TABLE OF CONTENTS

DECLARATION

I declare that the work presented in this dissertation was conducted exclusively by me, under the dual supervision of W.A.L. van Otterlo and C. B. de Koning. It is being submitted for the degree of Master of Science at the University of the Witwatersrand, Johannesburg. It has not been submitted before for any other degree or examination at any other university.

Tanya Dushanka Jeftic

07 October 2011

ABSTRACT

In the initial, methodological part of this MSc project we intended to expand upon and improve various aspects of the ultrasound accelerated, iodine catalyzed, conjugate addition reaction of amines with 1,4-naphthoquinones first reported by Ji and co-workers in *Synthetic Communications* (2008, **38**, 1201-1211). In recent times, the synthesis of 2-amino-1,4-naphthoquinones has become a heated area of research as a direct consequence of their multitude of diverse pharmaceutical activities; including anticancer, antimalarial, antifungal and trypanocidal properties.

Sonochemical transformations, reactions accelerated by ultrasound irradiation, have attracted considerable attention of late due to the shorter reaction durations, higher yields and milder reaction conditions associated with these processes. Additionally, as a result of its unique catalytic properties, iodine has been extensively exploited in diverse, atom-economical and accelerated organic reactions to afford the corresponding products in excellent yields with high selectivity.

With these considerations in mind a combinative library of eleven 2-amino-1,4-naphthoquinones with promising anticancer activity were successfully constructed in moderate to exceptional yields, with greatly reduced reaction times, 60 - 90 minutes, using the environmentally friendly, protic solvent ethanol.

ACKNOWLEDGEMENTS

Crossing that tenuous bridge, ever onwards toward the ultimate goals of this project has been a true test of spirit and endurance. But I could never have made those final steps without the many hands that sometimes carried me, held my hand or just pointed the way.

I would like to extend my sincere gratitude to my supervisors Professor W.A.L. van Otterlo and Professor C. B. de Koning for their guidance, patience, support and encouragement throughout the project. Willem, despite your travels you never forgot about me and the work that we were doing; your letters and many patient discussions paved the way to the end of this journey. Dr. A. Dinsmore for his creative ideas, passion for chemistry and his interesting take on life. Professor Carlton, for teaching me so much about NMR spectroscopy and for coming up with inventive solutions to some of the most stubborn compounds that evaded elucidation. Demi Levendis, thank you for reminding me again and again how wondrous chemistry is and what a privilege it is to have this knowledge.

Special thanks goes to Richard Mampa for accepting my bouquets of NMR tubes with grace and for running countless NMR experiments with diligence and enthusiasm. Marelize Ferreira and Dr. A. Dinsmore of the mass spectroscopy department who, despite many technical difficulties, managed to characterise many of my compounds and who imparted such valuable knowledge.

To the members of Lab 321 who made some of the gloomiest, failed-reaction days bright with music and laughter, your friendship and company will not be soon forgotten. In particular I would like to thank Jenny Lee Panayides and Darren Riley for answering a million questions and offering me their friendship. Warren Thompson and Lee Madeley for being close allies and for inspiring me with their brilliance.

J. R., I could never truly measure the investment you made in me, just a small girl in a lab coat with a big dream. Dr. Kali Trichoridis, for always keeping me focused and believing in me. Anthony Posner, for all your support and encouragement and for helping me find my way back to the lab.

Adushan Pillay, for your love of chemistry, your stern guidance, your creative synthetic ideas and for making it fun to be in the lab.

Thank you Cyberrange for repairing my laptop countless times and recovering data I thought would be lost forever.

The generous financial assistance of the National Research Foundation and the University of the Witwatersrand is gratefully acknowledged.

I would also like to thank my group of friends for providing an island away from the lab: Miskar Chomse, Andrew Backhouse, Chris Ansara and Christopher Dando. Special thanks goes to Christopher Dando for the graphic, formatting assistance, friendship, love and support.

Thank you Mom, Dad and James for supporting me throughout all these years and for allowing me to stay in Never Never Land longer than anyone could ever hope for.

We shall not cease from exploration. And the end of all our exploring will be to arrive where we started and know the place for the first time.

-T.S. Eliot

LIST OF COMMONLY USED ABBREVIATIONS

aq	aqueous
as	in infrared spectroscopy; asymmetrical vibration
bs	in NMR spectroscopy; broad singlet
cm^{-1}	wavenumber
DEPT	distortionless enhancement by polarisation transfer
DMF	*N*, *N*-dimethylformamide
DMSO	dimethyl sulfoxide
Et	ethyl
hr	hour
HRMS	high-resolution mass spectrometry
HSQC	heteronuclear single quantum coherence: in NMR, a 2-D experiment that maps the chemical shifts of directly bonded ^{1}H and ^{13}C or ^{15}N heteronuclei
Hz	Hertz, s^{-1}
IR	Infrared Spectroscopy
Me	methyl
min	minutes
mp.	melting point
NMR	nuclear magnetic resonance
OMe	methoxy
Proton	a hydrogen atom, with particular reference to ^{1}H NMR spectroscopy
rt	room temperature
TLC	thin-layer chromatography

R_f	retention factor: in chromatography; the distance travelled by a given component divided by the distance travelled by the solvent front
sy	in infrared spectroscopy; symmetrical vibration
WITS	University of the Witwatersrand

PART A

NITROGEN-CONTAINING DERIVATIVES OF NAPHTHOQUINONE

CHAPTER 1: INTRODUCTION AND LITERATURE SURVEY

1.1 Introduction – Research Rationale

Proliferative diseases are expected to become the major cause of death plaguing the human race in the 21st century.[1] The crucial step in sourcing novel chemical leads from the vast chemical space is the identification of a promising parent structure.[1] Natural products can be viewed as a treasure-chest of evolutionarily pre-validated molecules that have likely evolved to possess highly specialized functions.[1] These valuable biologically-synthesized organic compounds represent the fraction of the chemical pool explored by nature thus far.[1] It is estimated that natural products and natural product-derived compounds constitute 74% of all novel anticancer leads.[1] Simpler analogues of more complex, biologically active molecules have remained the inspiration for many active compounds and have led to the discovery of potent anti-tumour treatments in the past.[1] Plant metabolites have been shown to disrupt abnormal cell-signalling pathways leading to cancer and work synergistically with current forms of chemotherapy and radiotherapy.[1] Compounds discovered in medicinal plants may also avoid many of the side-effects associated with synthetic drugs as they naturally accumulate within living cells.[1]

The aforementioned considerations led to the construction of a combinative library of potential anticancer agents utilizing two well-known biological scaffolds with cytotoxic potential, namely; 1,4-naphthoquinones and piperazines, which will be discussed in detail below.

1.2 The 1,4-Naphthoquinone Pharmacophore in Anti-Cancer Agents

The 1,4-naphthoquinone pharmacophore, illuminated in Figure 1 below, has been shown to impart anticancer activity in a number of pharmaceutics, for example; doxorubicin **1A** and idarubicin **1B**, (**Figure 1**).[2, 3] These compounds belong to a family of chemotherapeutic and antibiotic anthracycline drugs isolated from the bacterium *Streptomyces peucetius var*. or *Streptomyces parvalus*.[4, 5]

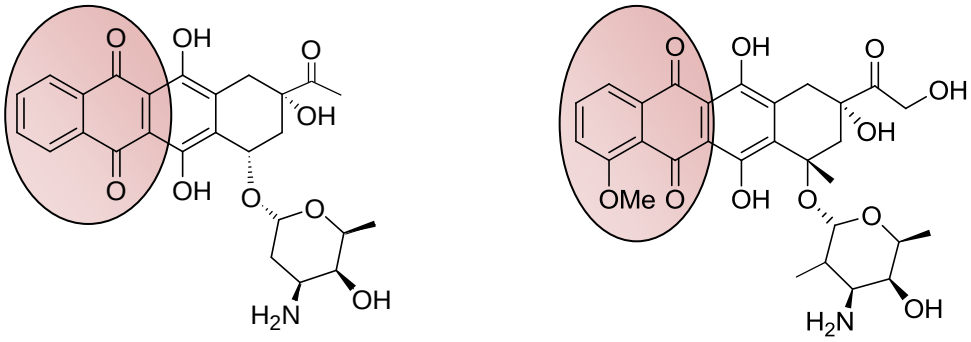

Doxorubicin
1A

Idarubicin
1B

Figure 1: Doxorubicin and Idarubicin with the 1,4-naphthoquinone pharmacophore highlighted

Most anthracyclines are thought to share similar modes of anticancer activity.[4] Ultimately, cell division is prevented through the disruption of the structure of DNA by intercalation between base pairs.[1, 4, 5] They are also known to inhibit topoisomerase II which hinders DNA replication, forms cytotoxic oxygen free-radicals and induces DNA breakage as well as chromosomal aberrations.[1, 4, 5]

Cyclin-dependent kinases (CDK) perform a vital regulatory role in the eukaryotic cell-cycle through the phosphorylation of proteins responsible for the activation of structural and regulatory genes.[2] Cdc25 A, B & C protein phosphatases control the activation of CDK by eliminating two inhibitory phosphate groups on adjoining threonine and tyrosine residues near the amino terminus.[2] Experimental evidence has shown that Cdc25 enzymes modify cells in culture and harbour oncogenic material.[2] The majority of highly effective Cdc25 regulators reported in the literature today contain the *quinone* moiety.[2] Several benzoquinones and fused quinones have been identified as potent *in vitro* Cdc25 inhibitors by high-throughput screening.[6] As a result of their unique redox capabilities, they modulate phosphatase behaviour via the generation of reactive oxygen species (ROS) and irreversibly oxidise the catalytic cysteine of Cdc25.[2] Exceptional biological activity is imparted on the 1,4-naphthoquinone pharmacophore due to the presence of two carbonyl groups that have the ability to accept electrons to produce the corresponding radical anion or di-anion species, as well as their acid-base properties.[7]

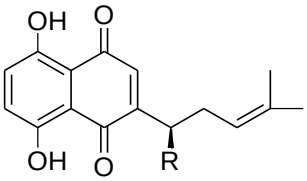

R = OH (Shikonin) **2A**
R = H (Arnebin) **2B**

Figure 2: The generic structure of two naphthoquinonyl natural products; Shikonin and Arnebin

Another example, shikonin **2A** (**Figure 2**), a natural product also bearing the naphthoquinone structure, isolated from the Chinese medicinal herb zicao (purple gromwell, the dried root of *Lithospermum erythrorhizon*) has demonstrated excellent anti-tumour potential through the inhibition of Epidermal growth Factor Receptor (EGFR) signalling in human epidermoid carcinoma cells.[8, 9] Mutations involving EGFR potentially result in constant over-activation, resulting in rampant cell division and a propensity to develop cancer.[8] Mutated EGFR has been isolated in several strains of cancer, is frequently resistant to chemotherapy and radiation therapy and has been identified as an attractive target for new therapeutic agents.[8]

Studies associated with the American National Cancer Institute have revealed that in addition to its anti-inflammatory and anticancer capabilities, shikonin **2A** possesses numerous pharmacological properties, including the ability to inhibit the human immunodeficiency virus (HIV) type 1.[9]

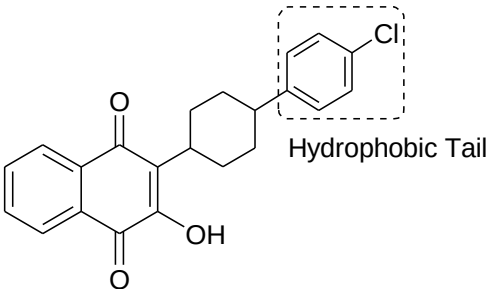

Atovaquone **3**

Figure 3

Another promising lead compound atovaquone **3** (**Figure 3**), a hydroxy-1,4-naphthoquinone, is an anti-parasitic drug that selectively targets the mitochondrial respiratory chain of the malaria parasite.[10, 11] It is a highly lipophilic molecule with poor bioavailability due to the presence of a hydrophobic 4- chlorophenyl tail in its chemical structure.[10, 11] After the tablet form of the drug was discontinued as a result of unreliable bioavailability it was reformulated as a yellow crystalline solid in citrus-flavoured liquid suspension.[10] Structural modifications of the parent structure have led to promising leads in the chemotherapeutic field and is pertinent as the sourcing of new applications for existing medicines remains an attractive means of accelerating drug development processes.[11]

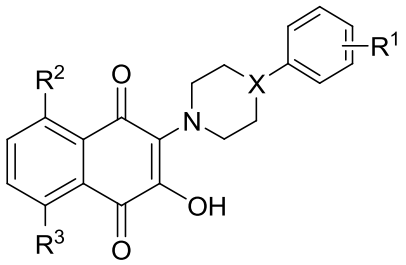

2-piperazinyl naphthoquinone (X=N) **4A**
2-piperidinyl naphthoquinone (X=CH) **4B**

Figure 4: The generalised structure of atovaquone analogues

In 2007, Zhou *et al*. reported the structural optimization and *in vitro* biological evaluation of atovaquone derivatives as new cytotoxic and apoptosis inducing agents.[11] The anti-cancer activity of 2-piperidinyl **4B** and 2-piperazinyl **4A** analogues (**Figure 4**) was evaluated on a range of human cancer cell lines using doxorubicin as a positive control.[11] Almost all of the aforementioned derivatives displayed broad-spectrum anti-proliferation activity against solid tumour cells.[11] In addition to the exciting experimental results, the aminonaphthoquinone analogues showed high selectivity in targeting tumour cells with no obvious cytotoxic activity in non-cancerous cell lines.[11]

Evaluation of the weight of the evidence thus indicates that aminonaphthoquinones are appealing targets, well worth pursuing as potential cytotoxic drug-precursors.

1.3 Antimalarial Activity of 1,4-Naphthoquinonyl Derivatives

Malaria is a devastating, tropical pathogen that is responsible for roughly two million deaths a year in the third world.[12] The population at risk for developing this disease has steadily increased as the *Anopheles* mosquito vector continues to thrive unchecked, coupled with the emergence of parasitic species resistant to conventional anti-malarial drugs.[12] Two virulent strains of *Plasmodium falciparum* have rendered the widely utilized antimalarial, chloroquine, ineffective, and resistance to other agents such as mefloquine and antifolates have arisen.[12] Thus there is currently an urgent need for the identification of lead compounds with novel mechanisms of action, which will be effective against all strains of the malaria parasite.[12]

The antiplasmodial activity of naphthoquinone and its derivatives was first reported almost fifty years ago.[13] Although none of these compounds have successfully passed through clinical trials to be developed into commercially viable antimalarials, a wide range of naphthoquinones and quinone-containing compounds have yielded promising results when tested against *P. falciparum* in veterinary models and *in vitro*.[13] This is hardly surprising as antiplasmodial effects have been observed for many compounds which produce elevated levels of oxidative stress in parasitized host erythrocytes.[13] It is proposed that naphthoquinones work to inhibit the enzyme dihydroorotate dehydrogenase and cause redox cycling, accounting for their antiparasitic action.[13]

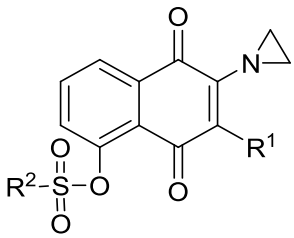

(R^1=H) 2-Arizidinyl-1,4-naphthoquinonyl Sulfonate **5A**

(R^1= ) 2,3-Bis(arizidinyl)-1,4-naphthoquinonyl Sulfonate **5B**

(R^2 = 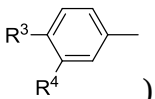) R^3 = CH_3, CH_2CH_3, $C(CH_3)_3$, Cl, Br, I, NO_2

R^4 = H, NO_2

Figure 5

Lin *et al*. of the Yale University School of Medicine research group synthesised 2-arizidinyl- **5A** and 2,3-bis-(arizidinyl)-1,4-naphthoquinonyl sulfonate **5B** and acylate derivatives (**Figure 5**) that are irreversibly bound and capable of redox cycling in malaria-infested red blood cells.[13] Their antiplasmodial activity was tested *in vitro* against the chloroquine-resistant human malaria parasite, *P. falciparum*.[13] The structure-activity relationships (SAR) revealed that the presence of nitrogen-containing substituents at the 2-position was associated with an increase in activity – specifically, the presence of an arizidinyl substituent at the 2-position of the naphthoquinone ring was associated with a substantial enhancement in antimalarial activity, while compounds with non-arizidinyl nitrogen-containing substituents at the 2-position demonstrated even greater activity.[13]

Furthermore, a drug discovery program in the School of Pharmacy at Howard University evaluated eighteen napththoquinonyl compounds, including synthetic derivatives and naturally occurring analogues, for potential antimalarial activity.[12] Their findings identified *aminonaphthoquinones* as a class of promising antiplasmodial agents against *P. falciparum*.[12] Interestingly, it was shown that the presence of an amino group is essential for antimalarial activity.[12] In particular, 2-amino-3-chloro-1,4-aminonaphthoquinone was identified as a potential lead compound for the design and development of a novel class of antimalarials.[12]

1.4 The Anti-Fungal Properties of 1,4-Naphthoquinone Derivatives

Patients with compromised immune systems arising through the use of cytotoxic drugs, immunosuppressant medications and HIV-related infections are at a high risk of developing fatal, systemic fungal diseases.[3] Existing treatments work only to suppress the proliferation of fungal populations, thereby encouraging the emergence of multidrug resistance.[3] Therefore, it has become imperative that new antimycotic agents with a broad gamut of antifungal activity are identified.[3] 2-Hydroxyjuglones **6A** isolated from the plant tissue of the black walnut (*Juglans nigra*), naturally occurring 2-methoxy-1,4-naphthoquinones **6B**, shikonin **2A** and arnebin **2B** include the naphthoquinone pharmacophore and exhibit pronounced anti-fungal properties against a number of fungal strains.[3] Juglone derivatives were found to suppress the respiratory functions of fungal spheroblasts and to inhibit RNA biosynthesis.[3] They are also known to obstruct the entrance and

exit of essential proteins, lipids and glucose by altering basic biochemical processes of membrane systems in the cells.[3]

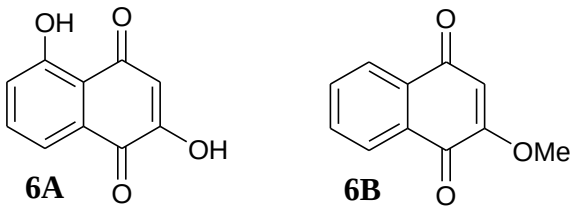

2-Hydroxyjuglone **6A**
2-Methoxy-1,4-naphthoquinone **6B**

Figure 6

1.5 The Application of 1,4-Naphthoquinone Derivatives in the Treatment of Other Diseases

Frequently used pharmaceuticals containing the naphthoquinone pharmacophore including; menadione (2-methyl-1,4-naphthoquinone) **7A**, plumbagin (2-methyl-5-hydroxy-1,4-naphthoquinone) **7B** and lapachol [2-hydroxy-3-(3-methyl-2-butenyl)-1,4-naphthoquinone] **7C** (**Figure 7**) exhibit trypanocidal activities against varied parasitic flagellate protozoa and *Leishmania* that are responsible for several human diseases such as African sleeping sickness (*Trypanosoma brucei rhodesiense* and *Trypanosoma brucei gambiense*), Kala-azar (*Leishmania donovani*) and Chagas disease (*Trypanosoma cruzi*).[7]

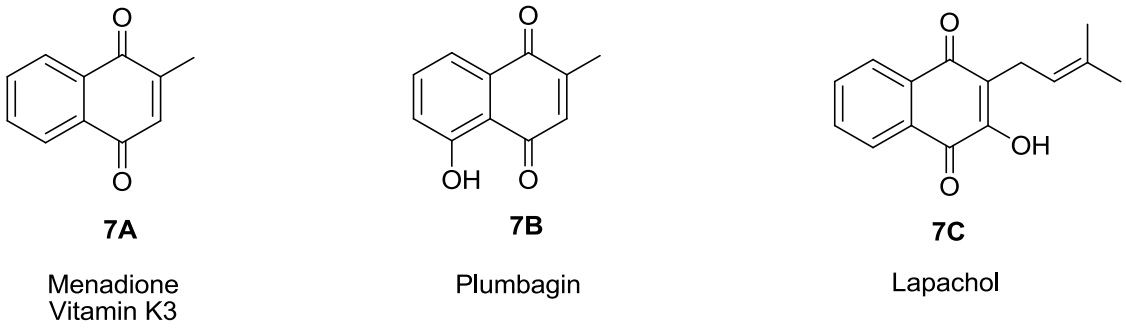

Figure 7: Trypanocidal Naphthoquinonyl Compounds

1.6 General, Domestic and Industrial Applications of (Alkylamino)naphthoquinones

In addition to their unmitigated chemotherapeutic, antimycotic, antimalarial and antiprotozoal uses, α-naphthoquinones have found widespread applications in colour chemistry, industrial dyeing processes, hair dying, cosmetics, home-remedies, agrochemistry and photostabilization.[7, 14]

For example, the 2-hydroxy-1,4-naphthoquinone containing leaves of the *Lawsonia alba* plant are ground and milled to produce a paste which is a commonly utilized dye known as henna.[7, 14] It has decorative value as a traditional, oriental stain of skin, hair, fingernails, leather, wool and silk.[7, 14]

Aminonaphthoquinones have also found diverse applications in the field of photography.[15] 2-Dialkylamino-1,4-naphthoquinones have been utilized as photosensitive molecules in silverless photographic materials with physical image development and in photoresist materials.[15] Photoresists are photosensitive materials exploited in several industrial processes including photolithography and photoengraving to facilitate the development of a patterned image on a surface.[15] This practical use is a direct result of a unique intramolecular photochemical redox reaction, resulting in the formation of naphtho[2,1-*d*]-2,3-dihydrooxazoles **8B** (**Scheme 1**).[15]

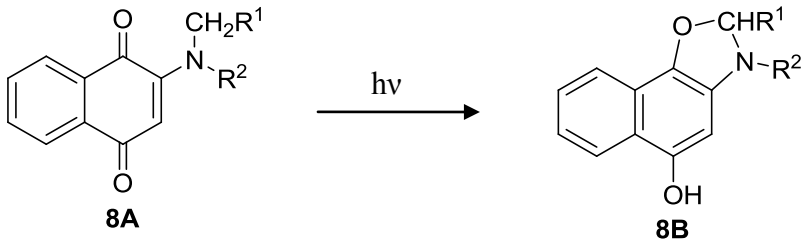

8A **8B**

Scheme 1: The Photoconversion of 2-Dialkylamino-1,4-naphthoquinones

α-Naphthoquinones, covalently bonded to various chromophores and fluorophores, possess reversible redox functions which potentially allow for unique "switching" properties.[16] A molecular switch is any molecule that can be reversibly shifted between two or more stable conformational states in response to a fluctuating stimulus, for example, pH, light, temperature, an electrical current or the presence of a ligand.[17] These switches find extensive applications in nanotechnology as

molecular computers and biological machines and physiology in allosteric regulation and vision.[17] The oldest and most widely encountered molecular switches are pH indicators, which display a distinctive set of colours as a function of hydronium ion concentration in solution.[17]

A conventional molecular switching system has two transformable stable state systems, resulting in four different integrated configurations.[17] In quinone optical switches the interconversion of the four states is as a result of two electrochromic states, namely quinone and hydroquinone.[17] Transmutation between these two states is achieved through the exchange of two protons and two electrons; thus allowing the redox couple to serve as the antenna subunit, influencing absorption or emission optical properties.[17] Illos *et al*. reported the design and synthesis of a novel "push-pull" molecular system bearing a fluorophore (dansyl) in electronic communication with an active redox quencher (phenyl-carbazoloquinone) through a secondary amine bridge.[17]

Based on the preceding considerations, it is undeniable that aminonaphthoquinone derivatives hold considerable value as synthetic targets. However, the synthetic procedures developed thus far for their production frequently remain unpredictable, time-consuming, cumbersome and harmful to the environment.[1]

1.7 Previously Reported Synthetic Procedures for Aminonaphthoquinones

The most commonly utilized synthetic strategies employed for the preparation of aminonaphthoquinones can be classified in two groups: one procedure involves a 1,4-Michael addition of a primary amine to the quinone moiety of a naphthoquinone **1** under acidic conditions (**Scheme 2**, eq. 1), whereas the other method entails the nucleophilic substitution of naphthoquinones bearing good leaving groups such as halogen atoms or methoxy groups with amines, leading to 2-amino-1,4-naphthoquinones **5** (**Scheme 2**, eq. 2).[1, 14, 18] However, these approaches are potentially laborious, usually give relatively low yields, afford many by-products and involve complex handling techniques.[14, 18] These drawbacks, in conjunction with the complications encountered during chromatographic purification, makes these methods synthetically unattractive.[14]

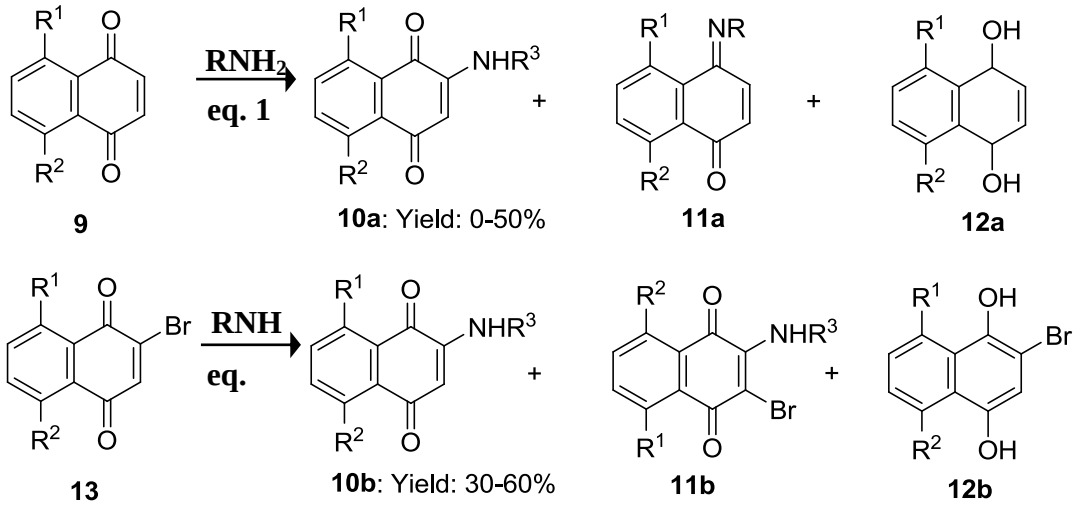

Scheme 2: General Methods for the Preparation of Aminonaphthoquinones

The possible side-products obtained in equations 1 and 2 in **Scheme 2** arise due to the unique redox properties of α-naphthoquinone.[14] This allows for the formation of the inert diol **12a** (or **12b**) and the presence of four equally reactive electrophilic centres permits the construction of 1,2- and 1,4-addition adducts, **11a** and **11b,** as well as bis-adducts not shown.[14]

Evaluation of the drawbacks associated with the synthetic procedures used thus far makes it evident that an improved, atom-economical methodology must be developed to include advanced catalytic processes which are inexpensive, readily available, and eco-friendly.[18]

1.8 The Utilization of Molecular Iodine as a Powerful Catalyst

Traditionally the Michael reaction, a 1,4-addition between nucleophiles and unsaturated carbonyl compounds, requires either acidic catalysts or basic conditions.[19] This approach involves the use of stoichiometric amounts of reagents, resulting in an increased likelihood of side-reactions occurring if the reaction-pair contains other reactive sites and allows for alternative reaction pathways.[19] In particular, due to the acid-induced conditions, polymerization of the unsaturated acceptor is commonly encountered.[19]

In recent times, molecular iodine has received increased consideration as an affordable, non-toxic and widely available catalyst for use in numerous organic transformations.[5] The moderate Lewis acidity associated with iodine has led to its recognition as an indispensable tool in numerous organic conversions using stoichiometric levels to catalytic amounts.[5]

In early 2006 Banik *et al*. reported a straightforward, rapid and high-yielding Michael addition between indoles and imidazoles with α,β-unsaturated ketones using a catalytic quantity of molecular iodine under solvent-free conditions.[19] That same year, Yao's group also revealed the use of iodine as a catalyst in the high-yielding, mild reaction of indoles with α,β-unsaturated ketones, or aldehydes at ambient temperature.[5] As part of a systematic study of hypervalent iodine chemistry, Kita *et al*. achieved the first total synthesis, a presumed biogenetic route, of discorhabdin C, a cytotoxic alkaloid isolated from the marine sponge *Latrunculia du Bocage* in New Zealand.[20] The generalised, concise synthetic route towards azacarbocyclic spiro-dienone systems entails an oxidative coupling reaction of the *O*-silylated phenolic aminoquinone, bearing both electron-poor and electron-rich sites at the *para* position, using phenyliodine(III)bis(trifluoroacetate).[20]

As a consequence of its unique catalytic properties, iodine has been extensively exploited in diverse, atom-economical and accelerated organic reactions to afford the corresponding products in excellent yields with high-selectivity.[18]

1.9 High-Power Ultrasound in Organic Synthesis

High-power ultrasonic waves drive a phenomenon known as cavitation within a liquid and through this process is capable of generating sufficient thermal energy, pressures, shock-waves and particle acceleration to promote chemical activation which enhances a wide-spectrum of organic processes proceeding via single electron transfer (SET) or radical routes.[21-23] The use of ultrasound irradiation in chemistry (sonochemistry) relies on relatively inexpensive equipment available in most general laboratories, results in higher yields, promises shorter reaction times and allows for the use of milder conditions.[22, 24] Sonochemistry, a green activation technique, shares with sustainable

chemistry such objectives as the use of less toxic reagents and solvents, lowered energy consumption and an increased product selectivity.[25-27]

Ultrasound is defined as sound of a frequency beyond the threshold of human detection.[23] It is considered to lie within the range of 20kHz to above 100MHz.[23] Sonochemistry is concerned with *conventional power ultrasound*, between 20 to 40kHz that influences chemical reactivity, produced by commercial laboratory instrumentation.[22, 26] At first glance, the ability of ultrasound to induce chemical change is unanticipated since the energies associated with sonication are insufficient to influence electronic, vibrational or rotational molecular properties.[26] However, this phenomenon is explained by a physical process that generates, expands and implodes vaporous lacunae in an irradiated liquid.[25]

Ultrasound, like all sound waves, is transmitted through a series of compression and rarefaction waves induced in the propagating material.[22] At sufficiently high power the rarefaction cycle may exceed the intermolecular van der Waals' forces of the liquid, resulting in an overall negative pressure being exerted on the medium.[22, 25, 28] The two most significant consequences are the formation of gas-filled microbubbles and the production of fine particles from solid reagents, resulting in substrates with large surface areas.[28] Upon nucleation, the cavities absorb energy from the US waves and expand over a few cycles.[25] The acoustic field surrounding a particular bubble is not static but changes continuously with the interference and resonance produced by the formation of new cavities.[22] As a result, bubbles unable to absorb energy sufficiently will undergo sudden inflation to an unstable size and implode violently.[22, 25] The rapid generation, expansion and disintegration of these micrometer-sized vesicles constitutes the phenomenon of *cavitation*.[26]

The "hot spot" theory explains that each collapsing bubble acts as a localised micro-reactor which, in aqueous systems, generates temperatures of around 5000K and pressures of approximately 1000 atm, sufficient to drive chemical reactions.[25, 27]

The first requirement for sonochemistry is an appropriate source of ultrasound.[22] Commonly, an ultrasonic cleaning bath and the ultrasonic horn or probe system are employed.[22] A simple sonicator is the most readily available, easy to operate and affordable point of supply of ultrasonic irradiation for the chemical laboratory.[22] Although, it is possible to use the chamber itself as a reaction vessel, this is not common practice since gases evolved cannot be contained and the bath walls are likely to corrode.[22] Conventional usage therefore involves the submersion of a standard glass reaction container, enclosing the reactants and solvent, into an ultrasound cleaner filled with tap water (**Figure 8**).[22] Additional thermostatic control may be required as temperature regulation in commercial cleaning baths is generally unsatisfactory.[22]

Figure 8: Sonochemical Reaction Set-Up Including Ultrasonic Cleaning Bath

Ultrasonic irradiation has been shown to be an effective technique for the activation and acceleration of various organic transformations.[23] Zeng *et al*. developed an ultrasound-accelerated reaction of indoles with (1*H*-indol-3-yl)(alkyl)methanol, catalyzed by ceric ammonium nitrate, at room temperature (**Scheme 3**).[23] This methodology was deemed superior to previously reported synthetic routes towards unsymmetrical bis(indolyl)alkanes (BIAs) **13C** (**Scheme 3**) due to its

relative speed, efficiency, use of non-toxic CAN, simple work-up and the possibility of using the same reaction to produce a number of unique BIAs simply by using different substrates.[23]

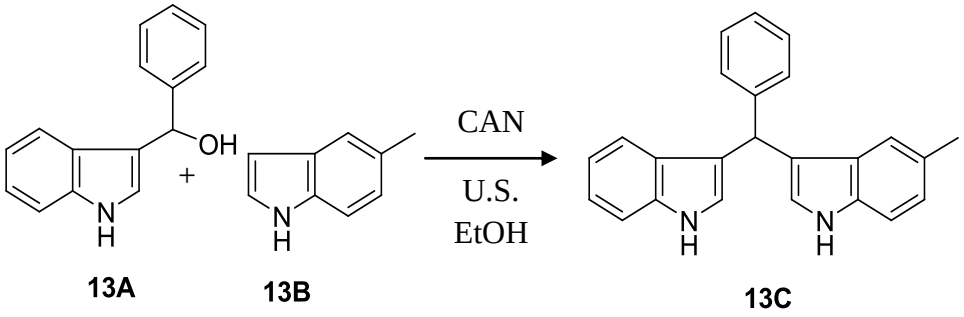

Scheme 3: Ultrasound-Accelerated Reaction of Indoles with (1*H*-indol-3-yl)(alkyl)methanol

The *O*-alkylation of 5-hydroxychromones (**Scheme 4**) is a non-facile, low-yielding reaction most likely as a result of hydrogen bonding between the carbonyl and hydroxyl group, thereby hindering ionization.[22] However, under sonication the yield was almost tripled and the range of the reaction was expanded using a variety of diverse haloalkanes.[22] It has also been shown that high power ultrasound acts to reduce the particle size of K_2CO_3 powder, thereby increasing the rate of the reaction and improving reactivity.[22]

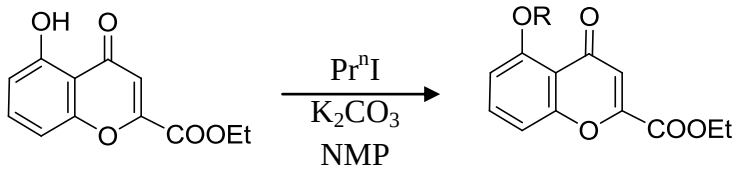

Scheme 4: Ultrasound-Mediated *O*-alkylation of 5-Hydroxychromones

Li *et al*. also reported the improved, high-yielding (96%) and rapid (30 min), sonicated Claisen-Schmidt condensation of cyclopentanone with aromatic aldehydes, catalyzed by KF/Al_2O_3.[24] Of importance, was that selectivity was highly specific.[24] To test this assertion, the reaction was performed on ratios of 2:1 and 1:1 furfural to cyclohexanone with the conclusion that both reactions produced α,α′-*bis*(furfurylidene)cyclohexanone **14A** exclusively and α-(furfurylidene)-cyclohexanone **14B** was not detected (**Scheme 5**).[24]

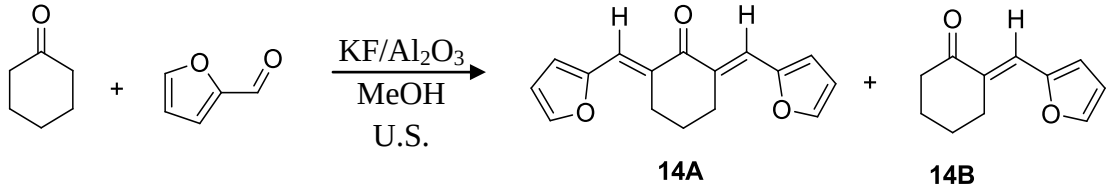

Scheme 5: Claisen-Schmidt Condensation of Cyclohexanone with Furfural

An improved Ullmann-Goldberg condensation of substituted 2-chlorobenzoic acid **15** with 2-aminopyridine **16** bearing various substituents, for the synthesis of 11-*H*-pyrido[2,1-*b*]quinazolin-11-one and derivatives **18** in *N*,*N*-dimethylformamide was described by Palacios *et al*. (**Scheme 6**).[29] The reaction duration under reflux conditions - 6 hours - lies in stark contrast to the mere 20 minutes required using ultrasound irradiation.[29] Additionally the average yield, for all derivatives, using sonochemistry was 74%, while that for reflux conditions was 60%.[29] At first glance, this may not appear to be a substantial improvement; however, it may be noted that the *lowest* yield attained using ultrasound irradiation was 63%, while that under reflux was 25%.[29] For all derivatives the yield obtained using ultrasound was substantially higher.[29]

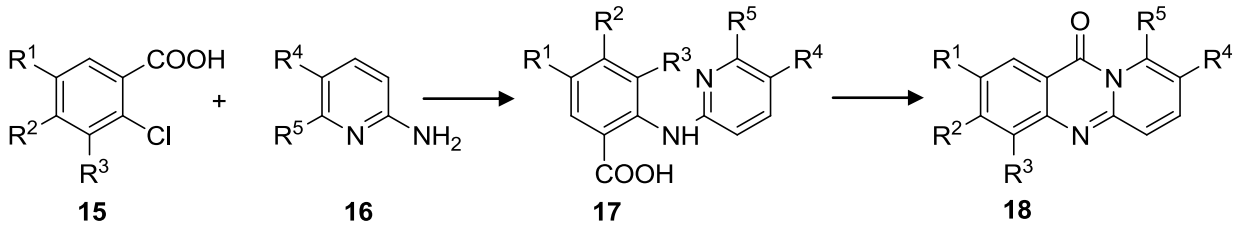

Scheme 6: Ultrasound-accelerated Ullmann-Goldberg Condensations

A journal letter submitted by Ji *et al*. was a crucial stepping stone leading to the groundwork research that inspired this MSc. project. They detailed the first sonicated Michael addition of indole **19** with α,β-unsaturated ketones **20**, using a catalytic amount of CAN in protic solvents at ambient temperature (**Scheme 7**).[30] Their methodology was applied to a wide-array of substrates and in most instances the reactions proceeded smoothly to produce the corresponding 3-(3-oxoalkyl)indole **21** in excellent yields (60-92%).[30] The transformations were also atom-economical, performed in non-

toxic solvents and highly specific.[30] Moreover, the formation of side-products, such as *N*-alkylation derivatives was not detected.[30]

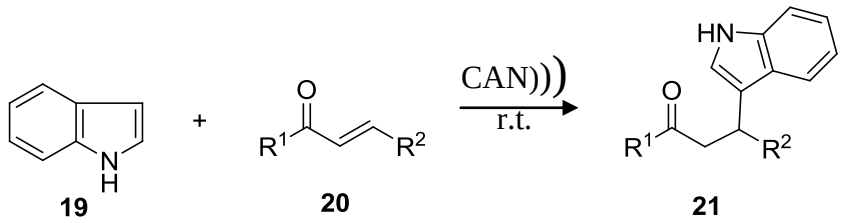

Scheme 7: Sonicated Michael Addition of Indole with Unsaturated Ketones

1.10 Groundwork Research Leading to Project Aims

The aforementioned considerations led to the pioneering work of Ji *et al*. which details the use of a variety of Lewis Acids such as CAN, $CeCl_3.7H_2O$, $Bi(NO_3)_3.5H_2O$, $FeCl_3.6H_2O$, *p*-toluenesulphonic acid (PTSA) and molecular iodine in the ultrasound-accelerated 1,4-addition of amines to α-naphthoquinone (**Scheme 8**).[18] However, it was found that the use of molecular iodine was associated with substantially higher yields and a shorter reaction duration.[18] Initial investigations were carried out on a 1:2 molar ratio of morpholine to 1,4-naphthoquinone, combined with a catalytic quantity of iodine whilst stirring at room temperature in anhydrous ethanol.[18] Notably, the yield was greatly improved (a 21% increase) under ultrasonic irradiation in the same reaction time (30 minutes).[18]

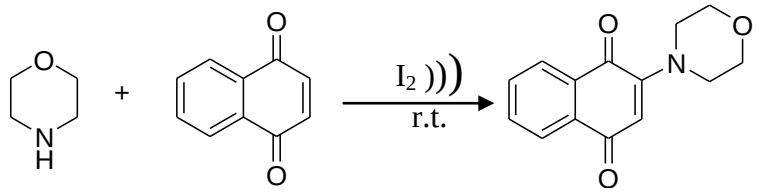

Scheme 8: Ultrasound-accelerated Conjugate Addition of Morpholine With 1,4-Naphthoquinone

The proposed mechanism for the reaction is outlined below in **Scheme 9**. At the outset, molecular iodine activates the carbonyl group by withdrawing electron density, inhibiting electron delocalisation and ultimately increasing the electrophilicity of the 3-position of α-naphthoquinone

to give intermediate **I**.[18] This is followed by amine attack at the unsaturated 3-position of intermediate **I**, giving rise to intermediate **II** after proton transfer.[18] Intermediate **II** then tautomerizes to the hydroquinone **III**, which subsequently undergoes rapid oxidation with a further equivalent of 1,4-naphthoquinone, resulting in the desired product- 2-amino-1,4-naphthoquinone **IV**.[18]

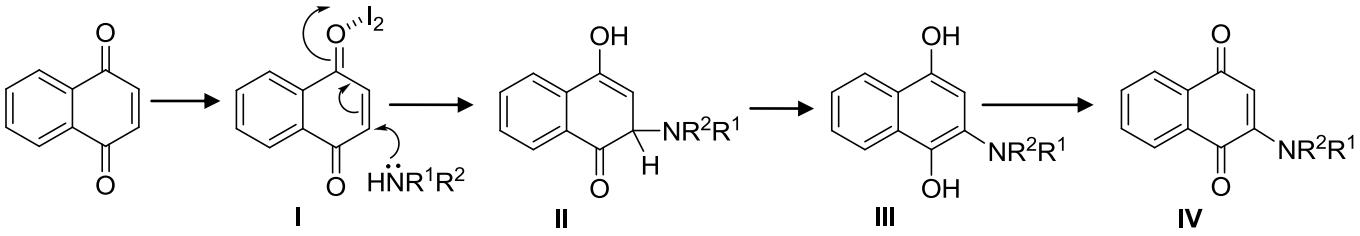

Scheme 9: Proposed Mechanistic Details for the Reaction of α-Naphthoquinone with a Generic Amine

Prompted by their unmitigated success, the basic reaction was extended to apply to the addition of aromatic amines, primary and secondary aliphatic amines such as piperidine **23** and pyrrolidine **24** to α-naphthoquinone, to afford the desired 2-amino derivatives in moderate to excellent yields (55-86%) (**Table 1**).[18]

Classes of Amines	Aromatic Amine	Aliphatic Amines			
Example	Aniline	Piperidine	Pyrrolidine	Morpholine	Piperazine
Structure	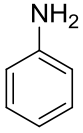 **22**	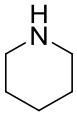 **23**	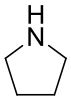 **24**	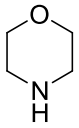 **25**	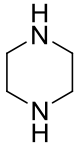 **26**

Table 1: A Table Outlining Two Major Classes of Amines with Examples

1.11 Project Aims for Part A

In this methodological research project, we plan to expand upon and improve various properties of the reaction first proposed by the organic chemistry research group of Suzhou University China, detailed above.[18] Their elegant synthesis allows for multiple extensions to produce a library of products through reactions with other classes of amines.

Our intention is to extend the reaction system to produce a library of 2-aminonaphthoquinones, containing piperazines **26** (**Table 1**), aryl-substituted piperazines and other unique branch-chained, aliphatic amines. Through repetition of the reaction process we plan to optimize reaction times and increase the previously reported mean yield of 65%. Although the solvent utilized in prior syntheses is protic and therefore environmentally friendly, we aspire is to repeat the synthesis under solvent-free conditions.

Ji *et al*. utilized a 1:2 molar ratio of amine to naphthoquinone in their research.[18] However, we hope to foster a more atom-economical process that allows for the use of a 1:1 molar ratio of reactants. During the aqueous work-up described by Ji *et al*., it was recommended that the reaction mixture be washed with a saturated solution of sodium hydrosulphite ($Na_2S_2O_4$) before extracting with dichloromethane.[18] In an effort to simplify the reaction, we propose to eliminate the use of $Na_2S_2O_4$ and wash with tap-water instead.

In certain instances, the method is so efficient that only one product is produced, as revealed by thin-layer chromatography (TLC). As a result, one is able to purify the crude-product rather simplistically, using a short silica plug. We aim to optimize the reaction to allow for the sparing use of column-chromatography which is often time-consuming, harmful to the environment, fairly costly and frequently leads to the decomposition of sensitive compounds.

In many instances naphthoquinone derivatives are found to be photo-sensitive and highly unstable. We intend to classify those compounds, in the proposed library, that are likely to decompose when exposed to light or when heated in the rotary evaporator. Water-bath temperature will therefore be noted, along with any other preventative measures needed to avoid product decomposition.

1.12 Summary of Aims

- Synthesize a library of piperazine-based 2-aminonaphthoquinones
- Optimize reaction times and increase the average reported yield
- Repeat one particularly facile reaction under solvent-free conditions
- Simplify the aqueous work-up and the purification process
- Identify photo-sensitive and thermo-sensitive compounds in the product library

CHAPTER 2: RESULTS AND DISCUSSION

This chapter will comprise a detailed commentary of the synthetic experiments conducted towards the proposed library of aminonaphthoquinone compounds. A discussion of the experiments will include a summary of the general procedure, followed by an overview of the results obtained. Relevant spectroscopic data, including NMR, IR and mass spectrometry will be presented as a means of confirming the identity and relative purity of each product.

2.1 Chasing the Molecule - Initial Forays into Aminonaphthoquinone Synthesis

2.1.1 Attempt 1 – Lewis Acid Promoted 1,4-Michael Type Addition

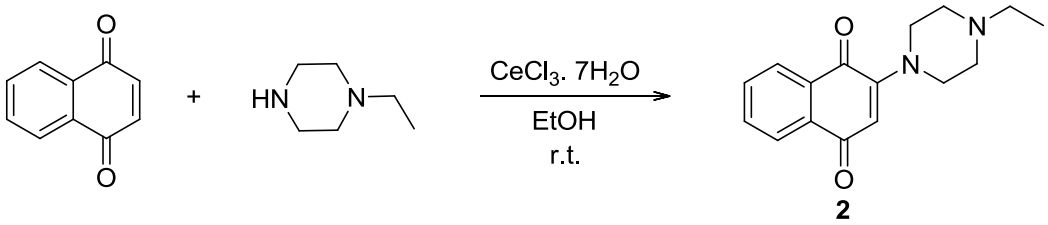

Scheme 10

This reaction involved a direct 1,4-Michael type addition of *N*-ethylpiperazine to the quinone moiety of 1,4-naphthoquinone in the presence of a Lewis acid, cerium (III) chloride, as outlined in the generalised procedure published by Keinan *et al*.[2] Crude α-naphthoquinone was dissolved in 96% ethanol, followed by the stoichiometric addition of the hydrate of cerium (III) chloride. The resulting solution was thoroughly stirred at room temperature until complete dissolution was achieved. Thereafter, *N*-ethylpiperazine was added to the reaction solution. The ensuing dark red mixture was then stirred overnight.

Prior to reaction work-up, the disappearance of starting materials was verified by TLC analysis with the eluent 50% EtOAc:hexane. The reduced form of Nile blue A was used as a developing and visualization reagent as recommended for naphthoquinones by Perrin and Armarego.[31] Under UV-light it became apparent that in excess of five compounds, all with highly similar R_f values, formed during the reaction. This result foreshadowed a potentially laborious and complex chromatographic separation which led to the rejection of the proposed reaction as a synthetically viable route towards the aminonaphthoquinone library.

The decision to abandon this methodological approach was substantiated by an article published in the *Journal of Organic Chemistry* by Couladouros *et al.*[14] Therein, it is suggested that this methodology is laborious and frequently gives low yields along with numerous side-products. These drawbacks, in conjunction with the complications encountered during the chromatographic purification, render this approach synthetically unfeasible.

An explanation for the appearance of several inseparable spots on the TLC plate originates from the intricate redox properties of naphthoquinone, which leads to the formation of the inert diol **2.4**.[14] The presence of four electrophilic sites of analogous reactivity often leads to the formation of a 1.2-addition adduct **2.3**, as well as a bis adduct **2.5**.[14]

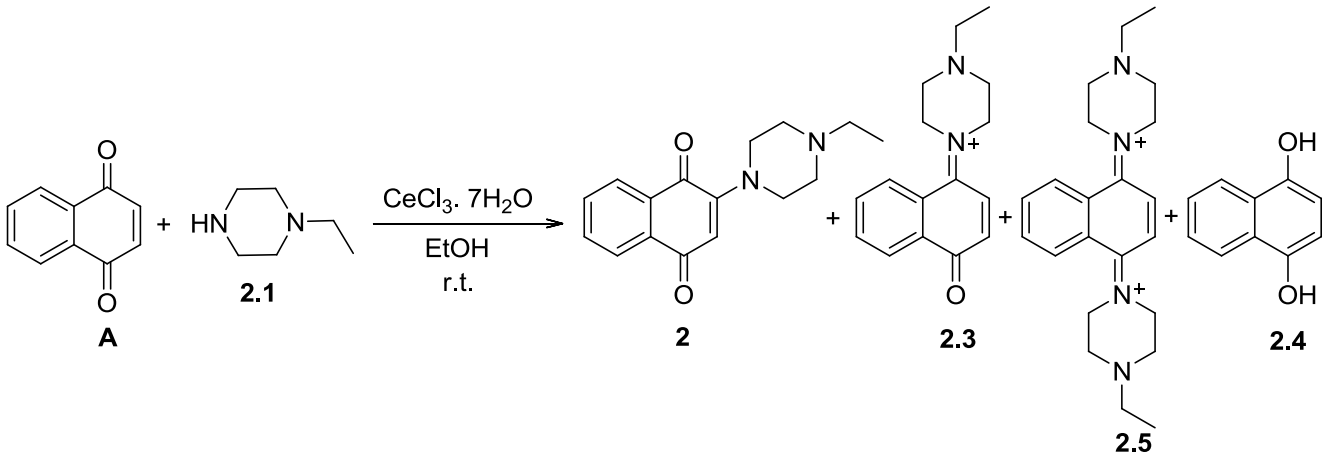

Scheme 11

2.1.2 Attempt 2 – Iodine-Catalyzed, Ultrasound accelerated 1,4-Michael Type Addition

Fortuitously, shortly after the initial set-back experienced with the classical approach to aminonaphthoquinone synthesis, Liu and co-workers of the Suzhou University in China reported a highly efficient, high-yielding conjugate addition reaction of morpholines, pyrrolidines, piperidines, aliphatic amines and substituted, aromatic amines with 1,4-naphthoquinone, accelerated with ultrasonic irradiation and catalyzed by molecular iodine at room temperature.[18]

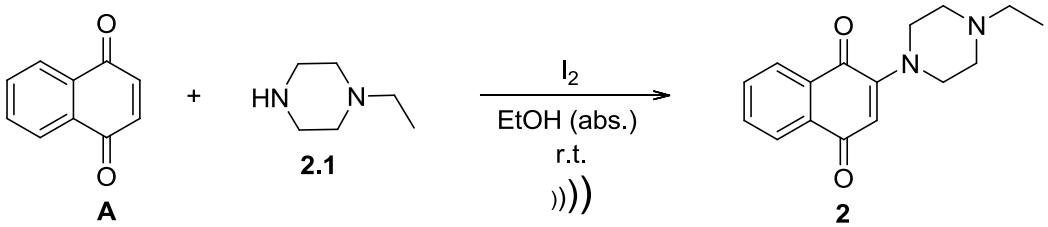

Scheme 12

A catalytic quantity of molecular iodine (10 mol %) was therefore added to a suspension of 1,4-naphthoquinone **A** and *N*-ethylpiperazine **2.1** in anhydrous ethanol. The resulting heterogeneous mixture was sonicated under ultrasound irradiation in a round-bottomed flask, open to the atmosphere and at room temperature, until the disappearance of starting material was noted under UV-light by thin-layer chromatography (TLC) at 60 minutes. The reaction contents were then evaporated under reduced pressure and the residue was washed with a saturated solution of sodium hydrosulphite ($Na_2S_2O_4$) and extracted with successive volumes of dichloromethane (CH_2Cl_2) until the organic layer remained clear. This was followed by drying the combined organic extracts over anhydrous sodium sulfate (Na_2SO_4) and subsequent filtration. The filtrate was then concentrated *in vacuo* and purified by column chromatography eluted with a 5% methanol-ethyl acetate solution. This ultimately led to the crude product oxidising on the silica, once more producing many inseparable compounds of similar R_f values as revealed by TLC analysis.

A ^{1}H NMR spectrum of the crude product revealed that the desired compound **2** (**Scheme 12**) was indeed successfully synthesised at an estimated, poor yield of 16%. The characteristic peaks unique to this compound were easily identified within the ^{1}H NMR spectrum; however additional peaks belonging to other unidentifiable side-products were also clearly observed. It appeared that this promising methodology was worth pursuing. Nevertheless, modifications of the reaction procedure would be necessary to achieve a better yield, facilitate full separation and allow for complete spectroscopic elucidation.

2.1.3 Purification of 1,4-Naphthoquinone

TLC analysis of the starting material, 1,4-naphthoquinone, showed that the material had oxidised in air during storage, making purification a necessity. It was anticipated that refinement of starting materials would ultimately ensure a more simplistic chromatographic separation.

Powdered 1,4-naphthoquinone was thus dissolved in dry benzene and the resulting solution was boiled over activated carbon for approximately 30 minutes. Whilst still hot, the mixture was filtered over compressed diatomaceous earth (celite) under reduced pressure. The purified solution was then reduced in volume *in vacuo* and allowed to recrystallise by slow evaporation. Bright yellow, needle-like crystals were subsequently collected by filtration, washed with a small quantity of chilled benzene and dried *in vacuo*.

2.2 On the Right Track- Building the Library of Molecules

2.2.1 Synthesis of Compound 1 – Reaction Between 1,4-Naphthoquinone and 2,6-Dimethylpiperazine

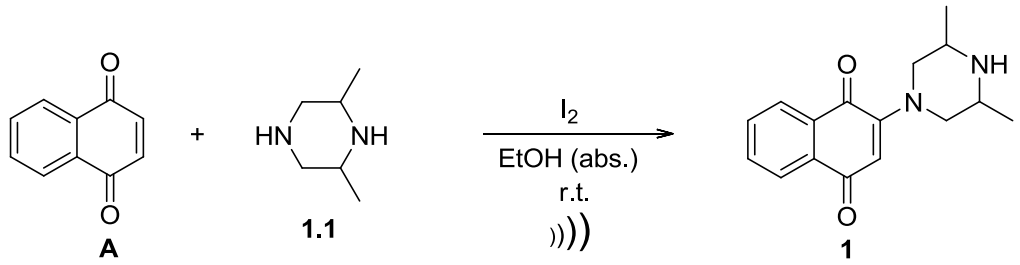

Scheme 13

It was decided to employ the promising work published by Liu and co-workers[18] as a core methodology from which, it was proposed, that each molecule in the aminonaphthoquinone library could be constructed in a mechanistic, handle-turning fashion.

This reaction involved the preparation of compound **1**, through a straightforward iodine-catalyzed, Michael-type addition of 2,6-dimethylpiperazine (**1.1**) (**Scheme 13**) to the quinone moiety of 1,4-naphthoquinone **A**, under ultrasonic irradiation as outlined in the generalised procedure published by Liu and Ji.[18]

A heterogeneous mixture of 1,4-naphthoquinone, 2,6-dimethylpiperazine and a catalytic quantity of molecular iodine (10 mol %), in absolute ethanol, was therefore sonicated under ultrasound irradiation in a round-bottomed flask, open to the surroundings at ambient temperature, until the disappearance of starting material was noted under UV-light by thin-layer chromatography (TLC) at 120 minutes. These compounds are often brightly coloured and were easily viewed with the naked eye; however, the presence of starting material could only be confirmed with the aid of a UV-lamp.

The resulting mixture was then evaporated under reduced pressure and the residue was washed with tap water, instead of saturated sodium hydrosulphite ($Na_2S_2O_4$). Fortunately, it was found that washing with cold tap water was just as effective in removing residual inorganic and unreacted species. The aqueous layer was then extracted with successive volumes of dichloromethane (CH_2Cl_2) until the aqueous layer remained clear of any pigment. This was followed by drying the combined organic extracts over anhydrous sodium sulfate (Na_2SO_4) and subsequent filtration under reduced pressure. The filtrate was then concentrated *in vacuo* and purified by column chromatography eluted with a highly polar, ethyl acetate:methanol:triethylamine solution in a ratio of 79:20:1 respectively. More simplistic solvent systems, of lower polarity were not able to raise the product off of the baseline. This result is not surprising as the free-amine moiety of the piperazine portion of the molecule exhibits hydrogen-bonding which results in a fairly strong interaction between the compound and the Si-OH bond of the absorbent.

Chromatographic purification and subsequent drying *in vacuo* yielded a vermilion solid of intense hue, often characteristic of substituted naphthoquinones, with a respectable yield of 75%. It was necessary to freeze the crude product in dry benzene for storage prior to purification, as it rapidly decomposed, even at sub-zero temperatures. However, the neat, pure product remained stable over an extended period when stored in a laboratory freezer.

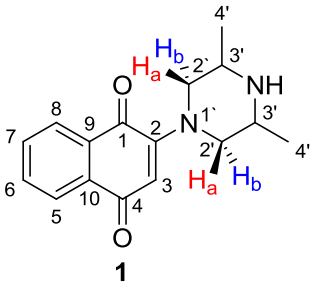

1

Figure 9

^{1}H NMR data / ppm		
H-6 & H-7	7.88	(2H, broad s)
H-5 & H-8	7.83-7.59	(2H, m)
H-3	5.99	(1H, s)
H-2′a	3.88	(2H, d)
H-3′	2.84	(2H, broad s)
H-2′b	2.47	(2H, d)
H-4′	0.98	(6H, d)

Table 2: ^{1}H NMR spectroscopic chemical shifts for compound **1**

The ^{1}H NMR spectrum of **1**, revealed two multiplets occurring in the chemical shift range of 7.88-7.59 ppm, integrating for four hydrogen atoms. These shifts were attributable to the four aromatic protons of the α-naphthoquinone moiety of the desired compound **1**. It is promising to note that these signals lie well within the range reported in the literature, 7.61-8.09 ppm,[18] for a structurally similar compound, a piperidine-based aminonaphthoquinone **1B**.[18]

A pronounced singlet occurring at 5.99 ppm integrating for one hydrogen atom is indicative of 1,4-naphthoquinone substituted at the 2-position and is within accordance with the literature reported value of 6.03 ppm[18] for the aforementioned piperidine-based aminonaphthoquinone **1B** (**Figure 10**).

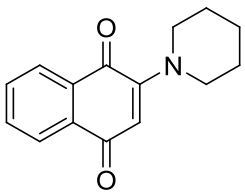

Figure 10: Compound **1B** – reported as compound 3h by Liu and Ji[18]

At 2.47 ppm a signal integrating for two hydrogen atoms lies underneath the overlapping solvent residual peak for deuterated dimethyl sulfoxide-d_6, typically occurring at 2.50 ppm.[32] The HSQC (C-H correlated) 2-D NMR spectrum showed that this signal, together with another signal arising at 3.88 ppm integrating for two protons, correlates with one carbon signal. These findings suggest that the impact of the stereogenic centre existing on C-3′ results in chemically non-equivalent, diastereotopic, geminal hydrogen atoms on C-2′. Furthermore, the piperazine ring is in a chair conformation which implies that H-2' is split into non-equivalent axial and equatorial protons. The hydrogen atoms found at both C-3′s are also accounted for by a broad singlet found at 2.84 ppm integrating for two hydrogen atoms. Compound **1B** does not exhibit diastereotopic hydrogen atoms on the piperidine moiety; however, it is useful to compare the reported chemical shift of 3.50 ppm to the experimentally determined range of 2.47-3.88 ppm for compound **1**. Lastly, a doublet at 0.98 ppm integrating for six hydrogen atoms was attributable to the presence of the two methyl groups at H-4′.

Two signals at 182.0 ppm and 182.8 ppm on the ^{13}C NMR spectrum were characteristic of the two carbonyl groups on 1,4-naphthoquinone (**Table 3**). The chemical shift quoted by Pretsch, Bűhlmann and Affolter, is 184.7 ppm for carbonyl carbon atoms lying on α-naphthoquinone.[32] The other aromatic carbon signals correlate well with the reported values of 133.7 ppm and 126.2 ppm.[32] The ^{13}C NMR signals which reveal the most about the substitution pattern of compound **1**, arise at 153.4 ppm (C-2) and 109.0 ppm (C-3). Instead of one signal occurring at 138.5 ppm for unsubstituted 1,4-naphthoquinones[32], two separate signals are found, with C-2 existing further downfield with respect to C-3, due to the pronounced deshielding effect of the electron-withdrawing nitrogen atom, N-1′.

The ^{13}C NMR spectrum also included: two signals at 132.5 ppm and 132.7 ppm which correspond to the two carbon atoms at C-9 and C-10 (*lit.*[32] 131.8 ppm), a chemical shift of 18.9 ppm which was assigned to the two methyl groups C-4″, the two chemically equivalent carbon atoms bearing the diastereotopic protons H-2′a and H-2′b are found at 55.0 ppm and the stereogenic centre C-3′ gives rise to a signal at 50.1 ppm.

^{13}C NMR data / ppm	
C-4	182.8
C-1	182.0
C-2	153.4
C-6 and C-7	133.9
C-10	132.7
C-9	132.5
C-5 and C-8	126.4
C-3	109.0
C-2′	55.0
C-3′	50.1
C-4″	18.9

Table 3: ^{13}C NMR chemical shifts for compound **1**

High-resolution mass spectrometry gave promising results and served to confirm the identity of the desired compound **1**. The molecular ion peak (M^+) which corresponds to the base peak at 270.1323, matched the calculated isotopic mass of 270.1369 ($C_{16}H_{18}N_2O_2$).

Lastly, in the infrared spectrum of compound **1** a strong C=O stretch occurred at 1672 cm^{-1} (*lit.*[18, 33] 1675 cm^{-1}), a weak C-H piperazine stretch was found at 2818 cm^{-1} (*lit.*[18, 34] 2811 cm^{-1}), a strong 1,4-napthoquinone C-C stretch was clearly observable at 1562 cm^{-1} (*lit.*[18, 33] 1559 cm^{-1}), an asymmetric C-N piperazine stretch occurred at 1240 (*lit.*[18, 33] 1297 cm^{-1}) and lastly a strong aromatic C-H δ oop was apparent at 775 cm^{-1} (*lit.*[18, 32] 772 cm^{-1}).

These findings serve to suggest that the synthesis of compound **1** was a success and allowed for further investigation into the expansion of the aminonaphthoquinone library.

2.2.2 Synthesis of Compound 2 – Reaction Between 1,4-Naphthoquinone and 1-Ethylpiperazine

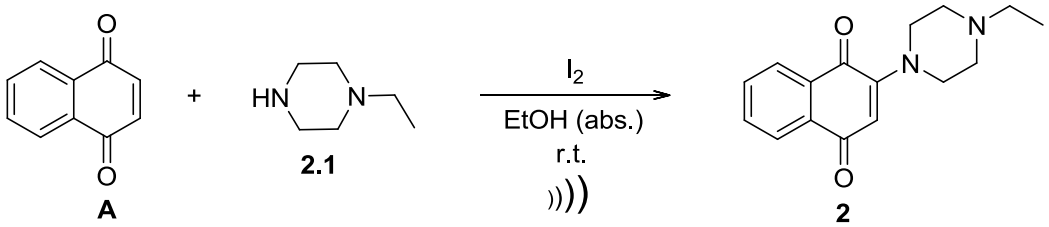

Scheme 14

Next a mixture of α-naphthoquinone, 1-ethylpiperazine **2.1** and a catalytic quantity of molecular iodine (10 mol %) in absolute ethanol, was sonicated under ultrasound irradiation at room temperature in a reaction vessel open to the surroundings. Progress of the reaction was monitored by thin-layer chromatography (eluent: EtOAc: 20% MeOH: 1% Et_3N), until the disappearance of starting-materials became evident under UV-light at 90 minutes. Remaining solvent was then removed under reduced pressure and the resulting residue was washed repeatedly with cold tap water until discolouration of the aqueous layer was no longer observed. The aqueous fractions were then extracted with successive volumes of dichloromethane and the combined organic portions were dried over anhydrous sodium sulfate, filtered under reduced pressure and concentrated *in vacuo*.

The solvent-system utilized in the chromatographic separation of compound **1** was not suitable for the purification of compound **2**, as it was seen to easily allow for elution of the compound from the silica gel, along with undesired impurities, instead of facilitating separation. A less-polar eluent was thus selected, that is a mixture of ethyl acetate: methanol: triethylamine in a ratio of 93:6:1 respectively. Isolation of the crude product was achieved by column chromatography, to reveal a dark-orange powder at a satisfactory percentage yield of 72 %.

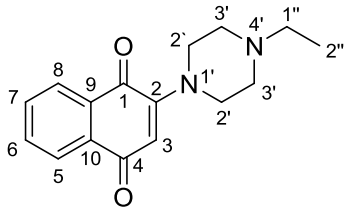

2

Figure 11

Contrary to what was expected, the axial and equatorial hydrogen atoms in the piperazine ring, H-2′a, H-3′a, H-2′e and H-3′e, were found to be chemically equivalent. Frequently, conformational changes occur faster than NMR spectroscopy can detect, as a result the observed chemical shift is half-way between the axial chemical shift and the equatorial chemical shift. This assertion is substantiated by the presence of two separate signals arising at 3.55 ppm (H-2′) and 2.62 ppm (H-3′), each integrating for four hydrogen atoms. The HSQC (C-H correlated) 2-D NMR spectrum also revealed that the four hydrogen atoms of H-2′ and H-3′ correlate to two separate carbon signals in the ^{13}C NMR spectrum at 48.9 ppm and 52.3 ppm respectively.

A triplet, J = 6.0 Hz, occurring at 1.12 ppm integrating for three protons was attributed to the terminal methyl group on the ethyl side-chain (H-2″) and a quartet, J=7.2 Hz, found further downfield at 2.48 ppm, integrating for two protons was assigned to the CH_2 group on the ethyl side chain (H-1″). Finally, the ^{13}C NMR spectrum revealed two aliphatic carbon atoms at 52.2 ppm and 11.9 ppm which were attributed to the CH_2 group and the terminal methyl group.

High-resolution mass spectrometry gave a molecular ion peak of mass 270.1323 which concurred well with the calculated isotopic mass of 270.1369 for $C_{16}H_{18}N_2O_2$. Finally, infrared spectroscopy revealed a strong carbonyl stretch at 1672 cm^{-1} (*lit.*[18, 33] 1675 cm^{-1}) and a strong C-N stretch occurring between the naphthoquinone and piperazine moieties was found at 983 cm^{-1}.

All in all, the spectroscopic data corresponded well with the literature[18] and with the spectroscopic findings for compound **1**.

2.2.3 Synthesis of Compound 3 – Reaction Between 1,4-Naphthoquinone and 1 Allylpiperazine

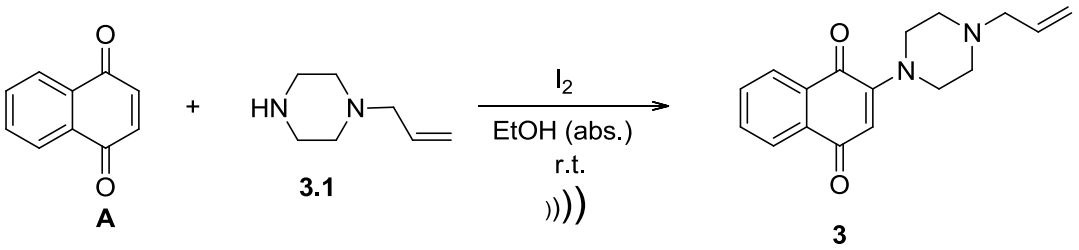

Scheme 15

Thereafter, α-naphthoquinone and 1-allylpiperazine **3.1** were reacted according to the general procedure outlined for compound **1** and **2** above. Reaction progress was monitored at thirty minute intervals by thin-layer chromatography (eluent: 93% EtOAc: 6% MeOH: 1% Et_3N), until the absence of starting materials was observed under UV-light at 120 minutes. Purification was subsequently achieved using column chromatography on silica gel to reveal a bright orange amorphous solid at an ample yield of 87%.

Furthermore the highly facile nature of this reaction was keenly observed – the dry starting materials began to react almost instantaneously before the addition of solvent and prior to ultrasonic irradiation. Thin-layer chromatography also revealed that compound **3** began to form on the plate when the reactants were overlapped on the same point on the silica gel. This led to the suggestion that a solvent-free synthesis be attempted to compare and contrast yield and duration with the original reaction.

However, a crack began to appear in the seemingly perfect veneer; when evaporating *in vacuo* at 45°C the sample began to decompose to a dark brown powder. It was tempting to discard the

compound and begin again, but thin-layer chromatography revealed that the brown colour was in fact a tertiary combination of two colours; orange – a secondary colour and blue – a primary colour. The chromatographic separation was then repeated to isolate the mysterious blue compound and its orange-coloured predecessor. A kaleidoscope of colours; blue, green, yellow, orange and red, resolved into distinct chromatographic bands – a rare treat, seared onto the memory of an organic chemist accustomed to the whites, yellows and browns of the organic kingdom!

The fractions corresponding to the orange coloured chromatographic bands were collected, combined and concentrated *in vacuo* to allow for spectroscopic characterisation. Advantageously, the compound remained stable at room temperature after purification which allowed for ^{1}H and ^{13}C NMR elucidation. Long-term stability was ensured by storing the compound at sub-zero temperatures.

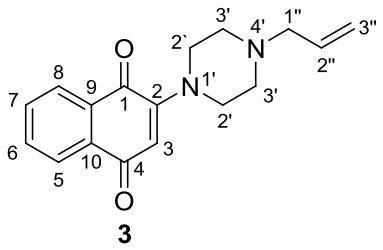

3

Figure 12

The ^{1}H NMR spectrum of compound **3** integrated for the correct number of total protons, 18, found in the structure of the expected product. The distinguishing peaks for the naphthoquinone and piperazinyl portion of the molecule lie within the same range as those assigned for compound **1** and compound **2**. A multiplet occurring in the chemical shift range 5.34-5.09 ppm, integrating for two protons, corresponded to the terminal CH_2 group (H-3″), a doublet, J= 6.6 Hz, found at 3.06 ppm, integrating for two hydrogen atoms was attributed to the CH_2 group (H-1″) and an intricate signal at 5.87 ppm, integrating for one proton was assigned to the CH group (H-2″). The three aforementioned signals were characteristic of the propenyl side-chain. The ^{13}C NMR spectrum also revealed three signals attributable to the propenyl side-chain: the terminal alkenyl carbon atom corresponded to a signal arising at 118.5 ppm (*lit.*[32] 113.5 ppm – 119 ppm), a chemical shift of

134.4 ppm was assigned to the central alkenyl CH group (C-2″) (*lit.*[32] 133 ppm – 140.5 ppm) and the CH_2 group existing closest to the piperazinyl moiety was attributed to a signal found at 61.5 ppm.

Infrared spectroscopic data showed a medium intensity stretch at 1671 cm^{-1} which was assigned to the carbonyl group of the naphthoquinone moiety, a strong stretch found at 1634 cm^{-1} was attributed to the $CH{=}CH_2$ group (*lit.*[32] 1650-1635 cm^{-1}) and a highly intense, distinguishing naphthoquinone-piperazinyl stretch occurred at 978 cm^{-1}.

High-resolution mass spectrometry revealed a molecular ion ($[M+H]^+$) of mass 283.1433 which corresponded well with the expected isotopic mass of 283.5301 for $C_{17}H_{19}N_2O_2$. Interestingly, a dimer $[(M+H)+(M+H)]^+$ of mass 566.87 also matched the expected isotopic mass of 566.7001 for $C_{34}H_{38}N_4O_4$.

The ^1H NMR spectrum of the blue compound was overwhelmed by base-line impurities and other peaks that evaded assignment. Therefore, elucidation of the molecular structure was unfeasible. However, certain characteristic peaks could be cautiously identified. Two aromatic multiplets occurring in the chemical shift range of 8.08-7.59 ppm could be attributed to the aromatic moiety of 1,4-naphthoquinone and the singlet arising at 6.0 ppm was recognised as the distinctive quinone C-H singlet of substituted naphthoquinones. A doublet found at a chemical shift of 3.53 ppm matched the piperazinyl hygrogen atoms, the terminal CH_2 group was identified at 5.28-5.22 ppm and a multiplet arising at 5.89-5.77 ppm corresponded to the allyl CH group.

Owing to the lack of definitive spectroscopic data one can only speculate that the blue compound is structurally similar to compound **3**. However, repeating the synthesis at a higher mass in the future, followed by gentle heating for two hours should afford a greater quantity of the blue compound. It would also be beneficial to determine whether or not the compound is thermosensitive or photosensitive. This would potentially allow for full spectroscopic characterisation and perhaps structural elucidation.

2.2.3′ Synthesis of Compound 3 – Solvent-Free Reaction Between 1,4-Naphthoquinone and 1-Allylpiperazine

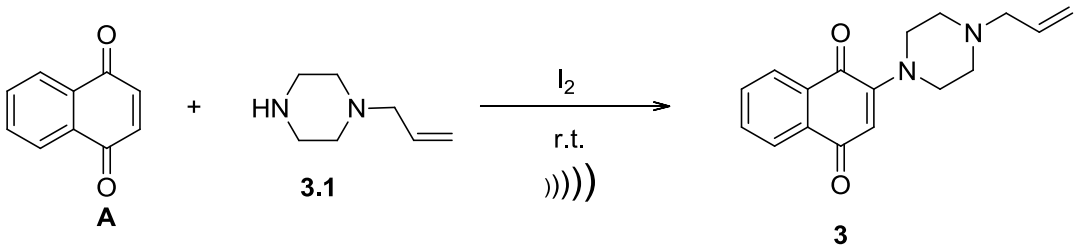

Scheme 16

Prompted by the highly facile nature of the transformation outlined in **Scheme 15** above, it was decided to attempt a solvent-free reaction based on the original generic experimental procedure detailed for the synthesis of compound **1** and **2** discussed previously.

It is suggested that when one of the reactants in a sonochemical reaction exists in the solid phase ultrasonic irradiation can yield several additional enhancement effects such as acceleration of reaction rate, reduction of induction period and overall improvement of catalyst efficiency, especially when the solid species behaves as a catalyst.[35] These beneficial factors occur as a direct consequence of cavitation in the liquid medium – micro-jets of solvent bombard the solid surface, exposing unreacted facets, ultimately increasing the surface area able to react.[35] Fortunately, 1-allylpiperazine exists in the liquid phase at room temperature and the catalytic species utilized is solid molecular iodine.

Consequently, 1-allylpiperazine **3.1** was added to the dry starting materials: α-naphthoquinone and iodine, in the absence of solvent. The resulting reaction mixture was suspended in an ultrasonic cleaning bath in a reaction vessel exposed to the surroundings at room temperature and sonicated for 90 minutes. Thereafter, the crude residue was partitioned between cold tap water and dichloromethane. The organic components were then extracted with dichloromethane, dried over anhydrous sodium sulfate and concentrated *in vacuo*. Purification was achieved using flash column

chromatography on silica gel to reveal a bright red semi-solid of compound **3** at a disappointingly low yield of 18%.

The sub-standard yield was attributed to the occurrence of extensive product decomposition during purification. It remains unclear as to an explanation for the product's (compound **3**) instability during column chromatography. However, compound **3**, synthesized under conventional reaction conditions, exhibited thermal decomposition at temperatures higher than 40°C. Curiously, the blue compound described in detail above, was not isolated in this instance.

Favourably, despite the apparent unpredictable nature of the product **3**, the compound remained stable at room temperature after purification which allowed for ^{1}H and ^{13}C NMR characterisation. Long-term stability was ensured by storing the compound at sub-zero temperatures.

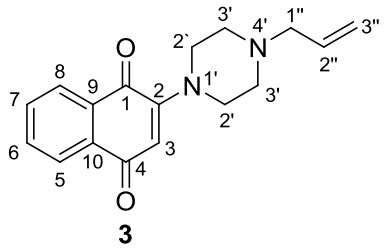

3

Figure 13

The ^{1}H NMR spectrum of compound ***3′*** corresponded perfectly with that of compound **3**: a doublet, J= 6.6 Hz, arising at 3.06 ppm, integrating for two protons, was assigned to the first CH_2 group (H-1″) found on the propenyl side-chain, the central CH group was identified as a complex multiplet, integrating for one hydrogen atom occurring in the chemical shift range 5.97-5.66 ppm, lastly the terminal CH_2 group (H-3″) matched a multiplet, integrating for two protons, found in the chemical shift range 5.36-5.09 ppm. The signals attributable to the propenyl side-chain in the ^{13}C NMR spectrum were found at the exact chemical shift positions as those assigned for the same compound **3** synthesized previously.

The combined spectroscopic data served to confirm that the solvent-free reaction was indeed a success and proved that the structure of the pure product attained in this methodological approach matched the expected structure of compound **3**.

2.2.4 Synthesis of Compound 4 - Reaction Between 1,4-Naphthoquinone and *Trans* – 1-allyl-2,5-dimethyl piperazine (racemic)

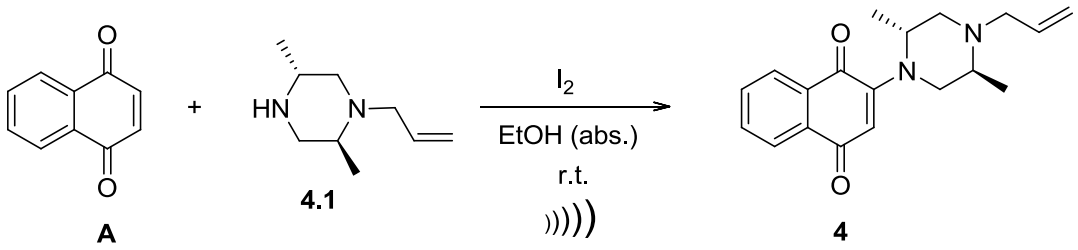

Scheme 17

Following on, 1,4-naphthoquinone and *trans*-1-allyl-2,5-dimethyl piperazine (racemic) were reacted according to the general experimental procedure detailed for compound **1** and **2** above. Reaction progress was monitored at thirty minute intervals by thin-layer chromatography (eluent: 93% EtOAc: 6% MeOH: 1% Et_3N), until the disappearance of reactants was detected under UV-light at 100 minutes. Purification was achieved using flash column chromatography on silica gel to reveal a bright-red, viscous oil, at an inferior yield of merely 19%, after drying *in vacuo* for twelve hours.

The percentage yield attained was well below the expected range of between 70-90% attained thus far. A plausible explanation for this finding may be that the sample potentially underwent photodimerization due to the presence of the highly reactive, terminal, alkenyl group. A side-product, corresponding to bright pink chromatographic bands, was eluted first during chromatographic separation. Within a matter of minutes these fractions transformed to a dull orange colour. As a result of its extreme lability and minuscule mass, spectral elucidation of the pink-coloured compound was not possible. However, the presence of this side-product may be

confirmation of a photo-dimer or could perhaps be attributed to the formation of a compound analogous to the blue compound isolated for compound **3**.

Despite the apparent instability of some of the aminonaphthoquinone compounds in the library, it was observed that once the pure product had been obtained following chromatographic purification, the sample remained stable at room temperature and long-term stability could be ensured by storing the compound at temperatures below 0°C. Compound **4** was no exception to this generalisation, which allowed for complete spectroscopic characterisation.

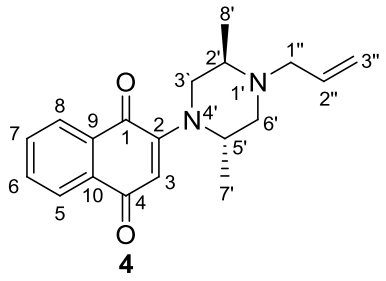

4

Figure 14

In general the ^{1}H NMR spectrum of compound **4** corresponded well with that of compound **3** which is structurally related. However, further complexity was introduced into the spectrum by the presence of two stereogenic centres, of the same configuration, found on C-2′ (R) and C-5′ (R) in the piperazinyl portion of the molecule. H-2′ and H-5′ were attributed to a single complex multiplet comprised of a pair of overlapping doublet of doublets of quartets (ddq), clearly integrating for two non-equivalent hydrogen atoms at a chemical shift range of 3.13-2.98 ppm. The axial and equatorial protons H-3' a/H-4′a and H-3′e/H-4′e were also revealed to be diastereotopic as a result of their close proximity to the chiral centres C-2′ (R) and C-5′ (R). Consequently, the splitting pattern ascribed to H-2′ and H-5′ can be explained by spin-spin coupling to axial H-3' /H-4' , equatorial H-3' /H-4' and to the methyl group H-7' /H-8' . The HSQC (C-H correlated) 2-D NMR spectrum revealed that the signals corresponding to C-2′ and C-5′ were located at chemical shifts of 57.5 ppm and 51.87 ppm in the ^{13}C NMR spectrum.

Furthermore, H-7′ and H-8′ corresponded to two doublets, J = 6.6 Hz, each integrating for three protons found at 1.38 ppm and 1.08 ppm. A doublet of doublets, J = 12.8 Hz and J = 3.0 Hz, arising at a chemical shift of 3.83 ppm, integrating for one hydrogen atom and the corresponding peak, an additional doublet of doublets, J = 12.9 Hz and J = 3.5 Hz, also integrating for one proton, found at a chemical shift of 3.53 ppm were attributed to the geminal protons H-6′a and H-6′e. Analogously, H-3′a and H-3′e were identified as two doublet of doublets, J = 11.9 Hz and J = 4.1 Hz/J = 2.43 Hz, each integrating for one hydrogen atom, found at 2.85 ppm and further upfield at 2.43 ppm. The HSQC (C-H correlated) 2-D NMR spectrum showed that these signals correlated with two carbon signals located at a chemical shift of 49.8 ppm (C-3′) and 49.1 ppm (C-6′) in the ^{13}C NMR spectrum.

Furthermore, infrared spectroscopic data coincided well with that of compound **3** and an additional stretch of strong intensity at 1298 cm^{-1} (*lit.*[32] 1400-1000 cm^{-1}, C-N, st) was tentatively identified as the stretch between the piperazinyl portion of the molecule and the propenyl tail. While relatively inconclusive, this data point is highly suggestive of the substitution pattern in the molecule.

Lastly, low-resolution mass spectrometry revealed a molecular ion ($[M+H]^+$) of mass 311.22 which corresponded well with the expected isotopic mass of 311.4038 for $C_{19}H_{23}N_2O_2$. Similar to that observed for compound **3**, a dimer $[(M+M)]^+$ of mass 620.61 was also observed which coincided with the expected isotopic mass of 620.7918 for $C_{38}H_{44}N_4O_4$.

Overall, the spectroscopic data corresponded well with the spectroscopic findings for the parent molecule, compound **3**, and accounted for the expected complexities that emerged as a consequence of the stereogenic centres in the piperazine ring.

2.2.5 Synthesis of Compound 5 - Reaction Between 1,4-Naphthoquinone and 1-[2-(dimethylamino)ethyl]piperazine

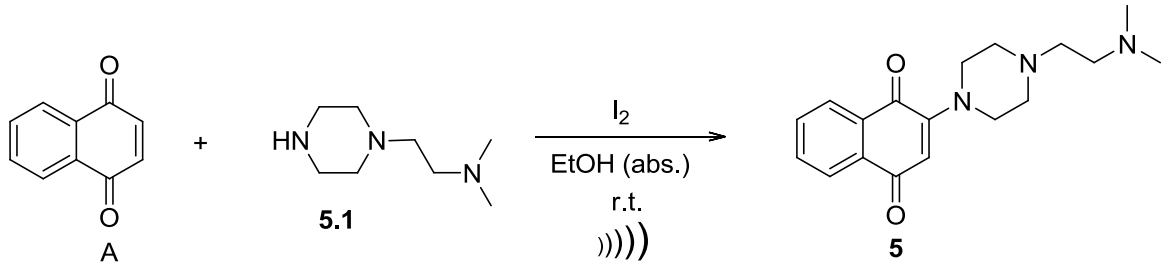

Scheme 18

Next it was discovered that the following piperazine selected as a building-block for the aminonaphthoquinone library, 1-[2-(dimethylamino)ethyl]piperazine, is sensitive to carbon dioxide which necessitated storage and handling under inert gases. This complication required the implementation of modifications to the original synthetic procedure followed thus far. The density of the liquid piperazine was also not quoted on the sample-bottle, on the Sigma-Aldrich website or in their handbook of fine chemicals. Therefore, an approximation of the sample's density, 1.000 g/ml, was then employed to calculate estimated stoichiometric quantities.

To ensure stringent anhydrous conditions, all glassware, including vacuum attachments, was dried overnight in a laboratory oven followed by additional flame-drying *in vacuo*. The two-necked round-bottomed flask was then flooded with argon and the solid starting materials 1,4-naphthoquinone and a catalytic amount of molecular iodine were swiftly added. The flask was then evacuated and filled with argon a second time until the reactants were submerged under a blanket of argon. 1-[2-(Dimethylamino)ethyl]piperazine was injected through a rubber septum into the reaction vessel while a steady flow of argon was bubbled into the sample bottle through a Pasteur pipette. Thereafter, absolute ethanol, distilled over oven-dried magnesium turnings, was injected through the septum. The resulting reaction mixture was then sonicated under ultrasound irradiation at ambient temperature in a sealed reaction vessel submerged in water. Reaction progress was monitored by thin-layer chromatography (eluent: 50% EtOAc: Hexane), until the disappearance of

starting-materials became evident under UV-light at 120 minutes. It was found that using solvent-systems of successively higher polarity, (50% EtOAc: Hexane), (EtOAc: 1% Et_3N), (5% MeOH: 1% Et_3N: EtOAc and MeOH: 1% Et_3N), did not lift the product off of the baseline during TLC analysis. This observation is not uncharacteristic of the anticipated product as the three nitrogen atoms in the piperazinyl and aliphatic portions of the molecule are expected to adhere firmly to the Si-OH bond of the absorbent. Consequently, the use of column chromatography as a purification technique was rejected. Following reaction completion the remaining solvent was removed under reduced pressure and the resulting residue was then purified by acid-base extraction, summarised in **Figure 15** below.

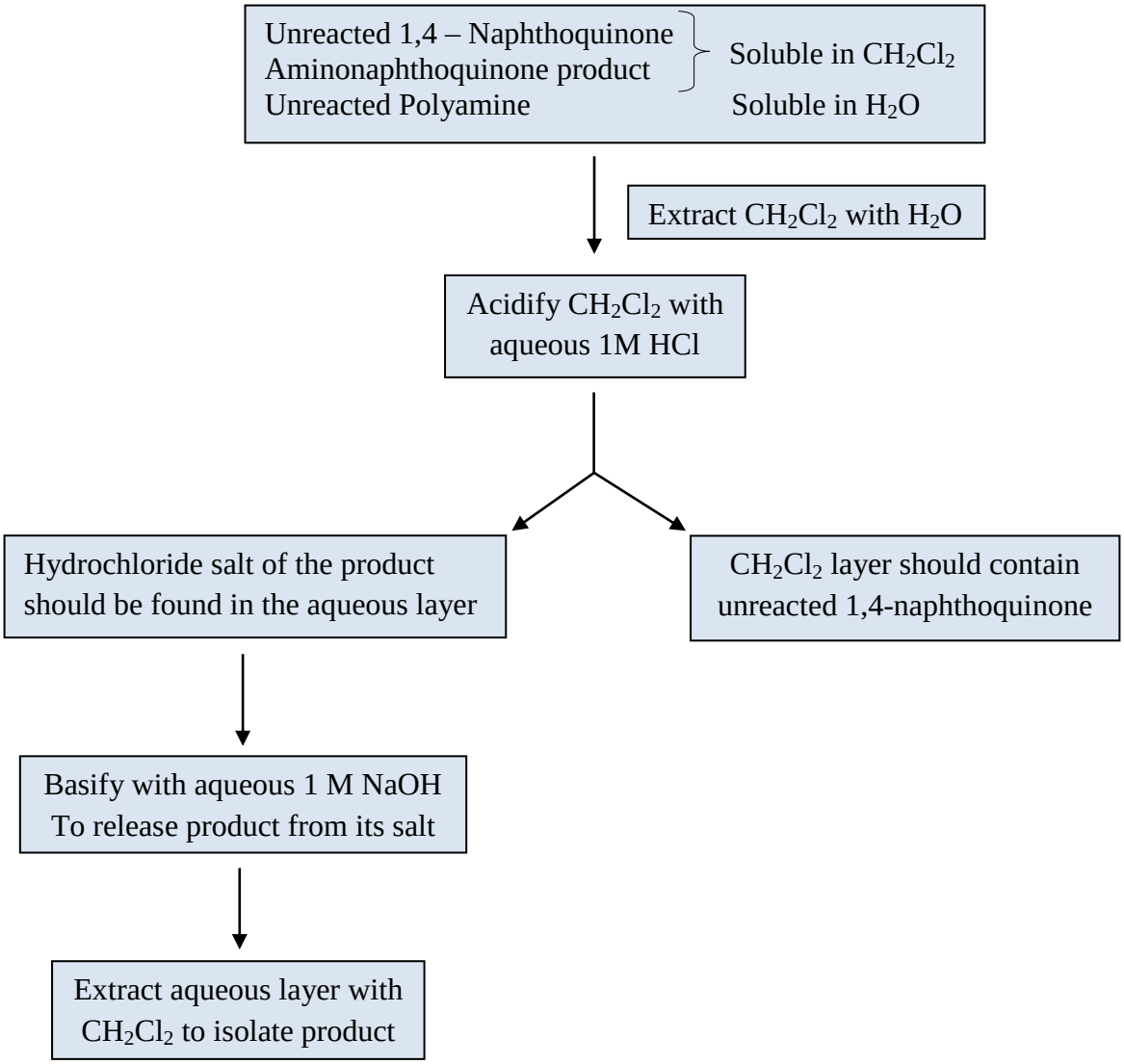

Figure 15

Finally, the combined organic portions were dried over anhydrous sodium sulfate, filtered under reduced pressure and concentrated *in vacuo* for 12 hours to reveal a dark red solid at a yield of 32%.

The use of acid-base extraction may account for the relatively low yield attained for this reaction. More specifically, complexities arising due to the partial miscibility of DCM in aqueous solutions in conjunction with the less precise nature of this type of purification may provide hints as to the reason for the disappointing percentage yield.

The identity of the compound was confirmed using mass spectrometry, infrared analysis, ^{1}H NMR, ^{13}C NMR and C-H Correlation NMR spectra.

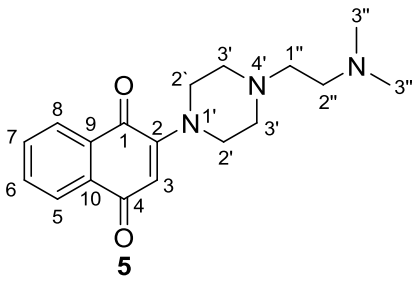

5

Figure 16

High-resolution mass spectrometry gave promising results. A molecular ion ($[M+H]^{+}$) of mass 314.1861 correlated well with the expected isotopic mass of 314.4075 for $C_{18}H_{24}N_3O_2$. The infrared spectrum revealed a weak, C-N stretch occurring at 1306 cm^{-1} which was assigned to the C3′-N stretch and another weak C-N band at 1252 cm^{-1} accounted for the CH_2-N stretch found on the ethylamino side-chain. These wavenumbers are within the expected range for carbon-nitrogen stretches, 1000-1400 cm^{-1}.[32]

The ^{1}H NMR spectrum of compound **5** integrated for the correct number of total protons, 23, found in the structure of the expected product. The distinguishing peaks for the naphthoquinone and

piperazinyl portions of the molecule lie within the same range as those assigned for compound **1** and compound **2**. A highly distinctive singlet arising at a chemical shift of 2.30 ppm and integrating for six hydrogen atoms was indicative of the two homotopic methyl groups, H-3″, and the two aliphatic CH_2 groups corresponded to a multiplet, integrating for four hydrogen atoms, identified at a chemical shift range of 2.60-2.39 ppm. Three signals in the ^{13}C NMR spectrum found at 56.3 ppm, 56.7 ppm and 45.8 ppm were assigned to C-1″, C-2″ and C-3″ respectively. These findings serve to confirm the identity of the expected product and imply that the reaction was a success.

2.2.6 Synthesis of Compound 6 - Reaction Between 1,4-Naphthoquinone and 1-[3-(Dimethylamino)propyl]piperazine

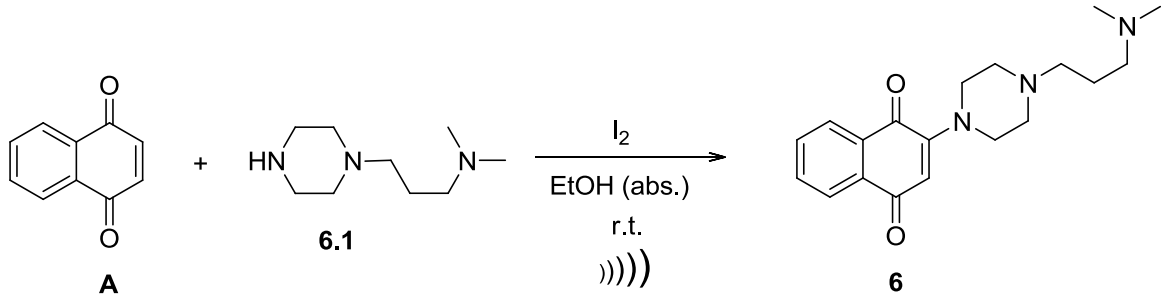

Scheme 19

Compound **6.1**, 1-[3-(dimethylamino)propyl]piperazine, differs structurally from compound **5.1**, 1-[2-(dimethylamino)ethyl]piperazine, by only one CH_2 group in the aliphatic side-chain. It was also found to be sensitive to atmospheric levels of carbon dioxide, therefore, 1,4-naphthoquinone and 1-[3-(dimethylamino)propyl]piperazine were reacted according to the general experimental procedure detailed for compound **5** above and the density of the liquid piperazine was approximated as, 1.000 g/ml**.** Reaction progress was monitored by thin-layer chromatography (eluent: EtOAc), until the disappearance of starting-materials became evident under UV-light at 120 minutes. The crude sample of compound **6** adhered to the absorbent on the TLC plates in the same manner as observed for compound **5**. Consequently, compound **6** was purified by acid-base extraction summarised in **Figure 15** above. Finally, the combined organic portions were dried over anhydrous sodium sulfate, filtered under reduced pressure and concentrated *in vacuo* for 12 hours to reveal a dark red solid at an improved yield of 47%.

The structure of compound **6** was substantiated using mass spectrometry, infrared analysis, ^{1}H NMR, ^{13}C NMR and C-H Correlation NMR spectroscopy.

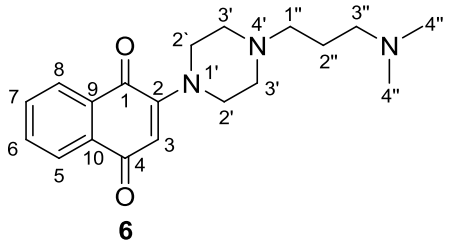

6

Figure 17

The ^{1}H NMR spectrum of compound **6** integrated for the correct number of total protons, 25, found in the structure of the expected product. The distinguishing peaks for the naphthoquinone, piperazinyl and aliphatic sections of the molecule lie within the same range as those assigned for compound **5**. H-1″ and H-3″ are homotopic and were identified as a multiplet, integrating for four hydrogen atoms, found in the chemical shift range, 2.50-2.27 ppm, while H-2″ was assigned to another multiplet, integrating for two protons, occurring further upfield at a chemical shift of 1.70 ppm. The signal for H-4″ coincided perfectly with H-3″ for compound **5**. In the ^{13}C NMR spectrum C-1″ and C-3″ were chemically equivalent and arose at a chemical shift of 56.3 ppm, C-2″ was found at 56.3 ppm and C-4″ was observed at the same chemical shift as C-3″ for compound **5**.

The infrared spectrum for compound **6** was almost identical to the spectrum attained for compound **5**, and revealed no unique substantiating peaks. Furthermore, high-resolution mass spectrometry gave a base-peak (M^{+}) of mass 328.2015 which corresponded with the expected isotopic mass of 328.2025 for $C_{19}H_{25}N_3O_2$.

All in all, the spectroscopic data coincided well the spectroscopic findings for compound **5** and served to verify the structural identity of compound **6**.

2.2.7 Synthesis of Compound 7 - Reaction Between 1,4-Naphthoquinone and 3,3′-Iminobis(N,N-dimethylpropylamine)

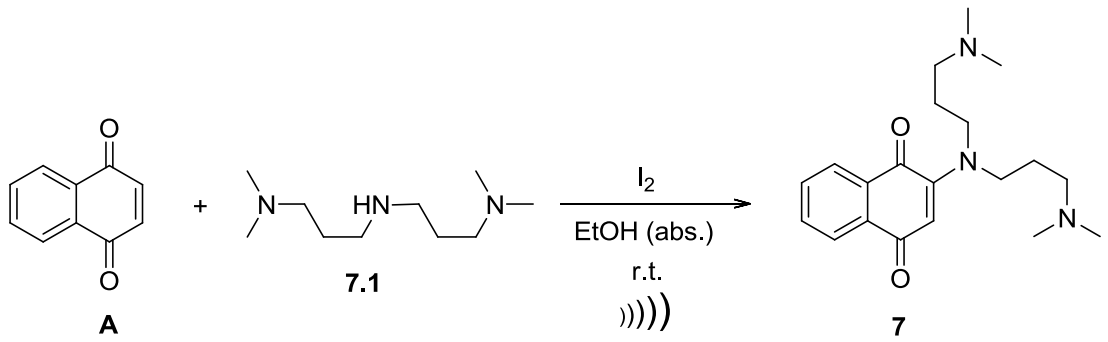

Scheme 20

Compound **7.1,** 3,3′-iminobis(*N*,*N*-dimethylpropylamine)**,** was the only aminonaphthoquinone precursor in the library that was not a substituted piperazine-derivative but rather an aliphatic polyamine. It was found to be stable in the presence of carbon dioxide and as a result 1,4-naphthoquinone and 3,3′-iminobis(*N*,*N*-dimethylpropylamine) were reacted according to the general experimental procedure detailed for compound **1** and **2**. Reaction progress was monitored by thin-layer chromatography (eluent: EtOAc) at ten minute intervals starting from 70 minutes, until the consumption of starting-materials was detected under UV-light at 120 minutes. Purification was achieved using acid-base extraction, outlined in **Figure 15**, due to the compound's strong affinity for the TLC plate absorbent as observed for compound **5** and compound **6** above. After purification, the combined organic portions were dried over anhydrous sodium sulfate, filtered under reduced pressure and concentrated *in vacuo* for 12 hours to reveal a highly viscous, dark-red, oil at a yield of 18%.

The structure of compound **7** was confirmed using mass spectrometry, infrared spectroscopy, ^{1}H NMR, ^{13}C NMR and C-H Correlation 2-D NMR spectroscopy.

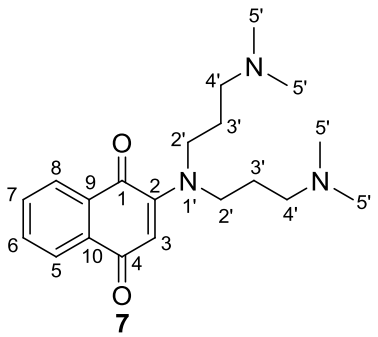

7

Figure 18

Low-resolution mass spectrometry gave a molecular ion ($[M+H]^+$) of mass 344.22 which coincided well with the expected isotopic mass of 344.4771 for $C_{20}H_{30}N_3O_2$. The infrared spectrum revealed two C-N stretches of weak intensity occurring at 1325 cm^{-1} and 1265 cm^{-1} which were characteristic of the vibrations between C-5′ and nitrogen and C-4′ and nitrogen. These bands are representative of the polyamine moiety of the molecule.

The ^1H NMR spectrum revealed two multiplets, integrating for four protons each, found in the chemical shift ranges of 1.88-1.65 ppm and 2.28-2.12 ppm were assigned to H-3′ and H′4 respectively. A distinctive singlet arising at a chemical shift of 2.06 ppm was attributed to H-5′ and a complex multiplet, observed at a chemical shift range of 3.47-3.52 ppm was identified as H-2′. The HSQC (C-H correlated) 2-D NMR spectrum showed that these signals correlate with four carbon signals in the ^{13}C NMR spectrum: 52.7 ppm (C-2′), 25.0 ppm (C-3′), 57.7 ppm (C-4′) and 48.9 ppm (C-5′). The distinguishing peaks for the naphthoquinonyl portion of the molecule lie within the same range as those assigned for compound **5** and compound **6**.

The combined spectroscopic data proved that the reaction was a success and confirmed the structure of the desired compound **7**.

2.2.8 Synthesis of Compound 8 - Reaction Between 1,4-Naphthoquinone and Ethyl 1-piperazinecarboxylate

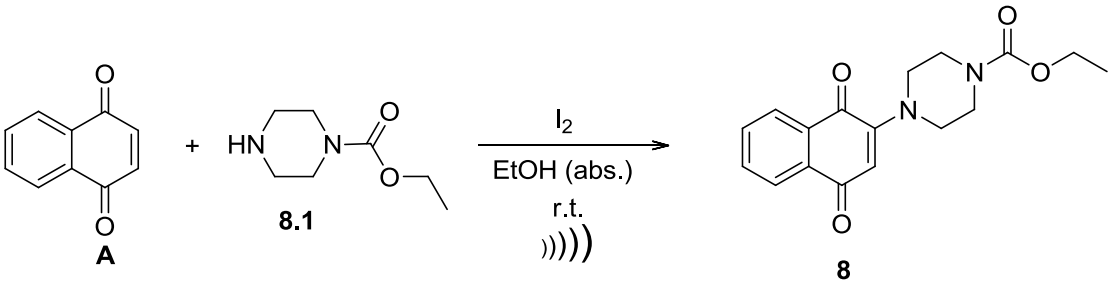

Scheme 21

Following on, 1,4-naphthoquinone and ethyl 1-piperazinecarboxylate were reacted according to the general experimental procedure detailed for compounds **1**-**4** above. Reaction progress was monitored at thirty minute intervals by thin-layer chromatography (eluent: 50% EtOAc: Hexane), until the disappearance of reactants was detected under UV-light at 90 minutes. Purification was achieved using flash column chromatography on silica gel to reveal a bright-orange, lustrous powder, in a yield of 60%, after drying *in vacuo* for twelve hours.

The structure of compound **8** was elucidated using mass spectrometry, infrared spectroscopy, ^{1}H NMR, ^{13}C NMR and C-H Correlation 2-D NMR spectroscopy.

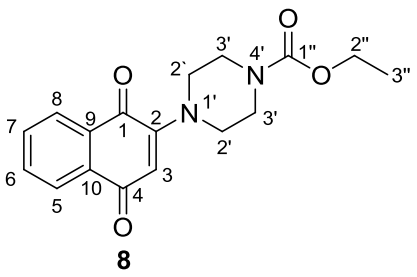

Figure 19

Low-resolution mass spectrometry gave a molecular ion ($[M+H]^+$) of mass 315.07 which corresponded well with the expected isotopic mass of 315.3489 for $C_{17}H_{19}N_2O_4$. In the infrared spectrum, a strong ester-like C=O stretch occurred at 1703 cm^{-1} (*lit.*[32] 1790-1650 cm^{-1}) and two strong intensity stretches found at 1171 cm^{-1} (symmetric) (*lit.*[32] 1260-990 cm^{-1}) and 1207 cm^{-1} (asymmetric) (*lit.*[32] 1310-1000 cm^{-1}) were representative of the ester-like tail of the molecule.

The ^1H NMR spectrum of compound **8** integrated for the correct number of total protons, 18, found in the structure of the expected product and the distinguishing peaks for the naphthoquinonyl and piperazinyl sections of the molecule lie within the same range as those assigned for compounds **1-7**. A quartet, J = 7.1 Hz, integrating for two protons, found at a chemical shift of 4.18 ppm was assigned to H-2″ and a triplet, J = 7.1 Hz, integrating for three protons, arising at a chemical shift of 1.29 ppm was attributed to the terminal methyl group. A signal observed at 155.4 ppm in the ^{13}C NMR spectrum was assigned to the carboxylate carbonyl carbon C-1″. Typically, according to Pretsch *et al.*, the signal should be found in a chemical shift range of 170.3-171.3 ppm, however the significant shielding effect of the proximal nitrogen atom causes the signal to be shifted further upfield in the spectrum. The signals corresponding to C-2″ and C-3″ were found at 61.7 ppm and 14.7 ppm respectively. These spectroscopic findings substantiated that the reaction was a success and served to validate the structure of the desired compound **8**.

2.2.9 Synthesis of Compound 9 - Reaction Between 1,4-Naphthoquinone and 1-Phenylpiperazine

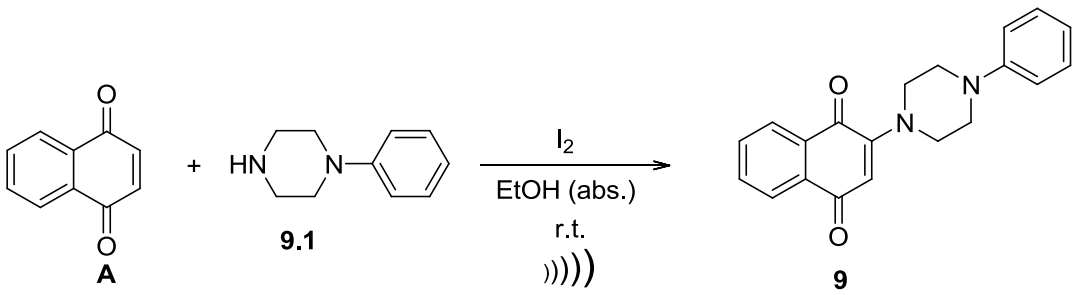

Scheme 22

Subsequently, 1,4-naphthoquinone and 1-phenylpiperazine were reacted according to the general experimental procedure detailed for compounds **1**-**4** above. Reaction progress was monitored at thirty minute intervals by thin-layer chromatography (eluent: 50% EtOAc: Hexane), until the consumption of starting-materials was observed under UV-light at 60 minutes. Purification was achieved using column chromatography on silica gel to reveal a bright-orange powder, at a yield of 68%, after drying *in vacuo* overnight.

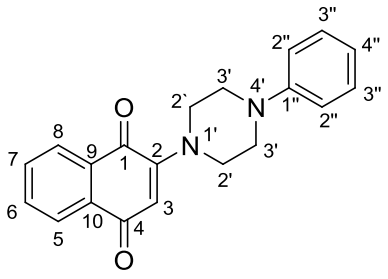

9

Figure 20

The calculated isotopic mass of 318.1369 ($C_{20}H_{18}N_2O_2$) corresponded with the peak of highest mass, 319.07 ($[M+H]^+$) as observed in the low-resolution mass spectrum. Additionally, in the infrared spectrum, a weak intensity, aromatic C-H stretch was observed at 3060 cm^{-1} and a C-C stretch of medium intensity was found at 1494 cm^{-1}. These bands were characteristic of mono-substituted aromatic rings[32] and served to confirm that the piperazinyl aromatic ring was indeed present in the structure of compound **9**.

In the ^1H NMR spectrum of compound **9** the distinguishing peaks for the naphthoquinonyl and piperazinyl sections of the molecule occur in the same chemical shift range as those assigned for compounds **1-8** and the ^1H NMR spectrum integrated for the correct number of total protons, 18, found in the structure of the expected product. A multiplet, integrating for two hydrogen atoms, observed at a chemical shift range of 6.96-6.88 ppm was assigned to H-2″ and H-4″. At first glance, the assertion that H-2″ and H-4″ are chemically equivalent, should stand out as erroneous to the trained eye. However, the HSQC (C-H correlated) 2-D NMR spectrum showed that these ^1H NMR signals correlated with two signals in the ^{13}C NMR, 130.0 (C-2″) and 121.0 (C-4″). On closer

inspection, it appears that the aforementioned multiplet in the ^{1}H NMR spectrum was not, in fact, one signal but two overlapping signals occurring in the same chemical shift range. Another multiplet, integrating for two protons, occurring further downfield at a chemical shift range of, 7.33-7.26 ppm, in the ^{1}H NMR spectrum was attributed to H-3″. The HSQC (C-H correlated) 2-D NMR spectrum revealed that this signal corresponded with a signal at a chemical shift of 113.8 ppm in the ^{13}C NMR spectrum. Lastly, C-1″, a non-hydrogen bearing aromatic carbon atom was identified at a chemical shift of 150.6 ppm. These spectroscopic findings substantiated that the reaction was a success and served to validate the structure of the desired aminonaphthoquinone **9**.

2.2.10 Synthesis of Compound 10 - Reaction Between 1,4-Naphthoquinone and 1-(2-Pyridyl)piperazine

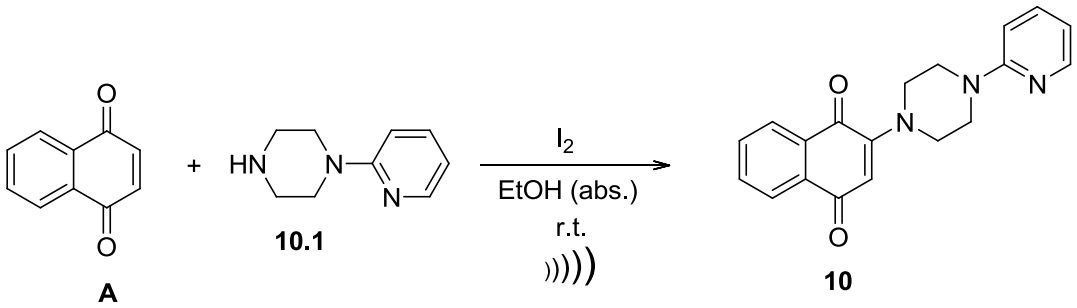

Scheme 23

Thereafter, 1,4-naphthoquinone and 1-(2-pyridyl)piperazine were reacted in accordance with the general experimental procedure detailed for compounds **1-4** and **7-9** above. Reaction progress was monitored at thirty minute intervals by thin-layer chromatography (eluent: 50% EtOAc: Hexane), until the consumption of starting-materials was observed under UV-light at 60 minutes. Purification was achieved using column chromatography on silica gel to reveal a bright-orange powder, at a yield of 70%, after drying *in vacuo* overnight.

Mass spectrometry, infrared spectroscopy, ^{1}H NMR, ^{13}C NMR and C-H Correlation 2-D NMR spectroscopy were used in combination to confirm the relative purity and elucidate the structure of compound **10**.

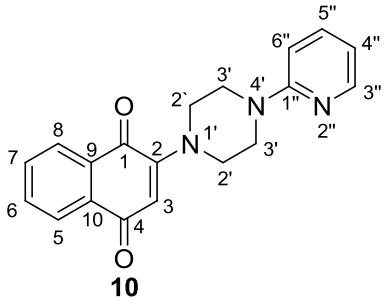

10

Figure 21

The calculated isotopic mass of 319.1447 ($C_{19}H_{17}N_3O_2$) corresponded with the peak of highest mass, 319.1321 (M^+) in the high-resolution mass spectrum. Additionally, a stretch of strong intensity, found at 1307 cm^{-1} was attributed to an aromatic amino C-N stretch and a medium intensity C-C band at 1478 cm^{-1} was characteristic of mono-substituted aromatic rings in the infrared spectrum.

The ^{1}H NMR spectrum of compound **10** showed that the signals corresponding to the 1,4-naphthoquinone and piperazine moieties arose in the same chemical shift range as those assigned for compounds **1-9** and furthermore, the signals integrated for the correct number of total protons, 17, found in the structure of the expected product. A multiplet arising at a chemical shift range of 7.58-7.48 ppm, integrating for one hydrogen atom was assigned to H-5″ and another multiplet arising further upfield at a chemical shift range of 6.75-6.57 ppm, also integrating for two protons, was identified as H-4″ and H-6″. As discussed for compound **9**, the multiplet identified as H-4″ and H-6″ may instead be viewed as an overlapping signal for two chemically unequivalent but closely related protons which corresponded to a pair of different carbon signals, 119.7 ppm (C-6″) and 120.3 ppm (C-4″), in the ^{13}C NMR spectrum. Furthermore a doublet of doublets, J = 4.9 Hz and J = 1.2 Hz, also integrating for one hydrogen atom, observed at a chemical shift of 8.22 ppm was attributed to H-3″. The remaining aromatic ^{13}C NMR signals were recognized as C-3″ (129.3 ppm), C-5″ (137.7 ppm) and C-1″ (150.7 ppm).

The weight of the spectroscopic data served to confirm the identity of the expected compound **10** and revealed that the reaction was a success.

2.2.11 Synthesis of Compound 11 - Reaction Between 1,4-Naphthoquinone and 1-(2-Pyrimidyl)piperazine

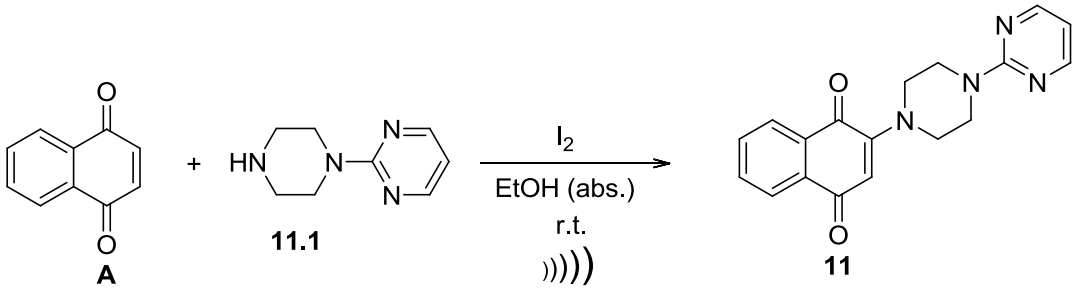

Scheme 24

Lastly, 1,4-naphthoquinone and 1-(2-pyrimidyl)piperazine were reacted in accordance with the general experimental procedure detailed for compounds **1-4** and **7-10** above. Reaction progress was monitored at thirty minute intervals by thin-layer chromatography (eluent: 50% EtOAc: Hexane), until the consumption of starting-materials was observed under UV-light at 60 minutes. Purification was achieved using column chromatography on silica gel to reveal a mustard-yellow powder, at a yield of 50%, after drying *in vacuo* overnight.

The structure of compound **11** was confirmed using mass spectrometry, infrared spectroscopy, ^{1}H NMR, ^{13}C NMR and C-H Correlation 2-D NMR spectroscopy.

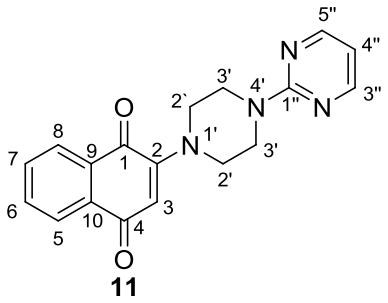

11

Figure 22

In the 1H NMR spectrum, a doublet, J = 4.7 Hz, integrating for two hydrogen atoms arising at a chemical shift of 8.34 ppm corresponded to the two homotopic aromatic protons H-3″ and H-5″ while H-4″ matched a triplet , J = 4.7 Hz, integrating for one proton at a chemical shift of 6.56 ppm. Three pyrimidyl aromatic signals were observed in the ^{13}C NMR spectrum: 111.1 ppm (C-4″), 153.4 ppm (C-3″ and C-5″) and 157.8 ppm (C-1″). Furthermore it was found that the characteristic peaks for the naphthoquinonyl and piperazinyl sections of the molecule were observed at the same chemical shift range as those assigned for compounds **1-10**.

Low-resolution mass spectrometry gave a molecular ion ($[M+H]^+$) of mass 321.14 which corresponded well with the expected isotopic mass of 321.3586 for $C_{18}H_{17}N_4O_2$. In the infrared spectrum a band of strong intensity found at 1307 cm^{-1} was attributed to an aromatic amino C-N stretch and an additional strong-intensity stretch arising at 1495 cm^{-1} was assigned to the C-C vibrations of the mono-substituted aromatic ring.

The spectroscopic data confirmed the identity of the expected compound **11** and the reaction was deemed a success.

2.3 Preliminary Anti-Cancer Testing

Preliminary cytotoxicity screening has been performed against three cancer cell lines and the results were extremely encouraging: these aminonaphthoquinone compounds have been proven to be cytotoxic to three cancer cell lines and some selectivity has been demonstrated, with two of the cell lines being more affected. However, it is important to bear in mind that the compounds must still be tested for cytotoxicity against healthy cells before more specific biochemical experiments can be conducted. Nevertheless, these initial findings suggest that it is worth extending the aminonaphthoquinone library in the future.

CHAPTER 3: CONCLUSIONS AND FUTURE POSSIBILITIES

AMINONAPHTHOQUINONE LIBRARY						
NO.	**STRUCTURE**	**GENERIC PROCEDURE NO.**	**REACTION DURATION (mins.)**	**PURIFICATION TECHNIQUE**	**% YIELD**	**PHOTO/ THERMO SENSITIVITY**
1	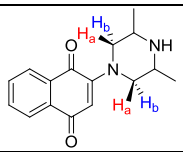	1	120	Column Chromatography	75	-
2	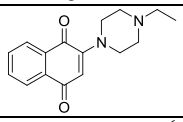	1	90	Column Chromatography	72	-
3	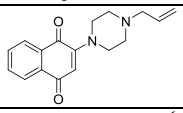	1	90	Column Chromatography	87	Thermo-sensitive >40°C
3′	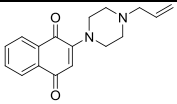	1 *Solvent-free*	90	Flash-Column Chromatography	18	Thermo-sensitive & Photo-sensitive >40°C
4	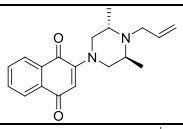	1	100	Flash-Column Chromatography	19	Photo-sensitive
5	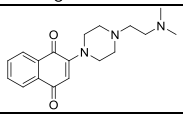	2	120	Acid-Base Extraction	32	-
6	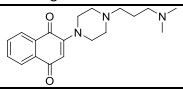	3	120	Acid-Base Extraction	47	-
7	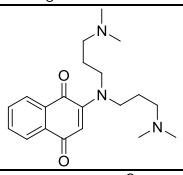	1	120	Acid-Base Extraction	14	-
8	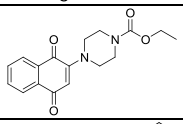	1	60	Flash-Column Chromatography	60	-
9	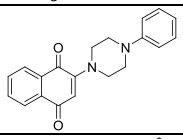	1	60	Column Chromatography	68	-
10	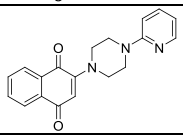	1	60	Column Chromatography	19	-
11	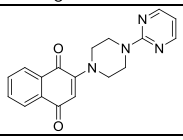	1	60	Column Chromatography	50	-

Table 4: A Table Summarising the Characteristics of the Library of Aminonaphthoquinones

The facile, iodine-catalyzed, ultrasound-accelerated, conjugate addition reaction of amines with 1,4-naphthoquinones, reported by Ji *et al*.[30] of the Suzhou University Organic Chemistry group of China was successfully extended to produce a library of 11 piperazine-based 2-aminonaphthoquinones. As was our aim, the aqueous work-up was simplified through the elimination of the use of aqueous, saturated, sodium hydrosulphite, $Na_2S_2O_4$. Fortunately, it was found that washing with cold tap water was just as effective in removing residual inorganic and unreacted species. Although, the purification technique was not necessarily improved upon, the use of acid-base extraction was utilized for some compounds in the library. Crystallisation proved to be ineffective as a purification method for this project due to extensive decomposition occurring in solution. These 2-aminonaphthoquinone compounds demonstrated long-term stability only after purification and at sub-zero temperatures.

It was our intention to optimize the reaction times quoted in the literature however, the average reaction duration achieved by Ji *et al*.[30] was quoted as 79 mins.[30] while the average reaction time attained in this research project was 99 mins. Further developments to this methodology could potentially involve the use of combined irradiation; the utilization of ultrasound and microwave technology. Additional beneficial effects are anticipated when one considers the extensive thermal energy released during cavitational collapse in combination with dielectic volumetric heating induced by microwave polarisation.[26] Technical complications have meant that this methodological approach has remained largely unexplored for synthetic purposes thus far.[26] However, simultaneous irradiation can be achieved in one reaction vessel through the direct insertion of a ceramic ultrasonic probe into a laboratory microwave oven.[26]

Furthermore, the average reported yield cited by Ji *et al*. was 65% while the average yield achieved in this project was 47%. Possible explanations for this finding include the relative instability of some of the piperazinyl-derivatives in the library and the use of the less precise acid-base extraction as a purification technique for compounds **5-7**.

Owing to the highly facile nature of the reaction keenly observed in TLC analysis and during the addition of starting-materials; starting-materials began to react within a matter of seconds on the

TLC plate and the dry ingredients were observed to change colour and react prior to the addition of solvent, it was decided to attempt a solvent-free reaction of one high-yielding process. Although the solventless attempt was a success synthetically, the yield was extremely low at only 18%. It appeared that the thermal sensitivity of compound **3**, observed in the original reaction, complicated the purification technique and resulted in a lower than expected reaction yield. In spite of the disappointing yield, this first attempt at a solvent-free 2-aminonaphthoquinone synthesis yielded promising results. Future revisions to the procedure could potentially involve the synthesis of less labile products that are proven to be stable during purification. One proposed suggestion was to grind the dry reactants together for ten minutes prior to subjecting the mixture to ultrasonic irradiation. Furthermore, the use of molecular iodine in solvent-free syntheses has been observed to be a highly efficient catalyst as revealed in the overall shortening of reaction duration and increase in reaction yields as reported by Ji *et al*.[36]

In an effort to elucidate the structure of the mysterious blue compound produced during the purification of compound **3** it may be worthwhile to repeat the reaction and remove the solvent at temperatures exceeding 40°C. Once, isolated by flash column chromatography, the blue compound should be stored under argon in an NMR tube, carefully sealed and kept in a laboratory freezer until low-temperature NMR experiments can be conducted.

Compounds **3** and **4** possess terminal alkenyl groups which could potentially be exploited in metathesis reactions as shown in **Figure 23** below.

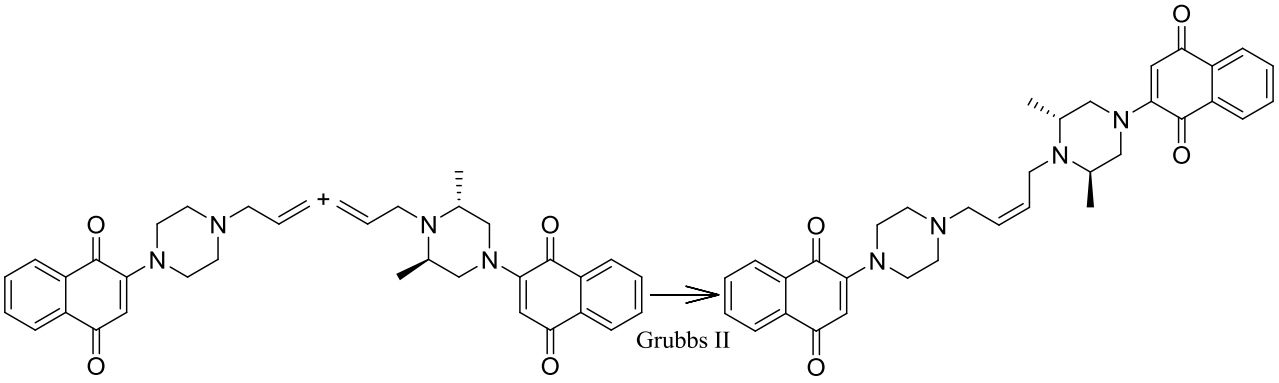

Figure 23

Extensive biological testing of the aminonaphthoquinone library should reveal the presence of any promising lead compounds with anti-cancer or antibiotic properties to pursue as synthetic targets. Ultimately it is our intention to extend the synthetic technique to include the 1,4-Michael addition of alcohols, sulphur-groups, fluorinated species and carbohydrates to the 1,4-naphthoquinone pharmacophore.

CHAPTER 4: EXPERIMENTAL PROCEDURES

4.1 General Experimental Procedures

4.1.1 Purification of Solvents and Reagents

All solvents utilized for preparative chromatography and for reactions occurring under anhydrous or inert conditions were distilled prior to use. Absolute ethanol was distilled from clean, dry magnesium turnings and triethylamine from calcium hydride.

1,4-Naphthoquinone was dissolved in dry benzene and boiled over activated charcoal for approximately 30 minutes. While still hot, the mixture was filtered over compressed celite. The purified solution was reduced in volume under reduced pressure and allowed to recrystallise by slow evaporation. The crystals were then collected by filtration, washed with chilled benzene and dried *in vacuo*. All other reagents were obtained from commercial sources and used without further purification.

4.1.2 Thin-layer Chromatography and Chromatographic Separations

Thin-layer chromatography (TLC) was conducted on Macherey-Nagel Alugram Sil G/UV_{254} plates pre-coated with 0.25 mm silica gel 60. Compounds were detected under ultraviolet light (254 nm or 366 nm) in a Bayer UV-cabinet II (BYL00596) to generate the quoted R_f (retention factor) values. Macherey-Nagel Kieselgel 60 silica gel (particle size 0.063-0.020 mm), with a mass 30 times that of the material to be purified, was used as the absorbent for conventional preparative column chromatography. The desired product was then loaded onto the surface of wet-packed silica and coated with a thin layer of acid-washed sand. Elution was accomplished using solvent-mixtures of EtOAc and hexane or EtOAc, Et_3N and MeOH as the mobile phase.

4.1.3 Physical and Spectroscopic Data

All melting points were obtained on a JK-MAM-4 hot-stage, melting-point apparatus with microscope. Samples were mounted on ground-glass slides and secured with clear glass microscope cover-slips (1.0-1.2mm thickness). The measurement range is from 25°C-320°C, the optic magnification is 10 × (eye lens) and 4 × (objective lens) and the repeatability is quoted as: < 200°C: ± 1°C, 200-300°C: ± 2°C.

^{1}H nuclear magnetic resonance (NMR) spectra were recorded on a Bruker AVANCE 300 (300.13 MHz) or a Bruker 400 (400.13 MHz) spectrometer. Unless otherwise indicated, the NMR spectra were measured in deuterated chloroform (C*D*Cl$_3$) and the chemical shifts were reported in parts per million (ppm) downfield from tetramethylsilane, the internal standard. Coupling constants are given in Hertz. Abbreviations used include: s-singlet, d-doublet, t-triplet, q-quartet and m-multiplet. NMR data are reported as follows: chemical shift (integration of signal, splitting pattern, coupling constant(s), assignment).

^{13}C NMR (^{1}H decoupled) spectra were recorded on a Bruker ADVANCE 300 (75.47 MHz) or Bruker 400 (100.63 MHz) spectrometer. Unless noted to the contrary, spectra were recorded in C*D*Cl$_3$ and chemical shifts were reported in ppm relative to the central signal of C*D*Cl$_3$, taken as δ 77.00.

Infrared Spectra (IR) were recorded on a Bruker TENSOR 2007 IFS-25 Fourier Transform spectrometer. The spectra were then manipulated and analysed using OPUS™ software. Signals were defined as a st-stretch, rock, or δ oop of vw-very weak, w-weak, m-medium or s-strong intensity. IR spectral data are reported as follows: wavenumber (intensity, assignment).

Mass spectra were recorded on a Kratos MS 9/50, VG70EMS or a VG70SEQ mass spectrometer at 70ev and 200μA utilizing **EI** (electron impact), **ESI** (electrospray ionization) or **APCI** (atmospheric pressure chemical ionization) systems.

4.1.4 Other General Procedures

Ultrasound sonication of the various reaction mixtures was achieved by submerging the reaction vessel in an ULTRASONS, P SELECTA® sonicator filled with water.

Evaporation of a solvent under reduced pressure refers to the removal of a solvent on a rotary evaporator at approximately 45°C.

Evaporation of a solvent *in vacuo* refers to the removal of a solvent on a rotary evaporator at approximately 45°C followed by further evaporation under high-vacuum.

Evaporation of a solvent under high vacuum refers to the removal of a solvent under high-vacuum exclusively.

4.2 Generic Experimental Procedures

4.2.1 Generic Experimental Procedure 1 – The synthesis of compounds 1-4 and 7-11

A mixture of piperazine, 1,4-naphthoquinone (0.079 g, 0.50 mmoles), a catalytic amount of I_2 (0.0012 g, 0.50 mmoles, 10 mol%) and EtOH (abs.) (2.0 cm^3) was sonicated under high-power ultrasound at ambient temperature in a round-bottomed flask open to the atmosphere. The reaction was monitored by thin-layer chromatography until the disappearance of starting materials was noted under UV-light. The crude product was evaporated under reduced pressure and the resulting residue was washed with tap water (*c.a.* 50 cm^3) and extracted with dichloromethane (3 × 50 cm^3). The combined organic layers were dried over anhydrous Na_2SO_4, filtered under water pressure and concentrated *in vacuo*. The crude product was then purified by column chromatography on silica gel.

4.2.2 Generic Experimental Procedure 2 - The synthesis of compounds 5 & 6

All glassware, including vacuum attachments, was thoroughly dried overnight in a laboratory oven, followed by further flame-drying *in vacuo*. The 2-necked, round-bottomed flask was flooded with argon and the dried starting materials; 1,4-naphthoquinone (0.079 g, 0.50 mmoles) and molecular iodine (0.0012 g, 0.50 mmoles, 10 mol%) were swiftly added. The reaction vessel was then evacuated *in vacuo*, followed by flooding with argon for a second time. 1-[2-(Dimethylamino)ethyl]piperazine (0.079 cm^3 *c.a.*, 78 mg, 0.50 mmoles, 1.0 equiv.) was then injected through a septum into the flask, while argon was bubbled through a Pasteur pipette into the sample bottle containing the piperazine. Lastly, EtOH (abs.) (2.00 cm^3), distilled over oven-dried Mg turnings, was injected through the septum into the round-bottomed flask. The resulting reaction mixture was next irradiated under high-power ultrasound for 120 mins, followed by the removal of solvent under reduced pressure. The crude product was then purified by acid/base extraction, and finally, the residue was suspended between CH_2Cl_2 (60 cm^3) and tap water (60 cm^3) in a separating funnel. Any remaining α-naphthoquinone, along with the desired product was found in the organic

layer. Repeated washings with tap water (4 × 60 cm^3) ensured that unreacted piperazine was removed. The CH_2Cl_2 solution was then acidified with 1 M HCl (pH=4 *c.a.*). The salt of the desired product should now be dissolved in the acidic layer while unreacted α-naphthoquinone remains dissolved in CH_2Cl_2. NaOH (1 M) was then added in a drop-wise manner to the aqueous acidic fraction, until the pH was 11 units. This releases the compound from the hydrochloride salt, which was then extracted with CH_2Cl_2 (3 × 20 cm^3), dried over anhydrous Na_2SO_4 and concentrated *in vacuo* for 12 hours.

4.3 Experimental Data

4.3.1 Synthesis of 2-(3,5-dimethylpiperazin-1-yl)-1,4-naphthoquinone – compound 1

Quantity of 2,6-Dimethylpiperazine	(57 mg, 0.50 mmoles, 1.0 equiv.)
Generic Experimental Procedure	1
Reaction Duration	120 mins
Solvent System used for Column Chromatography	1% triethylamine: 20% methanol

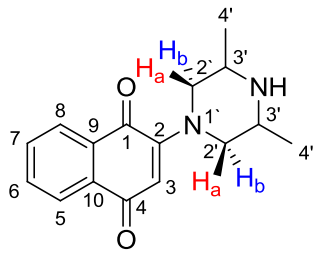

A brilliant red powder of the pure product was obtained according to generic experimental procedure **1** (101.4 mg, 75%, $C_{16}H_{18}N_2O_2$, 270.33 $g.mol^{-1}$); **mp** 48°C; $\mathbf{R}_f$ = 0.25 (EtOAc: 1% Et_3N: 20% MeOH); **IR** : ν_{max} (cm^{-1}) = 2923 (m, st, N-H), 2853 (w, st, C-H, piperazine ring (PR)), 1675 (m, st, C=O), 1560 (s, st, C-C, NQ), 1246 (m, st, as, C-N, PR), 1123 (w, st, as, C-C, PR), 1011 (w, st, C-C, NH-**C**H-**C**H_3), 779 (m, ar C-H δ oop), 727 (m, C-H rock, PR); **HRMS *m/z* (EI)** Found M^+, 270.13531. (M^+ 100%, $C_{16}H_{18}N_2O_2$ requires 270.13694); 269 (54), 268 (6), 271 (20), 272 (4), 274 (6), 275 (2); **LRMS *m/z* (EI)** Found M^+, 270. (M^+ 80%), 255 (4), 241 (18), 213 (8), 200 (100), 185 (42), 172 (8), 158 (30), 129 (12), 102 (28), 92 (36), 84 (42), 70 (64); **^{1}H NMR** δ_H (300 MHz, DMSO) 7.88 (2 H, bs, H-6 and H-7), 7.83 – 7.59 (2 H, m, H-5 and H-8), 5.99 (1 H, s, H-3), 3.88 (2 H, d, *J* 12.2 Hz, H-2′a), 2.84 (2 H, bs, H-3′), 2.47 (2 H, d, *J* 12.0 Hz, H-

2′b), 0.98 (6 H, d, *J* 5.7 Hz, H-4′); **^{13}C NMR** 182.8 (C-4), 182.0 (C-1), 153.4 (C-2), 133.9 (C-6 and C-7), 132.7 (C-10), 132.5 (C-9), 126.4 (C-5 and C-8), 109.0 (C-3), 55.0 (C-2′), 50.1 (C-3′), 18.9 (C-4′).

4.3.2 Synthesis of 2-(4-ethylpiperazin-1-yl)-1,4-naphthoquinone – compound 2

Quantity of 1-Ethylpiperazine	(0.064 cm^3, 57 mg, 0.50 mmoles, 1.0 equiv.)
Generic Experimental Procedure	1
Reaction Duration	90 mins
Solvent System used for Column Chromatography	93% ethyl acetate: 6% methanol: 1% triethylamine

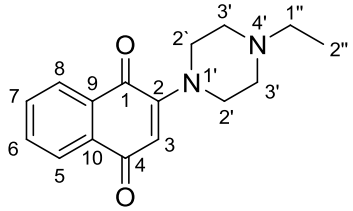

An ochre-orange powder of the pure product was attained according to generic experimental procedure **1** (97 mg, 72%, $C_{16}H_{18}N_2O_2$, 270.33 $g.mol^{-1}$); **mp** 100°C; $\mathbf{R}_f$ = 0.17 (93% EtOAc: 1% Et_3N: 6% MeOH); **IR** : ν_{max} (cm^{-1}) = 2818 (w, st, C-H, PR), 1672 (m, st, C=O), 1562 (s, st, C-C, NQ), 1240 (s, st, as, C-N), 1124 (m, st, as, C-C, PR), 983 (s, st, C-N, NQ-PR), 775 (s, ar C-H δ oop), 726 (s, C-H rock, PR); **HRMS *m/z* (EI)** Found M^+, 270.1323. (M^+ 100%, $C_{16}H_{18}N_2O_2$ requires 270.1369); **LRMS *m/z* (EI)** Found M^+, 270.02. (M^+ 100%), 255 (10), 227 (4), 213 (28), 185 (8), 158 (14), 115 (8), 102 (18), 85 (26), 84 (100), 71 (34), 64 (57); **^{1}H NMR** δ_H (300 MHz, $CDCl_3$) 8.22 – 7.87 (2 H, m, H-6 and H-7), 7.79 – 7.45 (2 H, m, H-5 and H-8), 6.03 (1 H, s, H-3), 3.55 (4 H, t, *J* 6.0 Hz, H-2′), 2.62 (4 H, t, *J* 4.5 Hz, H-3′), 2.48 (2 H, q, *J* 7.2 Hz, H-1″), 1.12 (3 H, t, *J* 7.2 Hz, H-2″); **^{13}C NMR** 183.6 (C-4), 183.1 (C-1), 153.7 (C-2), 133.8 (C-6 and C-7), 132.8 (C-10), 132.4 (C-9), 126.6 (C-5 and C-8), 111.63 (C-3), 52.2 (C-1″), 52.3 (C-3′), 48.9 (C-2′), 11.9 (C-2″).

4.3.3 Synthesis of 2-(4-allylpiperazin-1-yl)-1,4-naphthoquinone – compound 3

Quantity of 1-Allylpiperazine	(0.070 cm^3, 63 mg, 0.50 mmoles, 1.0 equiv.)
Generic Experimental Procedure	1
Reaction Duration	90 mins
Solvent System used for Column Chromatography	93% EtOAc: 6% MeOH: 1% Et_3N

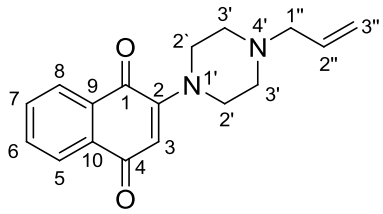

A bright orange powder of the pure product, that rapidly decomposes to a dark russet-brown solid at temperatures exceeding 45°C, was produced in accordance with generic experimental procedure **1** (0.1226 g, 87%, $C_{17}H_{18}N_2O_2$, 282.34 $g.mol^{-1}$); **mp** 78°C; $\mathbf{R}_f$ = 0.32 (93% EtOAc: 1% Et_3N: 6% MeOH); **IR** : ν_{max} (cm^{-1}) = 2796 (w, st, C-H, PR), 1671 (m, st, C=O), 1634 (s, st, $CH=CH_2$), 1558 (s, st, C-C, NQ), 1301 (s, st, $(CH_2)_2N$-CH_2), 1207 (s, st, as, C-N), 1122 (m, st, as, C-C, PR), 978 (s, st, C-N, NQ-PR), 777 (s, ar C-H δ oop), 724 (s, C-H rock, PR); **HRMS *m/z* (ESI)** Found $[M+H]^+$, 283.1433. ($[M+H]^+$ 100%, $C_{17}H_{19}N_2O_2$ requires 283.3501); **LRMS *m/z* (ESI)** Found $[M+H]^+$, 283.07. ($[M+H]^+$ 100%, $C_{17}H_{19}N_2O_2$ requires 283.1433), 200 (8); **LRMS *m/z* (APCI)** Found $[M+H]^+$, 283.12. ($[M+H]^+$ 100%, $C_{17}H_{19}N_2O_2$ requires 283.3501), 281 (8), 284 (18), 285 (2), Found $[(M+H)+(M+H)]^+$, 566.87. ($[(M+H)+(M+H)]^+$ 18%, $C_{34}H_{38}N_4O_4$ (dimer) requires 566.7001), 562 (2), 565 (74), 567 (4); **^{1}H NMR** δ_H (300 MHz, $CDCl_3$) 8.14 – 7.85 (2 H, m, H-6 and H-7), 7.78 – 7.54 (2 H, m, H-5 and H-8), 6.03 (1 H, s, H-3), 5.87 (1 H, ddt, *J* 16.8 and 10.1 and 6.6 Hz, H-2″), 5.34 – 5.09 (2 H, m, H-3″), 3.54 (4 H, t, *J* 6.0 Hz, H-3′), 3.06 (2 H, d, *J* 6.6, H-1″), 2.62 (4 H, t, *J* 6.0 Hz, H-2′); **^{13}C NMR** 183.6 (C-4), 183.1 (C-1), 153.8 (C-2), 134.4 (C-2″), 133.8 (C-6 and C-7), 132.8 (C-10), 132.4 (C-9), 126.6 (C-5 and C-8), 118.5 (C-3″), 111.7 (C-3), 61.5 (C-1″), 52.5 (C-2′), 48.9 (C-3′).

4.3.4 Synthesis of 2-(4-allylpiperazin-1-yl)naphthoquinone under solvent-free conditions – compound 3

Quantity of 1-Allylpiperazine	(0.070 cm^3, 63 mg, 0.50 mmoles, 1.0 equiv.)
Generic Experimental Procedure	1 (not including EtOH (abs.))
Reaction Duration	90 mins
Solvent System used for Column Chromatography	30% ethyl acetate: hexane

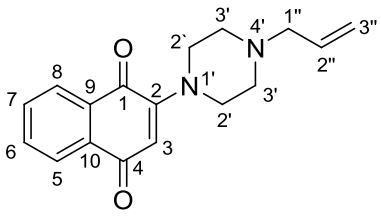

A bright red semi-solid of the pure product was obtained according to generic experimental procedure **1** performed in the absence of solvent (25.30 mg, 18%, $C_{17}H_{18}N_2O_2$, 282.34 $g.mol^{-1}$); **mp** 78°C; $\mathbf{R}_f$ = 0.47 (30% ethyl acetate-hexane); **^{1}H NMR** δ_H (300 MHz, $CDCl_3$) 8.15 – 7.90 (2 H, m, H-6 and H-7), 7.77 – 7.52 (2 H, m, H-5 and H-8), 6.02 (1 H, s, H-3), 5.97 – 5.66 (1 H, m, H-2″), 5.36 – 5.09 (2 H, m, H-3″), 3.53 (4 H, dd, *J* 14.3 and 9.2 Hz, H-3′), 3.06 (2 H, d, *J* 6.6 Hz, H-1″), 2.62 (4 H, t, *J* 6.0 Hz, H-2′); **^{13}C NMR** 183.7 (C-4), 183.1 (C-1), 153.8 (C-2), 134.4 (C-2″), 133.9 (C-6 and C-7), 132.8 (C-10), 132.4 (C-9), 126.7 (C-5 and C-8), 118.6 (C-3″), 111.7 (C-3), 61.5 (C-1″), 52.5 (C-2′), 48.9 (C-3′).

4.3.5 Synthesis of rac-2-[(2S,5R)-4-allyl-2,5-dimethylpiperazin-1-y]-1,4-naphthoquinone – compound 4

Quantity of trans-1-Allyl-2,5-dimethylpiperazine (racemic)	(0.085 cm^3, 77 mg, 0.50 mmoles, 1.0 equiv.)
Generic Experimental Procedure	1
Reaction Duration	100 mins
Solvent System used for Column Chromatography	30% ethyl acetate: hexane (flash column chromatography)

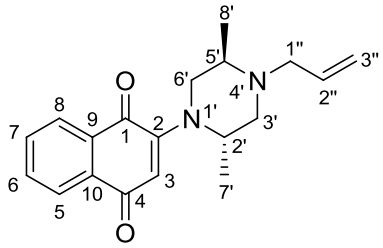

A bright red, viscous oil of the expected product was obtained according to generic experimental procedure **1** (30.1 mg, 19%, $C_{19}H_{22}N_2O_2$, 310.39 g.mol^{-1}); $\mathbf{R}_f$ = 0.13 (30% ethyl acetate: hexane); **IR** : ν_{max} (cm^{-1}) = 2816 (w, st, C-H, PR), 1672 (m, st, C=O), 1627 (s, st, CH=CH_2), 1551 (s, st, C-C, NQ), 1298 (s, st, $(CH)_2N$-CH_2), 1214 (w, st, as, C-N), 1169 (w, st, $CH(CH_3)$), 1124 (m, st, as, C-C, PR), 998 (s, st, C-N, NQ-PR), 776 (s, ar C-H δ oop), 722 (s, C-H rock, PR); **LRMS *m/z* (APCI)** Found $[M+H]^+$, 311.22. ($[M+H]^+$ 100%, $C_{19}H_{23}N_2O_2$ requires 311.4038), 312 (20), Found $[(M+M)]^+$, 620.61. ($[(M+M)]^+$ 10%, $C_{38}H_{44}N_4O_4$ (dimer) requires 620.7918), 622 (2); **^{1}H NMR** δ_H (300 MHz, $CDCl_3$) 8.21 – 7.87 (2 H, m, H-6 and H-7), 7.77 – 7.52 (2 H, m, H-5 and H-8), 6.01 (1 H, s, H-3), 5.83 (1 H, ddt, *J* 16.5 and 10.1 and 6.3 Hz, H-2″), 5.31 – 5.01 (2 H, m, H-3″), 3.83 (1 H, d, *J* 12.8 Hz, H-2.1′a), 3.53 (1 H, dd, *J* 12.9 and 3.5 Hz, H-2.1′b), 3.12 (2 H, dd, *J* 13.6 and 6.0 Hz, H-3′ and H-4′), 3.02 (1 H, dd, *J* 13.7 and 6.5 Hz, H-1″), 2.85 (1 H, dd, *J* 11.9 and 4.1 Hz, H-2.2′a), 2.43 (1 H, dd, *J* 11.9 and 2.4 Hz, H-2.2′b), 1.38 (3 H, d, *J* 6.7 Hz, H-5′ or H-6′), 1.08 (3 H, d, *J* 6.6 Hz, H-5′ or H-6′); **^{13}C NMR** 183.5 (C-4), 183.4 (C-1), 153.9 (C-2), 135.7 (C-2″), 133.7 (C-6 and C-7), 132.5 (C-10), 132.2 (C-9), 126.6 (C-5 and C-8), 117.3 (C-3″), 110.2 (C-3), 57.5 (C-3′ and C-4′), 53.2 (C-1″), 49.8 (C-2.2′), 49.1 (C-2.1′), 15.02 (C-5′ or C-6′), 8.8 (C-5′ or C-6′).

4.3.6 Synthesis of 2-{4-[2-(dimethylamino)ethyl]piperazin-1-yl}-1,4-naphthoquinone – compound 5

Quantity of 1-[2-(dimethylamino)ethyl]piperazine	(0.079 cm^3, 79 mg, 0.50 mmoles, 1.0 equiv.)
Generic Experimental Procedure	2
Reaction Duration	120 mins

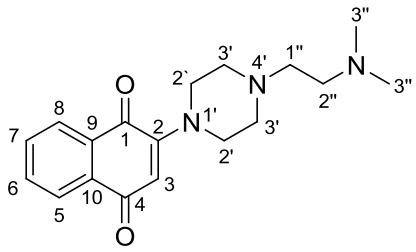

A dark red solid of the pure product was obtained according to generic experimental procedure **2** (50.1 mg, 32%, $C_{18}H_{23}N_3O_2$, 313.39 g.mol^{-1}); **mp** 93°C; $\mathbf{R}_f$ = 0.00 (compound adheres to the silica gel on the TLC plate) (EtOAc: 1% Et_3N: 5% MeOH) or

(MeOH: 1% Et_3N) or (50% EtOAc: Hexane) or (EtOAc: 1% Et3N); **IR** : ν_{max} (cm^{-1}) = 2750 (w, st, CH_2-N), 2800 (w, st, C-H, PR), 1665 (m, st, C=O), 1559 (s, st, C-C, NQ), 1306 (w, st, $(CH_3)_2$-N-CH_2R), 1252 (w, st, C-N, RCH_2-N$(CH_3)_2$), 1203 (s, st, as, C-N), 1120 (s, st, as, C-C, PR), 984 (s, st, C-N, NQ-PR), 780 (s, ar C-H δ oop), 724 (s, C-H rock, PR); **HRMS *m/z* (EI)** Found $[M+H]^+$, 314.1861. ($[M+H]^+$ 100%, $C_{18}H_{24}N_3O_2$ requires 314.4075), 330 (20), 282 (6), 269 (6); **LRMS *m/z* (ESI)** Found $[M+H]^+$, 314.07. ($[M+H]^+$ 54%, $C_{18}H_{24}N_3O_2$ requires 314.4075), 241 (6), 269 (100), 330 (25), 346 (2); **LRMS *m/z* (APCI)** Found $[M+H]^+$, 314.22. ($[M+H]^+$ 100%), 312 (1), 315 (20), 328 (4); **^{1}H NMR** δ_H (300 MHz, $CDCl_3$) 8.16 – 7.88 (2 H, m, H-6 and H-7), 7.78 – 7.52 (2 H, m, H-5 and H-8), 6.02 (1 H, s, H-3), 3.71 – 3.44 (5 H, m, H-2′), 2.64 (4 H, dd, *J* 14.3 and 9.7 Hz, H-3′), 2.60 – 2.39 (4 H, m, H-1″ and H-2″), 2.30 (6 H, s, H-3″); **^{13}C NMR** 183.6 (C-4), 183.1 (C-1), 153.7 (C-2), 133.8 (C-6 and C-7), 132.7 (C-10), 132.4 (C-9), 126.6 (C-5 and C-8), 111.6 (C-3), 56.3 (C-1″), 56.7 (C-2″), 53.1 (C-3′), 48.8 (C-2′), 45.8 (C-3″).

4.3.7 Synthesis of 2-{4-[3-(dimethylamino)propyl]piperazin-1-yl}-1,4-naphthoquinone – compound 6

Quantity of 1-[3-(Dimethylamino)propyl]piperazine	(0.086 cm^3 *c.a.*, 86 mg, 0.50 mmoles, 1.0 equiv.)
Generic Experimental Procedure	2
Reaction Duration	120 mins

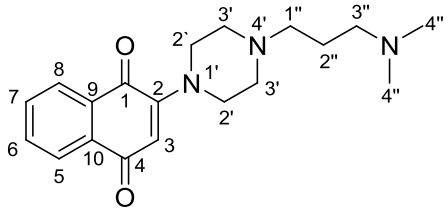

A maroon, amorphous solid of the pure product was obtained in accordance with generic experimental procedure **2** (77.1 mg, 47%, $C_{19}H_{25}N_3O_2$, 327.42 $g.mol^{-1}$); **mp** 87°C; $\mathbf{R}_f$ = 0.00 (compound adheres to the silica gel on the TLC plate) Developing solvents tested: (pure EtOAc) or (pure MeOH) or (EtOAc: 1% Et_3N: 5% MeOH) or (MeOH: 1% Et_3N) or (50% EtOAc: Hexane) or (EtOAc: 1% Et3N); **IR** : ν_{max} (cm^{-1}) = 2830 (w, st, C-H, PR), 2750 (vw, st, CH_2-N), 1668 (s, st, C=O), 1557 (s, st, C-C, NQ), 1306 (w, st, $(CH_3)_2$-**N-CH_2**), 1242 (s, st, C-N, **CH_2-N**$(CH_3)_2$), 1215 (w, st, as, C-N), 1123 (s, st, as, C-C, PR), 982 (s, st, C-N, NQ-PR), 785 (s, ar C-H δ oop), 729 (s, C-H rock, PR); **HRMS *m/z* (EI)** Found M^+, 328.2015. (M^+ 100%, $C_{19}H_{25}N_3O_2$ requires 328.2025); **LRMS *m/z* (ESI)** Found M^+, 328.13. (M^+ 100%,

$C_{19}H_{25}N_3O_2$ requires 328.2025), 149 (4), 344 (2), 255 (38), 283 (72); **LRMS *m/z* (APCI)** Found M^+, 328.24. (M^+ 100%), 329 (20), 330 (4); **^{1}H NMR** δ_H (300 MHz, $CDCl_3$) 8.13 – 7.90 (2 H, m, H-6 and H-7), 7.77 – 7.55 (2 H, m, H-5 and H-8), 6.02 (1 H, s, H-3), 3.56 (4 H, t, *J* 4.5 Hz, H-2′), 2.66 – 2.53 (4 H, m, H-3′), 2.50 – 2.27 (4 H, m, H-1″ and H-3″), 2.27 (6 H, s, H-4″), 1.70 (2H, m, H-2″); **^{13}C NMR** 183.2 (C-4), 182.7 (C-1), 152.7 (C-2), 133.4 (C-6 and C-7), 132.7 (C-10), 131.7 (C-9), 126.1 (C-5 and C-8), 105.9 (C-3), 56.3 (C-1″ and C-3″), 50.0 (C-2′ and C-3′), 45.1 (C-4″) 25.2 (C-2″).

4.3.8 Synthesis of 2-{bis[3-(dimethylamino)propyl]amino}-1,4-naphthoquinone – compound 7

Quantity of 3,3′-Iminobis(N,N-dimethylpropylamine)	(0.114 cm^3, 93.7 mg, 0.50 mmoles, 1.0 equiv.)
Generic Experimental Procedure	1
Reaction Duration	120 mins

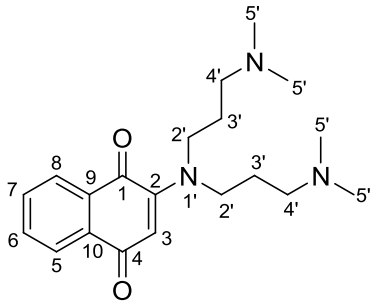

A highly viscous, crimson coloured oil of the pure product was obtained in accordance with generic experimental procedure **2** (30.0 mg, 14%, $C_{20}H_{29}N_3O_2$, 343.47 $g.mol^{-1}$); $\mathbf{R}_f$ = 0.00 (compound adheres to the silica gel on the TLC plate) Developing solvents tested: (pure EtOAc) or (pure MeOH) or (EtOAc: 1% Et_3N: 5% MeOH) or (MeOH: 1% Et_3N) or (50% EtOAc: Hexane) or (EtOAc: 1% Et3N); **IR** : ν_{max} (cm^{-1}) = 2942 (w, st, C-H, alkanes), 2750 (vw, st, CH_2-N), 1672 (w, st, C=O), 1622 (m, st, C=O), 1553 (s, st, C-C, NQ), 1461 (w, st, C-C, Ar), 1325 (w, st, $(CH_3)_2$-**N-CH$_2$**), 1265 (w, st, C-N, **CH$_2$-N**$(CH_3)_2$), 1216 (w, st, as, C-N), 1119 (s, st, as, C-C, aliphatic), 998 (s, st, C-N, NQ-N), 820 (s, ar C-H δ oop); **LRMS *m/z* (APCI)** Found $[M+H]^+$, 344.48. ($[M+H]^+$ 100%, $C_{20}H_{30}N_3O_2$ requires 342.4771), 383 (2), 382 (10), 380 (4), 346 (2), 297 (1), 260 (4), 259 (26), 319 (54); **^{1}H NMR** δ_H (300 MHz, $CDCl_3$) 7.98 (1 H, d, *J* 9.0 Hz, H-6), 7.86 (1 H, d, *J* 7.5 Hz, H-7), 7.70 – 7.40 (2 H, m, H-5 and H-8), 5.78 (1 H, s, H-3), 3.47 (4 H, m, H-2′), 2.28 – 2.12 (4 H, m, H-4′), 2.06 (12 H, s, H-5′), 1.88 – 1.65 (4 H, m, H-3′); **^{13}C NMR** 183.1 (C-4), 183.6 (C-1), 153.7 (C-2), 133.8 (C-6 and C-

7), 132.8 (C-10), 132.4 (C-9), 126.6 (C-5 and C-8), 111.5 (C-3), 57.7 (C-4′), 52.7 (C-2′), 48.9 (C-5′), 25.0 (C-3′).

4.3.9 Synthesis of ethyl 4-(1,4-dioxo-1,4-dihydronaphthalen-2-yl)piperazine-1-carboxylate – compound 8

Quantity of Ethyl 1-piperazinecarboxylate	(0.073 cm^3, 79.1 mg, 0.50 mmoles, 1.0 equiv.)
Generic Experimental Procedure	1
Reaction Duration	60 mins
Solvent System used for Column Chromatography	50% ethyl acetate: hexane (flash column chromatography)

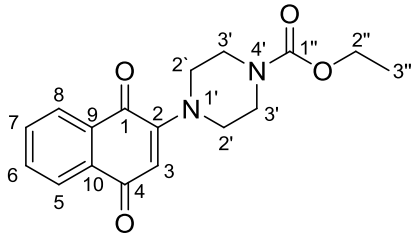

A bright orange, lustrous powder of the expected product was produced in accordance with generic experimental procedure **1** (95.9 mg, 60%, $C_{17}H_{18}N_2O_4$, 314.34 $g.mol^{-1}$); **mp** =160-162°C; $\mathbf{R}_f$ = 0.45 (50% ethyl acetate: hexane); **IR** : ν_{max} (cm^{-1}) = 3037 (w, st, C-H, NQ), 2750 (vw, st, CH_2-N), 1703 (s, st, C=O, ester), 1671 & 1626 (s, st, C=O), 1563 (s, st, C-C, NQ), 1234 (s, st, as, C-N), 1207 (s, st, as, CO-O), 1171 (s, st, sy, O-C-C), 1111 (s, st, as, C-C, PR), 983 (s, st, C-N, NQ-PR), 783 (s, ar C-H δ oop), 726 (s, C-H rock, PR); **LRMS *m/z* (ESI)** Found $[M+H]^+$, 315.07. ($[M+H]^+$ 100%, $C_{17}H_{19}N_2O_4$ requires 315.3489), 380 (14), 356 (2), 340 (4), 241 (26), 200 (4), 186 (4); **LRMS *m/z* (APCI)** Found $[M+H]^+$, 315.16. ($[M+H]^+$ 100%), 317 (2), 316 (18), 313 (6); **^{1}H NMR** δ_H (300 MHz, $CDCl_3$) 8.15 – 7.89 (2 H, m, H-6 and H-7), 7.84 – 7.55 (2 H, m, H-5 and H-8), 6.02 (1 H, s, H-3), 4.18 (2 H, q, *J* 7.1 Hz, H-2″), 3.85 – 3.58 (4 H, m, H-2′), 3.60 – 3.39 (4 H, m, H-3′), 1.29 (3 H, t, *J* 7.1 Hz, H-3″); **^{13}C NMR** 183.6 (C-4), 182.9 (C-1), 155.4 (C-1″), 153.4 (C-2), 134.0 (C-6 and C-7), 132.6 (C-10), 132.2 (C-9), 126.7 (C-5 and C-8), 112.0 (C-3), 61.7 (C-2″), 48.5 (C-2′), 43.1 (C-3′), 14.7 (C-3″).

4.3.10 Synthesis of 2-(4-phenylpiperazin-1-yl)-1,4-naphthoquinone – compound 9

Quantity of 1-Phenylpiperazine	(0.076 cm^3, 81 mg, 0.50 mmoles, 1.0 equiv.)
Generic Experimental Procedure	1
Reaction Duration	60 mins
Solvent System used for Column Chromatography	50% ethyl acetate: hexane

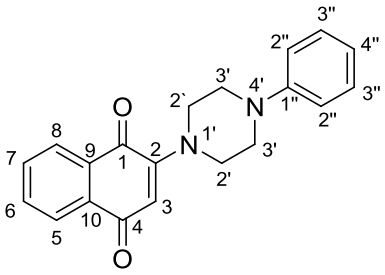

A bright orange powder of the pure product was obtained in accordance with generic experimental procedure **1** (107.8 mg, 68%, $C_{20}H_{18}N_2O_2$, 318.14 $g.mol^{-1}$); **mp** =161-164°C; $\mathbf{R}_f$ = 0.7 (50% ethyl acetate: hexane); **IR** : ν_{max} (cm^{-1}) = 3060 (vw, st, ar C-H, mono-substituted ar ring), 2831 (w, st, C-H, PR), 1667 (m, st, C=O), 1562 (s, st, C-C, NQ), 1494 (m, st, C-C, mono-substituted ar ring), 1228 (s, st, as, C-N, PR), 1206 (s, st, sy, C-N, PR), 984 (s, st, C-N, NQ-PR), 782 (s, ar C-H δ oop), 725 (s, C-H rock, PR); **LRMS *m/z* (ESI)** Found $[M+H]^+$, 319.07. ($[M+H]^+$ 100%, $C_{20}H_{19}N_2O_2$ requires 319.3831), 200 (12), 140 (8); **LRMS *m/z* (APCI)** Found $[M+H]^+$, 319.18. ($[M+H]^+$ 100%), 321 (2), 320 (20); **^{1}H NMR** δ_H (300 MHz, $CDCl_3$) 8.06 – 7.97 (2 H, m, H-6 and H-7), 7.73 – 7.62 (2 H, m, H-5 and H-8), 7.33 – 7.26 (2 H, m, H-3″), 6.96 – 6.88 (3 H, m, H-2″ and H-4″), 6.07 (1 H, s, H-3), 3.74 – 3.68 (2 H, m, H-3′), 3.39 – 3.35 (2 H, m, H-2′); **^{13}C NMR** 183.6 (C-4), 183.1 (C-1), 153.4 (C-2), 150.6 (C-1″), 134.1 (C-7), 133.9 (C-5 and C-6), 132.7 (C-10), 132.5 (C-9), 130.0 (C-2″), 125.6 (C-8), 121.0 (C-4″), 113.8 (C-3″), 111.0 (C-3), 48.8 (C-3′), 48.8 (C-2′).

4.3.11 Synthesis of 2-(4-pyridin-2-ylpiperazin-1-yl)-1,4-naphthoquinone – compound 10

Quantity of 1-(2-Pyridyl)Piperazine	(0.076 cm^3, 82 mg, 0.50 mmoles, 1.0 equiv.)
Generic Experimental Procedure	1
Reaction Duration	60 mins
Solvent System used for Column Chromatography	30% ethyl acetate: hexane

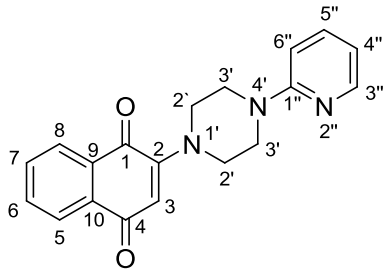

A bright orange, lustrous powder of the pure product was produced in accordance with generic experimental procedure **1** (29.6 mg, 19%, $C_{19}H_{17}N_3O_2$, 319.36 $g.mol^{-1}$); **mp** =130-135°C; $\mathbf{R}_f$ = 0.27 (30% ethyl acetate: hexane); **IR** : ν_{max} (cm^{-1}) = 3060 (vw, st, ar C-H, mono-substituted ar ring), 2831 (w, st, C-H, PR), 1666 (m, st, C=O), 1565 (s, st, C-C, NQ), 1478 (m, st, C-C, mono-substituted ar ring), 1307 (s, st, C-N, aromatic amine), 1242 (s, st, as, C-N, PR), 1208 (s, st, sy, C-N, PR), 1120 (w, st, as, C-C, PR), 982 (s, st, C-N, NQ-PR), 775 (s, ar C-H δ oop), 725 (s, C-H rock, PR); **HRMS *m/z* (ESI)** Found M^+, 319.1321. (M^+ 100%, $C_{19}H_{17}N_3O_2$ requires 319.1447); **LRMS *m/z* (ESI)** Found $[M+H]^+$, 320.07. ($[M+H]^+$ 100%, $C_{19}H_{17}N_3O_2$ requires 320.3708), 275 (4), 225 (4), 200 (10), 156 (4); **LRMS *m/z* (APCI)** Found $[M+H]^+$, 320.14. ($[M+H]^+$ 100%), 322 (2), 321 (20), 318 (2); **^{1}H NMR** δ_H (300 MHz, $CDCl_3$) 8.22 (1 H, dd, *J* 4.9 and 1.2 Hz, H-3″), 8.12 – 7.93 (2 H, m, H-6 and H-7), 7.68 (2 H, m, H-5 and H-8), 7.58 – 7.48 (1 H, m, H-5″), 6.75 – 6.57 (2 H, m, H-4″ and H-6″), 6.04 (1 H, s, H-3), 3.77 (4 H, dd, *J* 6.8 and 2.8 Hz, H-3′), 3.71 (4H, dd, *J* 6.8 and 2.7 Hz, H-2′); **^{13}C NMR** 183.6 (C-4), 183.2 (C-1), 158.9 (C-2), 150.7 (C-1″), 137.7 (C-5″), 134.0 (C-6 and C-7), 132.7 (C-10), 132.5 (C-9), 129.3 (C-3″), 126.7 (C-5), 125.6 (C-8), 120.3 (C-4″), 119.7 (C-6″), 111.6 (C-3), 48.8 (C-3′), 48.8 (C-2′).

4.3.12 Synthesis of 2-(4-pyrimidin-2-ylpiperazin-1-yl)-1,4-naphthoquinone – compound 11

Quantity of 1-(2-Pyrimidyl)piperazine	(82.1 mg, 0.50 mmoles, 1.0 equiv.)
Generic Experimental Procedure	1
Reaction Duration	60 mins
Solvent System used for Column Chromatography	30% ethyl acetate: hexane

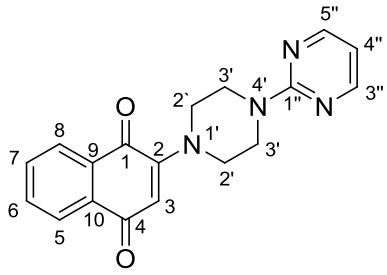

A mustard-yellow powder of the pure product was obtained according to generic experimental procedure **1** (68.2 mg, 50%, $C_{16}H_{16}N_4O_2$, 320.35 g.mol^{-1}); **mp** 175-182°C; $\mathbf{R}_f$ = 0.6 (30% ethyl acetate: hexane); **IR** : ν_{max} (cm^{-1}) = 3060 (vw, st, ar C-H, mono-substituted ar ring), 2831 (vw, st, C-H, PR), 1666 (m, st, C=O), 1586 (s, st, C-C, NQ), 1495 (m, st, C-C, mono-substituted ar ring), 1307 (s, st, C-N, aromatic amine), 1242 (s, st, as, C-N, PR), 1210 (s, st, sy, C-N, PR), 1123 (w, st, as, C-C, PR), 979 (s, st, C-N, NQ-PR), 773 (s, ar C-H δ oop), 726 (s, C-H rock, PR); **LRMS *m/z* (APCI)** Found $[M+H]^+$, 321.14. ($[M+H]^+$ 100%, $C_{18}H_{16}N_4O_2$ requires 321.3586), 322 (20), 323 (2), 319 (2); **^{1}H NMR** δ_H (300 MHz, $CDCl_3$) 8.34 (2 H, d, *J* 4.7 Hz, H-3″ and H-5″), 8.15 – 7.89 (2 H, m, H-6 and H-7), 7.83 – 7.51 (2 H, m, H-5 and H-8), 6.56 (1 H, t, *J* 4.7 Hz, H-4″), 6.04 (1 H, s, H-3), 4.02 (4 H, dd, *J* 6.3 and 4.3 Hz, H-3′), 3.75 – 3.54 (4 H, m, H-2′); **^{13}C NMR** 183.5 (C-4), 183.0 (C-1), 161.4 (C-2), 157.8 (C-1″), 153.4 (C-3″ and C-5″), 133.9 (C-6 and C-7), 132.7 (C-10), 132.5 (C-9), 126.7 (C-5), 125.6 (C-8), 111.1 (C-4″), 110.5 (C-3), 48.5 (C-2′), 43.1 (C-3′).

PART B

NITROGEN-CONTAINING DERIVATIVES OF PODOPHYLLOTOXIN

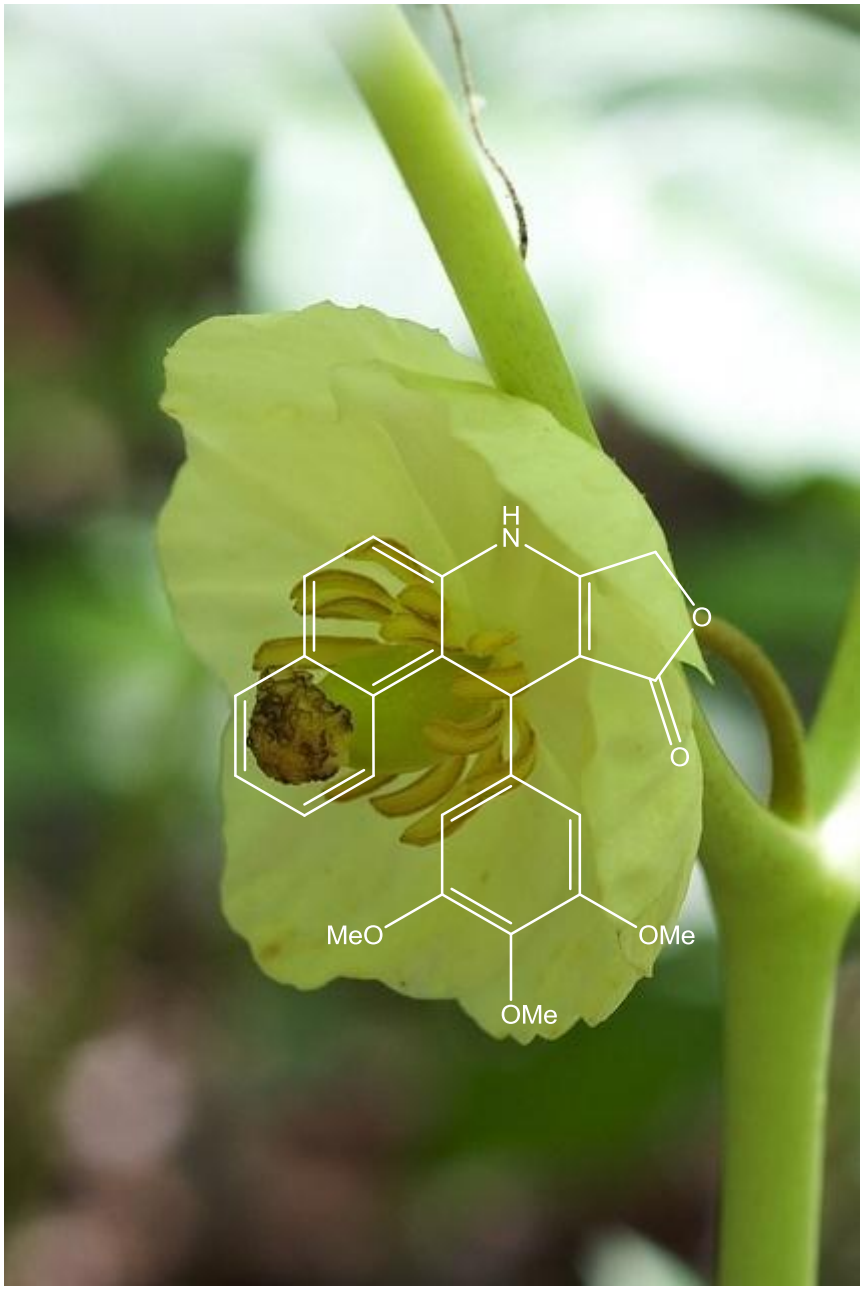

ABSTRACT

The antimitotic, aryltetralin lactone (−)-podophyllotoxin is the most abundant lignan isolated from the plant material of a genus (*Podophyllum*) of six species of herbaceous perennial plants in the family, Berberidaceae, native to eastern Asia and eastern North America. Plant extracts of the *Podophyllum* species have been used in oriental folk medicine and in the traditional pharmacopoeia of diverse cultures as antihelminthics, cathartics, purgatives and as antidotes to poisons dating back as far as 1000 years ago.

Once a promising lead compound has been sourced from the pool of evolutionary pre-validated natural products, and is proven to provoke a desired phenotypic response in a cell culture or *in vivo* experiment, several strategies, including photoaffinity labelling may be employed to map its protein target. Photolabile ligands can help to shed light on some central drug-interaction concerns: the identity of the protein target for a particular ligand, the protein's affinity for the ligand, the location of the target protein in the organism and the nature of the active site of the target. The aim of this part of the project was to synthesize a photolabeled, modified 4-aza-podophyllotoxin analogue with the intention of utilizing this photoprobe in future biochemical experiments to determine the mode of action and the preferred binding site of these nitrogen-containing derivatives.

(+)–Podophyllotoxin bears the distinction of being one of the most intriguing natural lignans due to its fascinating structure – four contiguous chiral centres, a rigid trans lactone and a pseudoaxial ring. The complex 4-aza-podophyllotoxin scaffold was successfully constructed in one pot utilizing a variation of the Hantzsch dihydropyridine multicomponent reaction fruitfully exploited in the Wits synthetic research group thus far. Thereafter, the "warhead" of the probe, pentafluorobenzoyl chloride, was efficiently installed through a facile acylation reaction with a primary amine group to reveal the photosensitive ligand rearing to go for cytotoxicity testing and biochemical analyses.

CHAPTER 1: INTRODUCTION AND LITERATURE SURVEY

1.1 Introduction – Research Rationale

The ability of low-molecular-weight organic compounds to induce observable changes in the physical or biochemical characteristics of a cell or an organism through the modulation of biopolymer (proteins, nucleic acids and polysaccharides for example) functioning has rendered them invaluable as pharmaceuticals and as tools in the elucidation of complex cell-signalling pathways.[37] The efficacy of countless successful drugs in use today was proven through direct observation of the phenotypic changes induced in a biological organism by the compound or extract.[37] Often, the drug's mechanism of action was only discovered years after its initial clinical implementation.[37] Despite significant technological advances, the mapping of specific bio-macromolecular targets of biologically active small molecules remains a major stumbling block in the fields of medicinal chemistry and chemical biology.[37] Thus, the illumination of the unique protein targets of bioactive small molecules is a fundamental step toward expanding the range of potential drug targets.[37]

Some of the most powerful modulators of cellular behaviour are complex, naturally-sourced, biological compounds and their semi-synthetic derivatives.[37] The utilization of these natural products as photoaffinity probes in the identification of cellular binding partners could lead to the formulation of as yet undiscovered strategies for the treatment of proliferative diseases.[37]

It is with these considerations in mind that the design and synthesis of a photolabeled, modified, 4-aza-podophyllotoxin analogue, with potential cytotoxic properties, was undertaken in this project.

1.2 Signal Transduction in Cell Membranes

Receptor proteins, located in the plasma membrane of target cells, selectively bind to signalling molecules; each kind of receptor can bind only certain ligand conformations.[38] A signalling molecule, typically referred to as a *ligand*, may be a peptide (short protein) or another small molecule such as a neurotransmitter, a hormone, a pharmaceutical drug or a toxin.[38] At the start of a signalling pathway a ligand binds with a receptor and the receptor is activated.[38] The activated receptor alters the conformation of a neighbouring protein, which then in turn becomes activated.[38] Ultimately, these sequential interactions result in the activation of an enzyme bound to the plasma membrane.[38] That enzyme may catalyse the biosynthesis of intracellular signalling molecules or it may activate related intracellular enzymes.[38] In this manner, the original biochemical signal is amplified and may profoundly alter the metabolism of the cell.[38] Simply stated, ligand-induced conformational changes in receptors result in cellular changes which constitute the biological activity of the ligand.[38]

1.3 Introduction to Photoaffinity Labelling

The first-step in the modern drug-development process is the recognition of macromolecular targets associated with particular disease-states; knowledge of the receptor-site and its function allows for the development of novel compounds that can selectively manipulate biological responses.[39] Conversely, once a promising lead compound has been sourced from the pool of evolutionary pre-validated natural products, and is proven to provoke a desired phenotypic response in a cell culture or *in vivo* experiment, several strategies may be employed to map its protein target.[37] The central principle of target-identification experiments is that a single binding event between the ligand and its receptor-site is used to elucidate the target biopolymer.[37] One critical assumption is that the induced phenotypic cellular response occurs as a direct consequence of the covalent or non-covalent bond between the small molecule and the target receptor site.[37]

Photoprobes have been identified as invaluable remotely-controlled tools in the drug-discovery process.[39] Their inherent stability under dark conditions and lability when exposed to light of a particular wavelength can be exploited at two stages.[39] Stage one involves the synthetic introduction of the photosensitive group to a biologically active compound, followed by the initiation of a specific photo-response by irradiation with light of a defined wavelength.[39] Consequently, a new covalent association is formed (photoaffinity labelling and photoimmobilization) or the cleavage of a particular bond results (photodeprotection).[39] Photolabile ligands can help to shed light on some central drug-interaction concerns: the identity of the protein target for a particular ligand, the protein's affinity for the ligand, the location of the target protein in the organism and the nature of the active site of the target.[39]

Photoaffinity labelling (PAL) is a biochemical technique, first described by Westheimer[40] and co-workers, that has been utilized to identify specific amino acid residues present in the binding sites of biological receptors.[41, 42] PAL not only reveals vital information about the structural nature of a particular binding-site but could potentially be harnessed to investigate the process of information transfer in biological receptors, for example their mode of action in signal transduction (the process in which the cell converts an extracellular signal into an intracellular signal that affects cell functioning).[38, 43]

In their groundbreaking research, which marked the invention of photoaffinity labelling, Westheimer and co-workers covalently linked a photosensitive diazo ester onto a serine-125 amino acid residue of the enzyme, α-chymotrypsin, and the bond was cleaved in the presence of light thereafter (**Scheme 1**).[40, 42] The results of this experiment allowed for the identification of specific amino acid resides comprising the ligand binding-site and revealed striking details about the architecture and mode of action of this enzyme.[42]

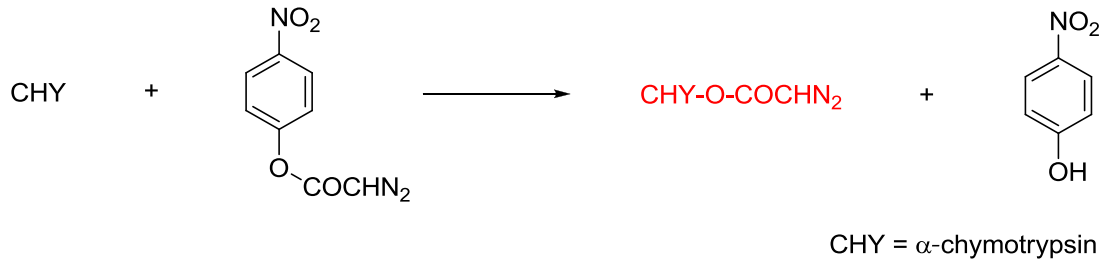

Scheme 1 (CHY = α-chymotrypsin)

In a typical PAL experiment a light-sensitive photophore (benzophenone for example) is adjoined to a natural ligand of an enzyme or target protein.[41, 42] The light-sensitive ligand is then permitted to bind to its target biological receptor.[42] Upon irradiation with light of a particular wavelength, photolysis of the complexed ligand occurs which liberates a highly reactive intermediate, usually a radical species, which reacts rapidly and irreversibly with a nearby amino acid residue to form a sturdy covalent bond between the labelling moiety and the receptor (**Scheme 2**).[42] As a consequence of the photoinitiated coupling reaction, a permanent, irreversible bond forms between the label and the target protein which can inactivate or activate the biochemical function of the biopolymer.[39, 42] An ideal reactive intermediate for PAL experiments would be indiscriminating and react irreversibly with the first bond encountered, even an inactivated CH bond.[39, 42] The PAL experiment would be compromised if the photogenerated intermediate was indiscriminating; as it could then potentially leave the binding site and react with other non-specific amino acid residues on the protein chain.[41] An ideal photoligand must also include an easily detectable photo-tag (for example radioactive, fluorescent or immunoreactive) which would allow for elucidation of the morphology of the macromolecule's ligand-binding site.[39] In addition to the commonly utilized aryl azides, a wide range of photosensitive probes have been used with some success, including diazirines, diazoketones, aryldiazonium salts and aromatic halides; pentafluorobenzoyl chloride is the photophore of choice in this project.[42] Fluorine has been shown to be a particularly auspicious elemental substituent for photoprobes in PAL experiments due to its relatively small atomic radius that does not impede upon substrate binding and the serendipitous availability of ^{19}F NMR spectroscopy as an additional analytical tool with which to examine the photolabelling mechanism.[42]

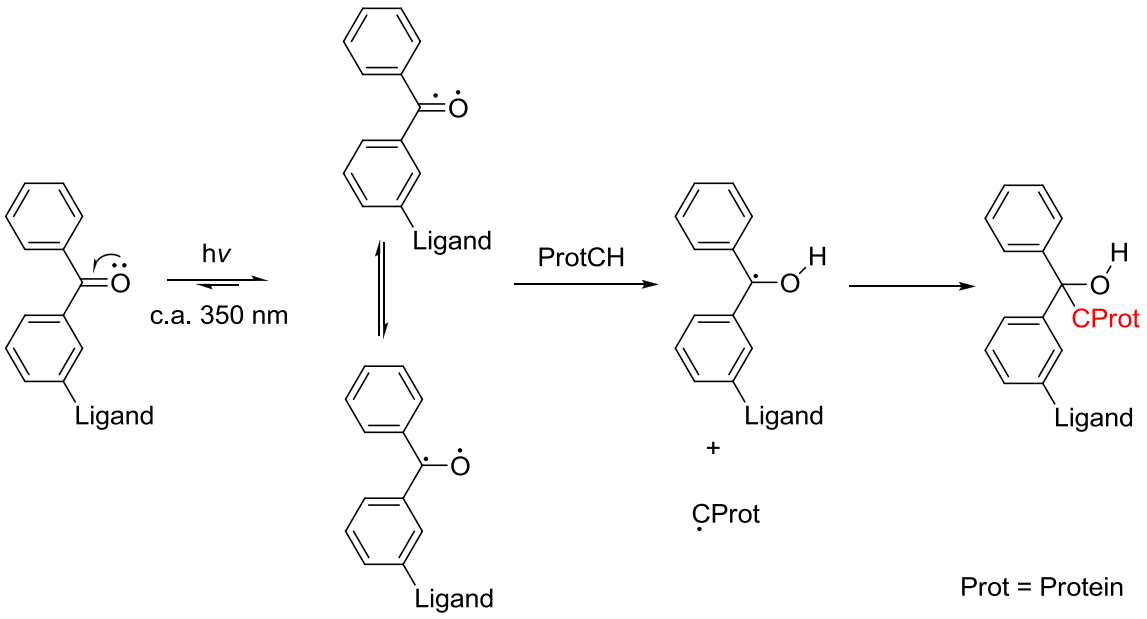

Scheme 2: Photochemical Events of the Benzophenone Photophore used in Photoaffinity Labelling

1.4 Podophyllotoxin – a Brief Introduction

Figure 1: The White Flower of the Mayapple

The antimitotic, aryltetralin lactone (−)-podophyllotoxin (**1, Figure 2)** is the most abundant lignan isolated from the roots, rhizomes, stems, leaves, fruits, seeds and in the resin, podophyllin, produced by a genus (*Podophyllum*) of six species of herbaceous perennial plants in the family, Berberidaceae, native to eastern Asia and eastern North America (one species, Mayapple *P. peltatum*) (**Figure 1**). [43,]

Plant extracts of the *Podophyllum* species have been used in oriental folk medicine and in the traditional pharmacopoeia of diverse cultures as antihelminthics, cathartics, purgatives and as antidotes to poisons dating back as far as 1000 years ago.[45] Podophyllin, the resin used by Native Americans to treat venereal warts, was included in the first edition of the Pharmacopoeia of the Massachusetts Medical Society in 1808, and gained entry into the United States Pharmacopoeia in

1820, wherein its biological activity was attributed to the compound, podophyllotoxin and remains the standard treatment for venereal warts today.[45] From the aqueous extract of *Podophyllum peltatum*, the antiviral properties of the most active component, podophyllotoxin, was keenly demonstrated in the inhibition of replication of measles and the herpes simplex type I virus.[45] Podophyllotoxin has also been widely used in dermatological preparations for the treatment of *Molluscum contagiousum* – a benign skin disease affecting children, adolescents and HIV-sufferers, *Condyloma acuminatum* caused by the human papilloma virus (HPV) and *Psoriasis vulgaris* a chronic autoimmune skin disease.[45] The potential antitumor properties of podophyllotoxin were extensively investigated in the treatment of human neoplasia but clinical trials were mostly unsuccessful and were complicated by severe gastrointestinal side effects.[46, 47] These findings led researchers in the pharmaceutical research department of Sandoz to investigate the possibility that podophyllotoxin may occur naturally as a glucoside derivative.[44] Extensive structural modifications, specifically the acetalization of the 4- and 6-hydroxy groups of the glucopyranose moiety using aldehydes, were performed on the original lead glucosidic compound in order to obtain more potent and less toxic semi-synthetic derivatives with anticancer properties.[44, 47, 48] This led to the discovery of etoposide (**2**), etoposide phosphate (**3**) and teniposide (**4**) which have been in clinical use as antineoplastic agents since the early 1970s (**Figure 2**).[48] Etoposide and etoposide phosphate are specifically used in the treatment of malignancies including lung and testicular cancers, lymphoma, nonlymphocytic leukaemia and glioblastoma multiforme, while teniposide is invaluable in the treatment of childhood acute lymphocytic leukaemia.[46]

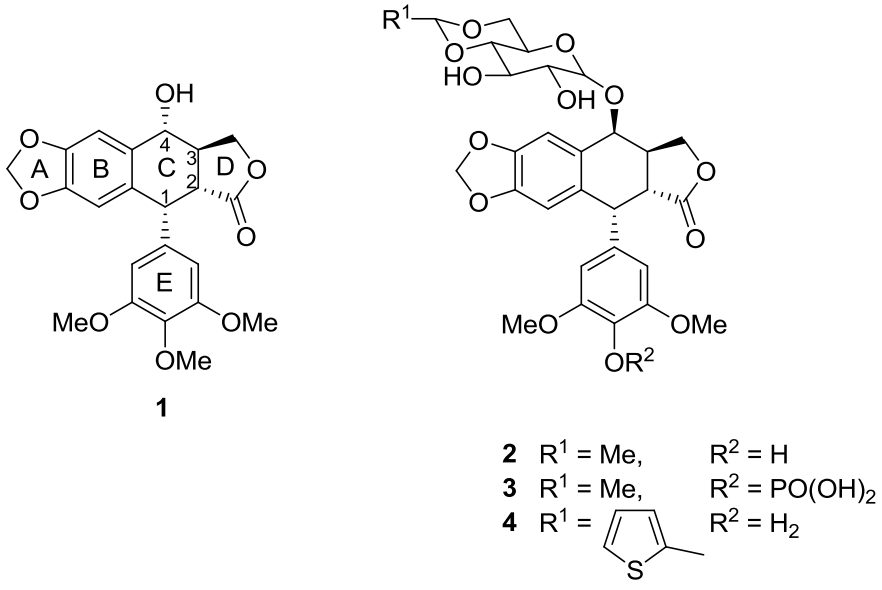

Figure 2: Structures of podophyllotoxin (**1**), etoposide (**2**), etoposide phosphate (**3**) and teniposide (**4**)

Despite the efficacy of the podophyllotoxin derivatives discussed thus far, the development of drug resistant cancer cells and the side-effects associated with clinical use, including myelosuppression, neutropenia and nausea, the hunt for novel anticancer drugs with podophyllotoxin as the lead pharmacophore remains a feverish topic of research.[46]

1.5 Mode of Action

The mechanism of action of podophyllotoxin is the obstruction of microtubule assembly through the inhibition of tubulin polymerization and arresting of the cell cycle in metaphase. [45, 49] Interestingly etoposide, etoposide phosphate and teniposide are not antimitotic agents but rather inhibitors of DNA topoisomerase II.[45] Their mode of action is based on the formation of a nucleic acid-pharmaceutical-enzyme complex which induces fractures in single- and double-stranded DNA as the initial step in a series of biochemical transformations that ultimately results in apoptosis - cell death.[45]

1.6 Biosynthesis of Podophyllotoxin and Derivatives

The complete biosynthetic pathway for cyclolignans has not been fully elucidated to date however, studies of various species of *Forsythia* (Oleaceae) *intermedia*, *Linum* and *Podophyllum* as model systems have led to the proposition of a suitable biochemical reaction scheme.[44, 45] The preliminary steps of the biosynthetic pathway reveal that coniferyl alcohol (**5**), the synthetic precursor, is synthesized from phenylalanine by phenylpropanoid enzymes (**Scheme 3**).[45] Several studies have suggested a common pathway starting from the transformation of coniferyl alcohol to (+)-pinoresinol (**6**) in the presence of a radical oxidant through the stereospecific dimerization of radical intermediates (**Scheme 3**).[45] Pinoresinol is subsequently reduced, in the presence of co-factor NADPH, to lariciresinol (**7**), which is ultimately converted to secoisolariciresinol (**8**) in a sequence of steps (**Scheme 3**).[45] Secoisolariciresinol gives rise to matairesinol (**9**) through the process of lactonization and matairesinol affords yatein (**10**), through appropriate quinomethane intermediates, which finally begets deoxypodophyllotoxin (**11**) (**Scheme 3**).[45]

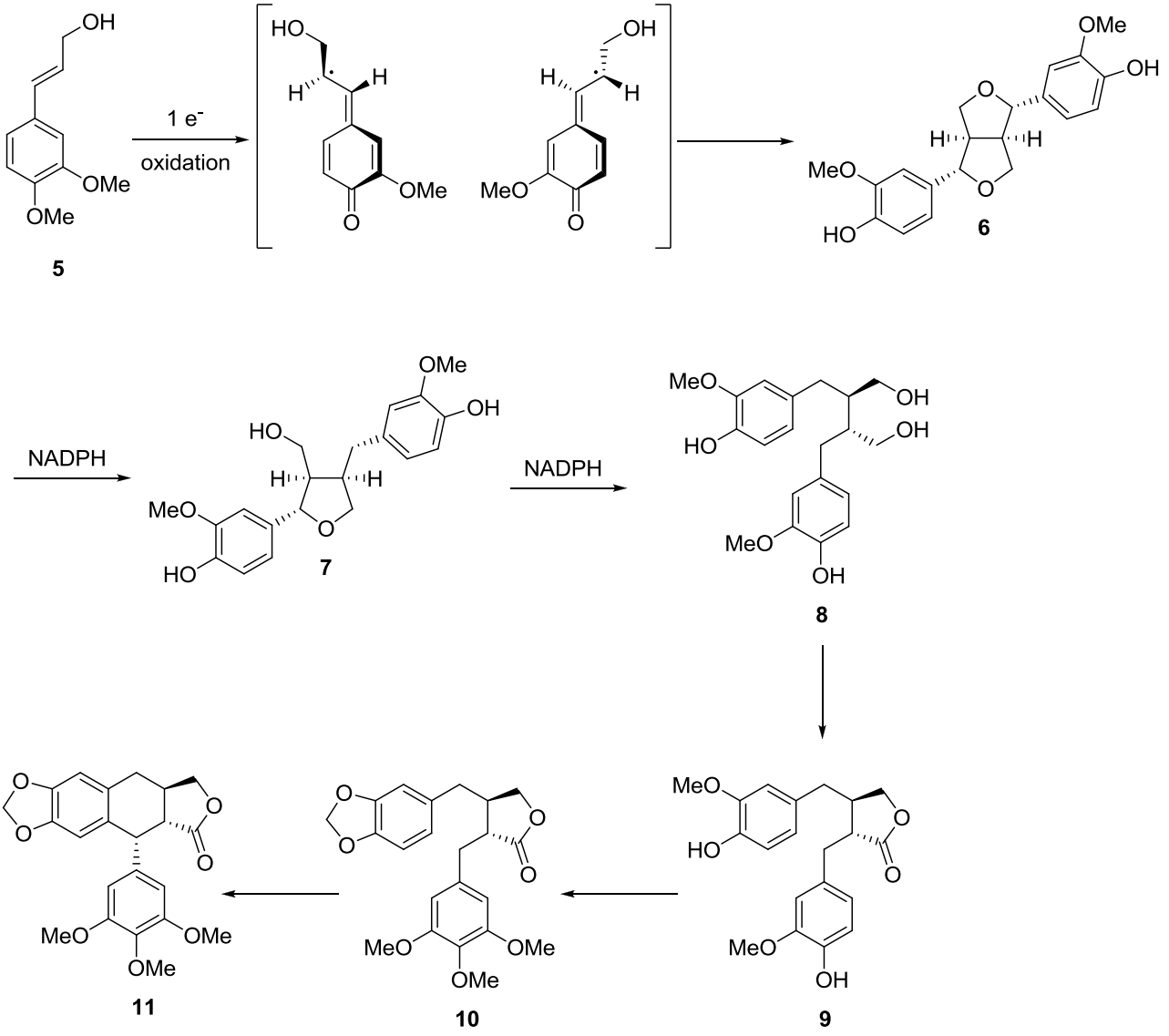

Scheme 3: Proposed Biosynthetic Pathway to Deoxypodophyllotoxin

1.7 Previously Reported Synthetic Methods Towards Podophyllotoxin

Four general methodologies for the synthesis of podophyllotoxin and its analogues have been developed; variations and novel approaches have also been demonstrated in the literature for each of the generic procedures .[44] These reactions involve the lactonization of a dihydroxy acid[50] (**14** → **1**), the cyclization of a tandem conjugate addition product[51] (**15** + **16** + **17** → **18** → **19**), the embellishment of an γ-oxo ester[52] (**12** → **13** → **1**) or the construction of the aryltetralin unit through an intermolecular Diels-Alder reaction[53] (**20** → **21**) (**Figure 3**).[44]

The Oxoester Route

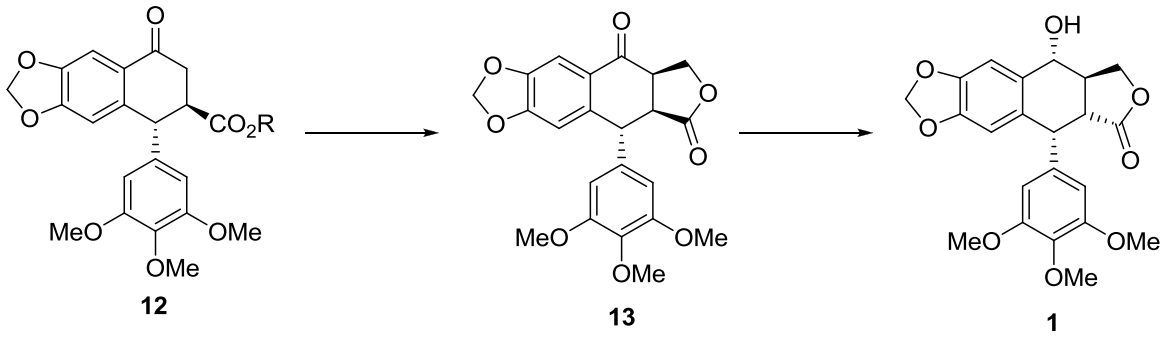

The Dihydroxy Acid Route

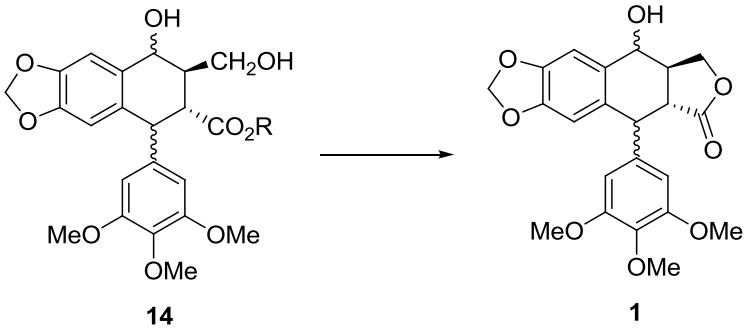

The Tandem Conjugate Addition Route

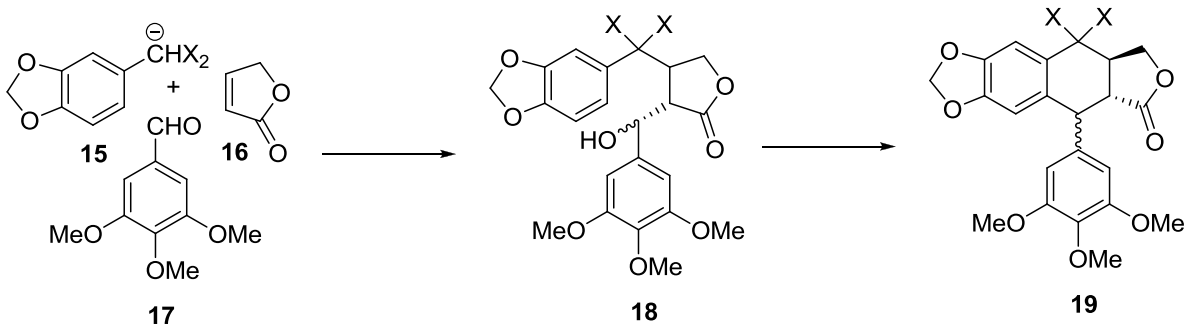

The Intramolecular Diels-Alder Route

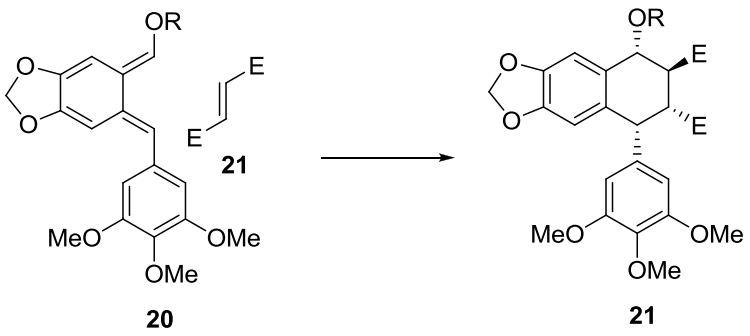

Figure 3: The Four General Approaches to the Synthesis of Podophyllotoxin and its Derivatives

1.8 Research Motivations

(+)–Podophyllotoxin bears the distinction of being one of the most intriguing natural lignans due to its fascinating structure – four contiguous chiral centres, a rigid trans lactone, a pseudoaxial ring E, and ready epimerization at C-2 and C-4 (**Figure 2**).[54] As a direct consequence of its intricate molecular architecture a great number of the structure-activity (SAR) studies performed on podophyllotoxin have been facilitated through synthetic derivatization of the parent natural lignan, rather than by total chemical synthesis.[46, 55] The hallmark of SAR studies is the chemical synthesis of a large library of structural analogues of the original lead compound and their biological testing to determine the result of substituent effects on activity or potency.[56] In this sphere, Itokawa and Takeya, reported the preparation of novel aza-podophyllotoxin analogues from commercially available reagents in a few simple steps.[49] Takeya and co-workers revealed that quinolines (**22**, **Fig. 4**), 4-aza-analogues of 1-arylnaphthalene lignans, could be prepared from anilines, benzaldehydes and tetronic acid or 2,3-cyclopentanedione via a sequence of condensation, cyclization and reduction reactions in good to excellent yields (**Scheme 4**).[47-49] Furthermore, the reduction of (**22**, **Fig. 4**) by an excess amount of sodium cyanoborohydride in acetic acid at ambient temperatures yielded 4-aza-2,3-dehydro-4-deoxypodophyllotoxin (**23**, **Fig. 4**) in excellent yield, which was shown to possess potent cytotoxicity; some derivatives of this compound were twice as cytotoxic as natural podophyllotoxin (**1**).[49] More importantly, the elimination of the stereogenic centres at C-2 and C-3 (**Fig. 2**) removes the possibility of epimerization at C-2 which has plagued the clinical development of podophyllotoxin, because the rapidly formed *in vivo cis*-lactone metabolite is inactive.[55]

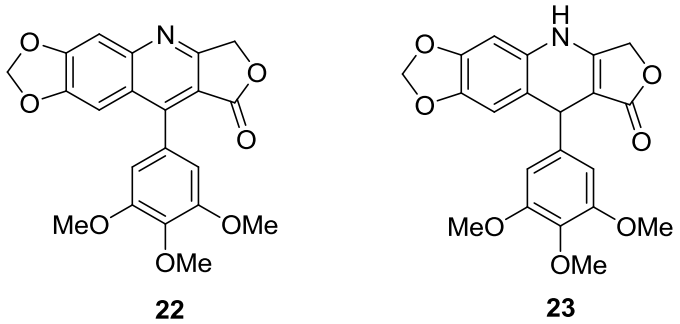

Figure 4: Aza-Podophyllotoxin Analogues

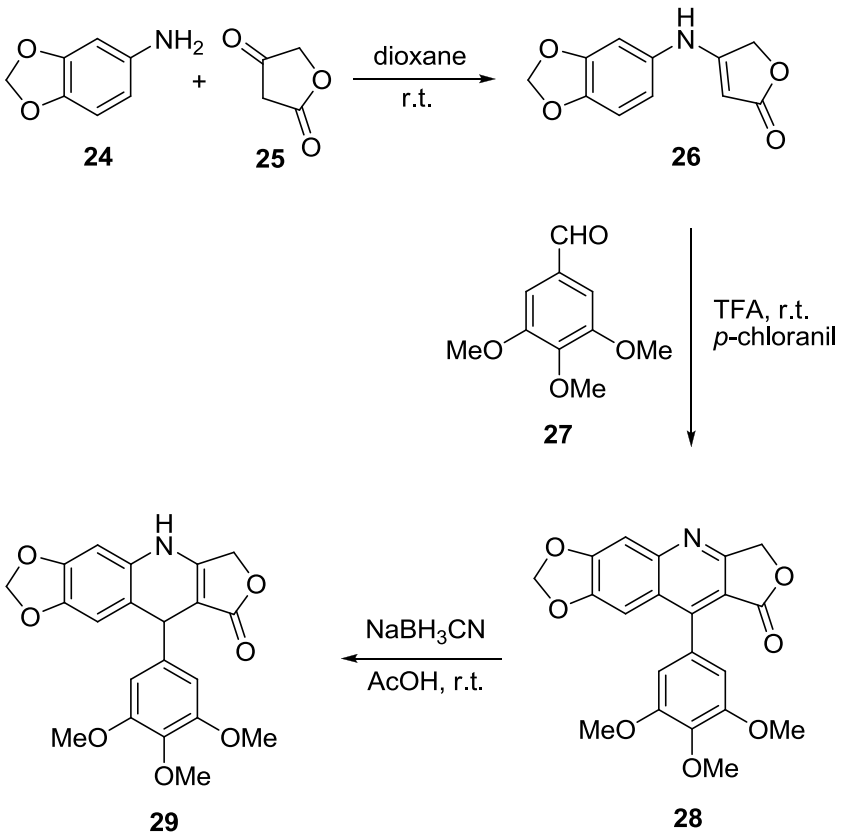

Scheme 4: Takeya's Method[49]

Later, Giorgi-Renault and Husson disclosed a more efficient, straight-forward synthesis of 4-aza-2,3-didehydropodophyllotoxins according to a multicomponent reaction (**Scheme 5**).[48] Both methods start with the same three reagent components and take advantage of the inherent electrophilicity and nucleophilicity of tetronic acid **25.**[48]

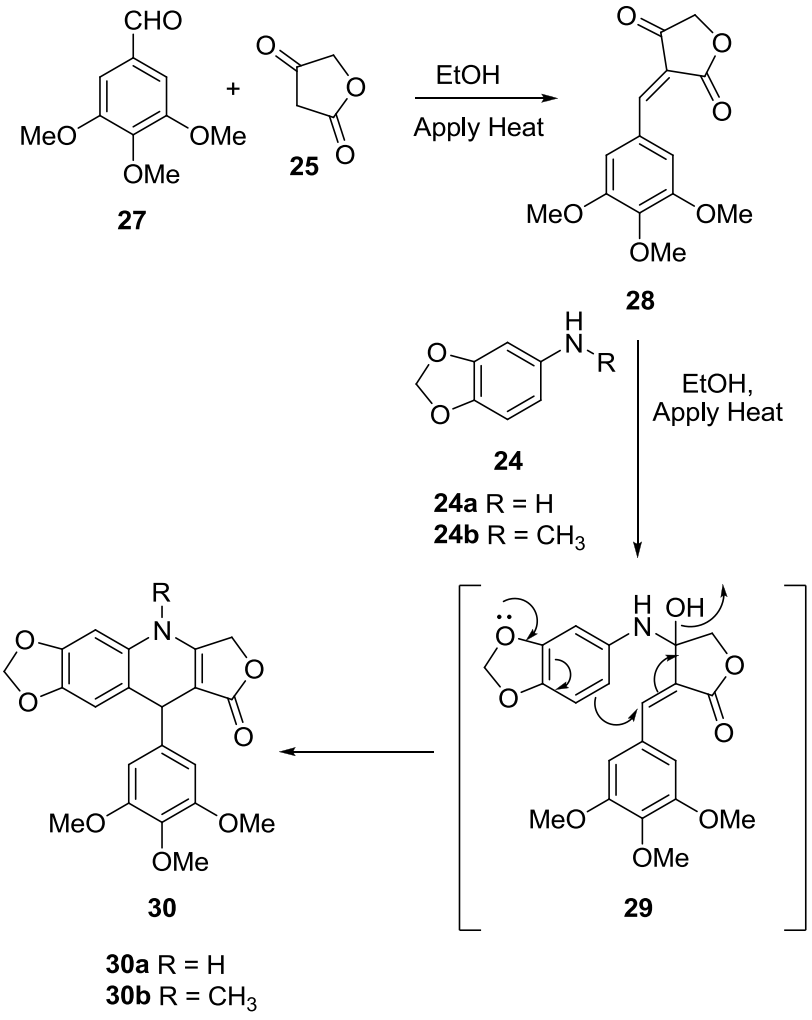

Scheme 5: Giorgi-Renault's Method[48]

1.9 Multicomponent Reactions

Multicomponent reactions (MCRs), in which several reactions are combined into a single synthetic transformation in one pot, have been extensively employed to create carbon-carbon bonds in synthetic chemistry.[47] A true MCR is a series of intermolecular and intramolecular events that continue sequentially until a final, irreversible convergent step traps the product.[57] These reactions allow for the construction of highly complex molecules that incorporate most of the atoms contained in commercially available or easy to prepare starting materials in one procedural step, thus avoiding complicated purification operations, ensuring atom-economy, energy saving and environmental friendliness.[46, 47] Unlike the conventional step-by-step construction of bonds leading

to a target molecular scaffold, the chief attribute of MCRs is the inherent formation of many distinct chemical bonds in a single procedure, preferably without isolating reaction intermediates, altering reaction conditions or adding further reagents.[57] The overall structure of a reaction product can be easily diversified by altering the chemical substituents on simple starting materials or by using alternative readily available reactants. In this way, MCRs can be used in automated synthesis to build a large combinative library of structurally diverse derivatives of a lead compound to be used in SAR studies.[57]

Myriad MCRs have been investigated over the years, starting with its earliest inception over 150 years ago in Hantzsch's dihydropyrimidine synthesis.[57]

1.10 Hantzsch's Dihydropyridine Synthesis

Arthur Hantzsch described the preparation of 1,4-dihydropyridine (**34**, **Scheme 6**), a structural relative of reduced nicotinamide adenine dinucleotide (NADH), more than a century ago.[58] The original synthesis involved a three-component MCR combining acetoacetic ester (**31**), benzaldehyde (**32**) and ammonia (**33**) in refluxing ethanol (**Scheme 6**).[58] Similarly, the preparation of dihydropyridine derivatives can be achieved through the condensation of an aldehyde with two equivalents of β-ketoester in the presence of ammonia (**Scheme 7**).[58] In 1986 the mechanism of the Hantzsch dihydropyridine synthesis was throroughly investigated through the use of NMR spectroscopy and it was established that the reaction proceeds through a Knoevenagel condensation product as a key intermediate.[58, 59] The condensation of the second equivalent of the β-ketoester with ammonia yields a second key intermediate, an ester amine (enamine intermediate) **35 (Scheme 8)**.[59] Further condensation between the two intermediary fragments yields the dihydropyridine derivative **38** (**Scheme 8**).[59]

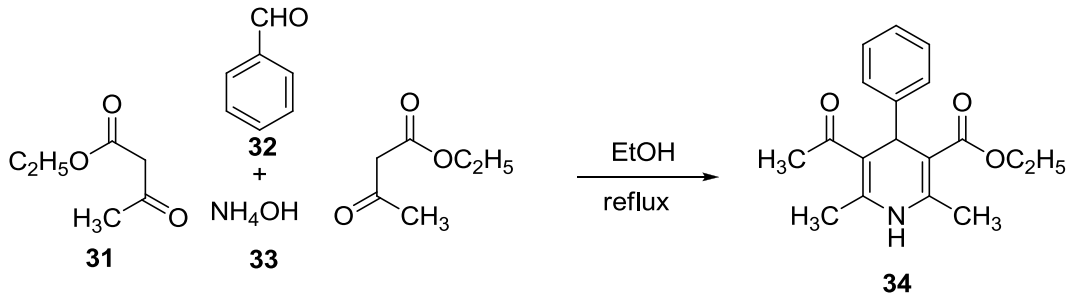

Scheme 6: The Original Hantzsch Reaction[58]

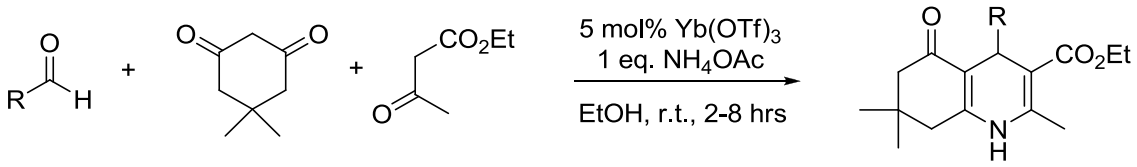

Scheme 7: $Yb(OTf)_3$ Catalyzed Hantzsch Reaction[60]

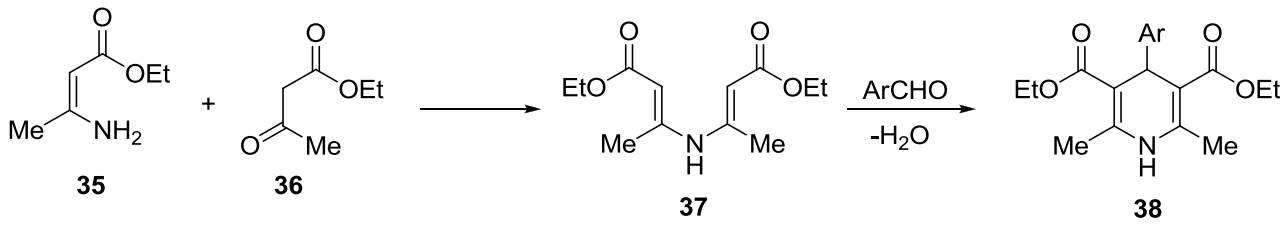

Scheme 8: The Mechanistic Pathway of the Hantzsch Reaction

Despite the widely-reported use of MCR for the construction of medicinal libraries, their use in natural product chemistry is uncommon.[46] As part of an effort aimed at expanding the use of MCRs leading to the preparation of privileged medicinal scaffolds, the Wits organic chemistry research group, in collaboration with Alexander Kornienko of the New Mexico Institute of Mining and Technology, utilized a variation of the Hantzsch Pyridine reaction to synthesize a library of between 30 and 40 synthetic derivatives of 4-aza-podophyllotoxin. However, a mystery lay waiting to be solved. As discussed previously, podophyllotoxin is an antimitotic agent which inhibits tubulin polymerization while etoposide and its derivatives are not antimitotics, but DNA topoisomerase II inhibitors. Despite the fact that 4-aza-podophyllotoxin and its derivatives exhibit potent cytotoxic

capabilities; their biochemical mode of action has not yet been elucidated. It is with these considerations in mind that it was decided to attach a photoprobe to one of the previously synthesized 4-aza-podophyllotoxin derivatives to allow for future biological testing, which will hopefully shed some light on their mode of action and reveal valuable structural information regarding their binding site.

1.11 Proposed Synthetic Route

Step one of our proposed synthesis will involve the alkylation of the free phenol in syringaldehyde (**39**, **Scheme 9**) with 2-(Boc-amino)ethyl bromide and 4 equivalents of potassium carbonate (K_2CO_3) in dimethylformamide. This is a standard protection procedure that will allow for stability in the presence of the mild base encountered during the MCR and will ensure that the MCR proceeds via the desired pathway. Next, the extended syringaldehyde will be heated in the presence of tetronic acid (**41**) and β-naphthylamine (**42**) in absolute ethanol, in a variation of the Hantzsch Pyridine MCR reaction to afford the 4-aza-podophyllotoxin derivative (**43**, **Scheme 10**). Following on, deprotection of the boc-group on the ethylamine tether in the presence of hydrogen chloride in dioxane should yield a hydrochloride salt of the 4-aza-podophyllotoxin analogue (**44**, **Scheme 11**). Lastly, this salt (**44**) will be reacted with the pentafluorobenzoyl chloride photophore (**45**) to form the photosensitive ligand (**46**). It is envisaged that this compound could then be utilized in future chemical biology experiments to confirm the location of the putative binding site(s).

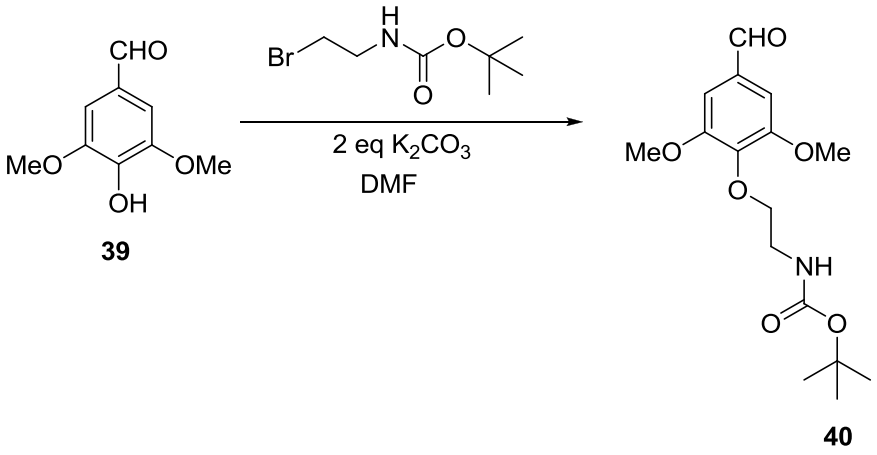

Scheme 9: Step 1 of the proposed synthetic route

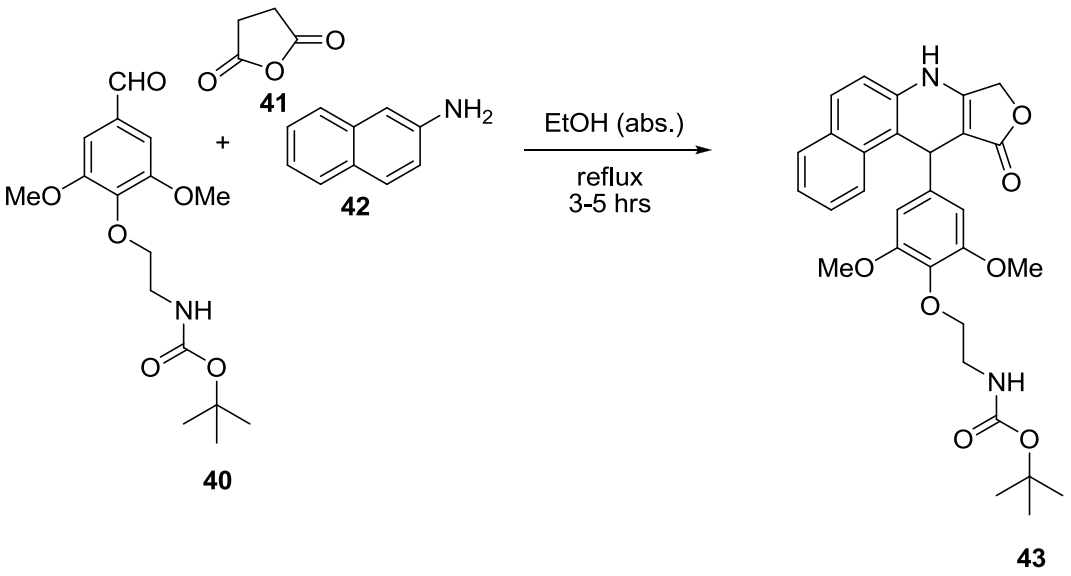

Scheme 10: Step 2 of the proposed synthetic route - MCR

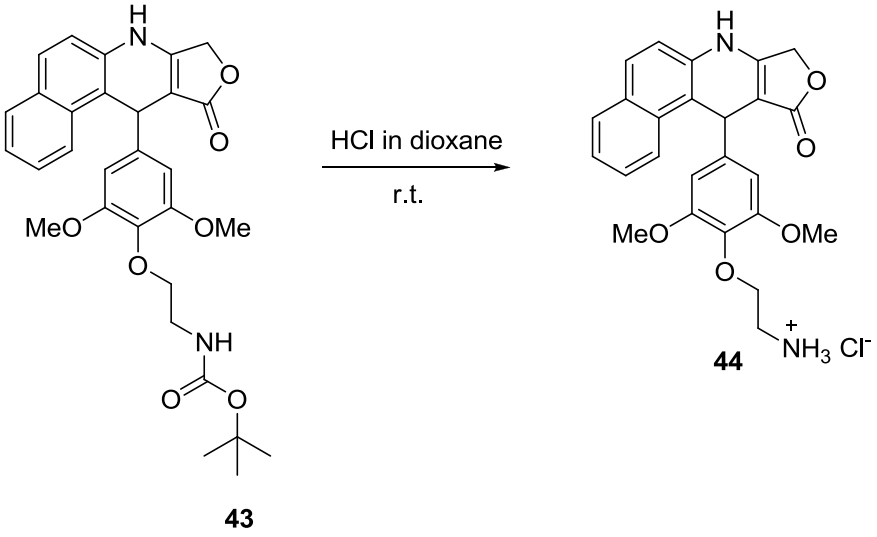

Scheme 11: Step 3 of the proposed synthetic route - Deprotection

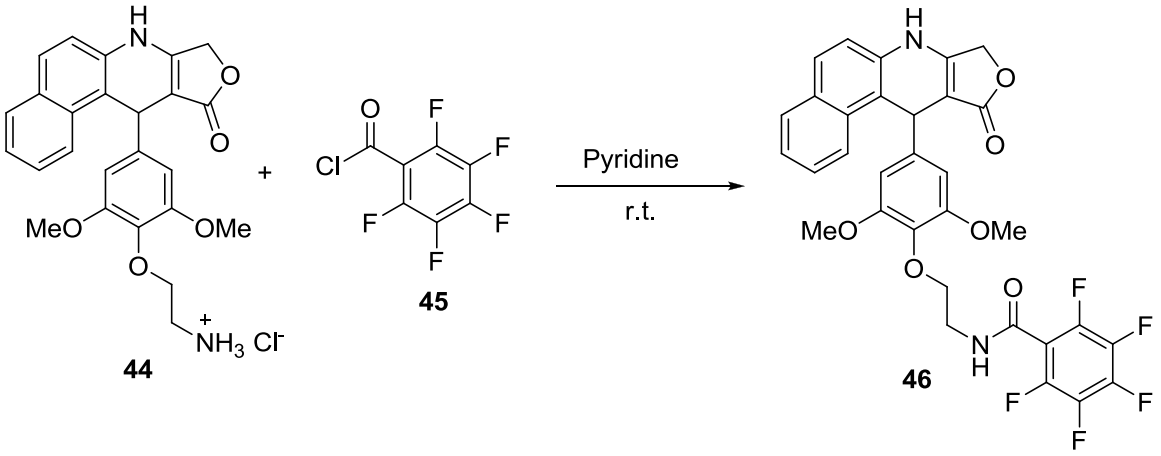

Scheme 12: Step 4 of the proposed synthetic route – Reaction with Photophore

CHAPTER 2: RESULTS AND DISCUSSION

This chapter will be separated into two principal sections; a preliminary rehearsal of the MCR synthetic protocol followed by the synthesis of the photosensitive ligand. Each main section will be further divided into appropriate sub-sections which will cover the individual experiments undertaken in this part of the MSc. research project. A discussion of the experiments will include a summary of the general procedure, followed by an overview of the results obtained. Relevant spectroscopic data, including NMR, IR and mass spectrometry will be presented as a means of confirming the identity and relative purity of each product.

2.1 Testing the Waters – Preliminary Rehearsal of the MCR

2.1.1 4-Azapodophyllotoxin Analogue Synthesis – A Variation of the Hanztsch Pyridine Reaction

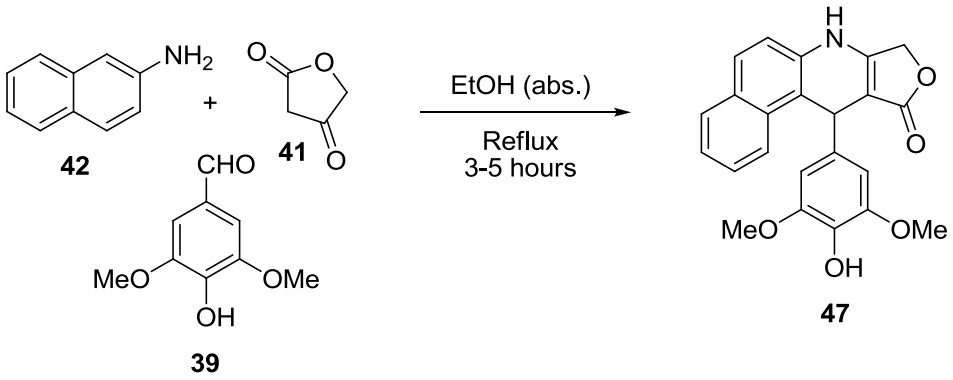

Scheme 13

It was thus decided to repeat one particularly facile MCR, a variation of the Hanztsch dihydropyridine synthesis, previously conducted in the Wits organic chemistry research group, in an

effort to familiarise ourselves with the synthetic techniques required to conduct the preparation of the photosensitive ligand discussed in the introduction.

To this end, a mixture of equimolar quantities of syringaldehyde, tetronic acid and β-naphthylamine in absolute ethanol was heated at reflux for 4 hours and the reaction progress was monitored by thin-layer chromatography (TLC) hourly until the disappearance of starting materials was noted under UV-light at 4 hours. The reaction mixture was then allowed to cool to room temperature, whereupon the product was observed to precipitate out of solution. Thereafter, the precipitated product was collected by filtration, washed with a minimum of chilled ethanol and thoroughly dried *in vacuo*. In this instance the product was deemed to be pure as judged by TLC and ^{1}H NMR spectroscopy and no further purification was required.

This procedure resulted in a dark brown powder that was collected in a yield of 54 %, which was only marginally lower than the yield of 59% reported by Tratrat *et al*. for the same compound.[48] Compound **47**, a 4-aza-podophyllotoxin analogue, was subsequently characterised by mass spectrometry, infrared analysis, ^{1}H NMR and ^{13}C NMR spectroscopy.

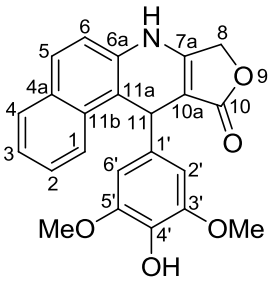

47

Figure 5

Low-resolution mass spectrometry revealed a molecular ion M^{+} of mass 389.17, which corresponded relatively well with the expected isotopic mass of 389.4028 for $C_{23}H_{19}NO_5$. Additionally, in the infrared spectrum of compound **47** a broad N-H stretch was clearly observed at 3500 cm^{-1}, a strong C=O stretch occurred at 1645 cm^{-1}, a characteristic strong C=C stretch was

found at 1534 cm^{-1}, a medium-intensity doublet band, typical of asymmetric and symmetric C-O-C stretches, was observed at 1196 and 1181 cm^{-1} and a strikingly intense stretch at 1107 cm^{-1} was attributed to a C-O vibration.

The ^{1}H NMR spectrum of **47**, revealed a broad singlet integrating for one hydrogen atom, occurring at a chemical shift of 10.24 ppm which was assigned to the amine proton (NH) (*lit.*[47] 10.27 ppm) and another broad singlet, arising further upfield, at a chemical shift of 8.16 ppm, also integrating for one hydrogen atom, corresponded to the OH proton. Two multiplets occurring at the chemical shift ranges of 7.96-7.76 ppm and 7.52-7.20 ppm, each integrating for three hydrogen atoms, were attributed to the six aromatic protons of the β-naphthylamine-derived moiety. It is promising to note that these signals lie well within the range reported in the literature, 7.86-7.27 ppm.[47] An aromatic singlet integrating for two protons, found at 6.44 ppm was assigned to the chemically equivalent aromatic hydrogen atoms, H-2′ and H-6′ and a doublet of doublets occurring at 4.93 ppm corresponds to the two chemically equivalent protons, H-8. Furthermore the proton bonded to the stereogenic centre C-11 was observed at a chemical shift of 5.58 ppm (*lit.*[47] 5.61 ppm) and an intense singlet arising at 3.59 ppm, integrating for 6 hydrogen atoms corresponded to the methoxy protons (*lit.*[47] 3.64 ppm).

The ^{13}C NMR signals found in the chemical shift range 147.8–104.5 ppm, corresponding to the syringaldehyde group and the β-naphthylamine moiety overlapped in the aromatic region and evaded definitive assignment. However, the pertinent signals arising in the ^{13}C NMR spectrum included: a chemical shift of 172.2 ppm, which was attributed to the carbonyl carbon, a peak observed further upfield at 57.0 ppm (2 × OMe), and a chemical shift of 55.1 ppm which corresponded to the stereogenic centre (C-11).

These findings serve to suggest that the synthesis of compound **47** was a success and allowed for further investigation into the synthesis of the photoprobe.

2.2 Synthesis of the Photosensitive Ligand

2.2.1 Step 1: Alkylation of the Free Phenol Moiety in Syringaldehyde

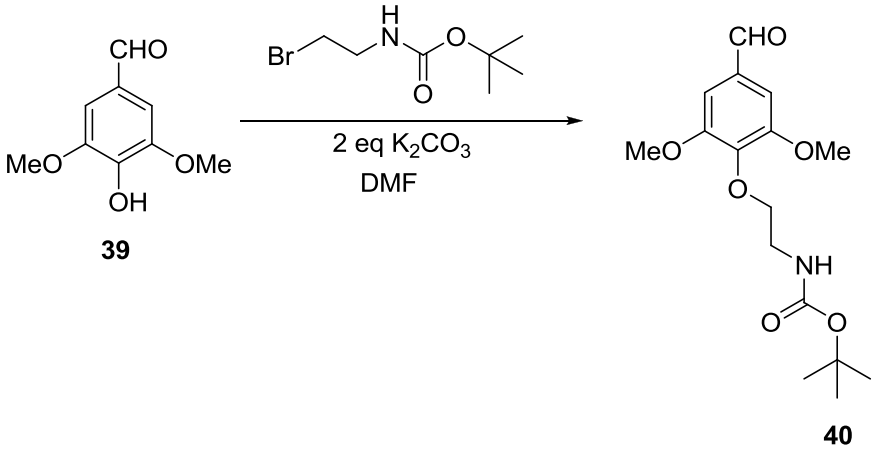

Scheme 14

This reaction involved the alkylation of syringaldehyde with one equivalent of 2-(Boc-amino)ethyl bromide in the presence of potassium carbonate (K_2CO_3) in DMF, as outlined in the general procedure reported by Brouwer, Mulders and Liskamp.[61] Impurities were next removed by column chromatography eluted with a 50% EtOAc: Hexane solvent system. Chromatographic purification revealed a light-yellow oil that solidified to a cream coloured solid after drying *in vacuo* for 12 hours. The yield obtained was 34% which was lower than the expected yield of 76% reported in the literature.[61]

The identity of the pure compound was next confirmed by mass spectrometry, infrared analysis, ^{1}H NMR and ^{13}C NMR spectroscopy.

Low-resolution mass spectrometry revealed a molecular ion (M^{+}) of mass 325.9 which matched the expected isotopic mass of 325.1525 for $C_{16}H_{23}NO_5$. An infrared spectrum of the sample showed a

strong intensity amide carbonyl stretch at 1727 cm^{-1} and another strong carbonyl vibration at 1687 cm^{-1}. Furthermore, two strong intensity bands were observed at 1329 cm^{-1} and 1123 cm^{-1}, which were assigned to a C-N and a C-O vibration respectively. Lastly, a medium intensity N-H band was readily identified at 3383 cm^{-1}.

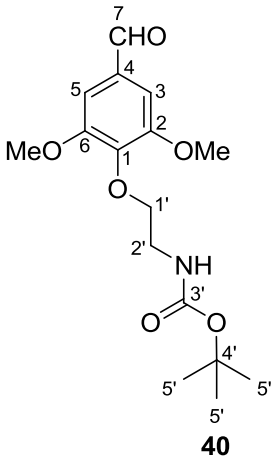

40

Figure 6

In the ^{1}H NMR spectrum of **40**, a triplet, *J*=4.8 Hz, occurring at 4.15 ppm and integrating for two protons was attributed to H-1′ on the ethyl chain and a doublet of doublets, with *J*=6.0 Hz and *J*=9.0 Hz, found further upfield at 3.41 ppm, integrating for two protons was assigned to the additional CH_2 group on the ethyl chain (H-2′). The homotopic aromatic protons, H-3 and H-5, were effortlessly identified at a chemical shift of 7.14 ppm and the tertiary butyl protons corresponded to an intense singlet integrating for nine hydrogen atoms at a chemical shift of 3.95 ppm. Favourably, the formyl hydrogen atom (C-7) was discovered at a chemical shift of 9.88 ppm (*lit.*[62] 9.74 ppm) and six homotopic methoxy hydrogen atoms were assigned to a singlet arising at a chemical shift of 3.95 ppm (*lit.*[62] 3.73 ppm).

The ^{13}C NMR spectrum revealed three quaternary aromatic signals at 153.7 ppm (C-2 and C-6), 142.2 ppm (C-1) and 132.1 (C-4) and a CH aromatic carbon signal at 106.5 ppm (C-3 and C-5). An amide carbonyl signal was identified at 156.1 ppm (C-3′) and another carbonyl signal arising at a chemical shift of 190.9 ppm (*lit.*[62] 192.0 ppm) corresponded to C-7. Lastly, the tertiary butyl moiety

(C-5′) was identified at 28.4 ppm (*lit*.[62] 28.6 ppm) and the chemically equivalent methoxy groups were observed at 65.3 ppm (*lit*.[62] 60.9 ppm).

Overall the spectroscopic data corresponded well with the literature[62] and served to confirm that the synthesis of compound **40** was a success.

2.2.2 Step 2: Multicomponent Reaction

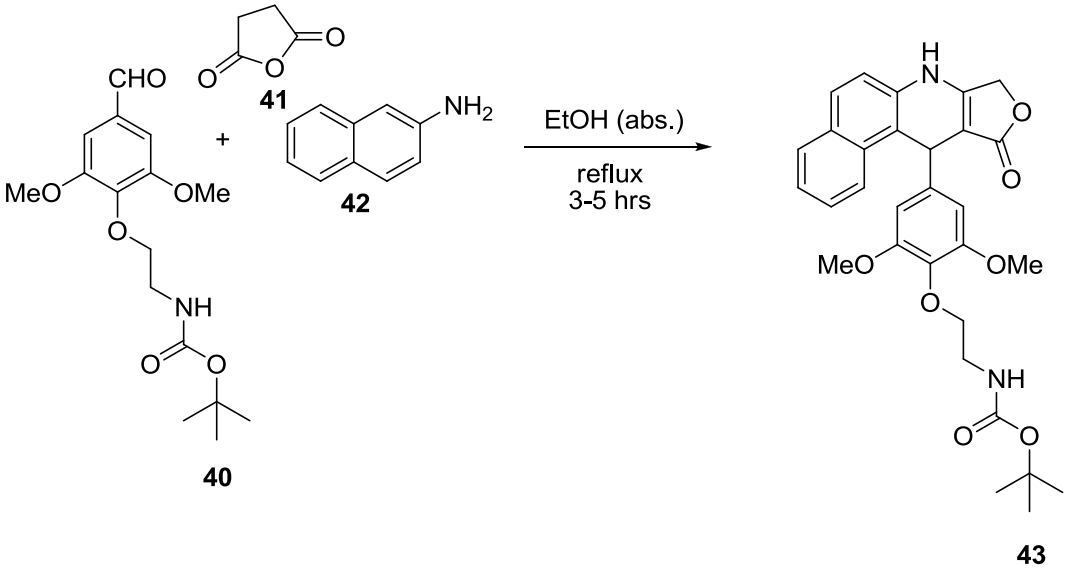

Scheme 15

Compound **43** was prepared according to the same experimental procedure detailed above in **2.1.1**. However, despite washing with cold ethanol, followed by further rinsing with distilled acetone, the product was determined to be impure as revealed by TLC analysis and ^{1}H NMR spectroscopy. The crude product was then purified by flash column chromatography, eluted with a 50% EtOAc: Hexane solvent system. The relevant chromatographic fractions were collected, combined and evaporated *in vacuo* to reveal a white, fluffy crystalline powder in a disappointingly low yield of 19%.

The low percentage yield could potentially be attributed to extensive loss of product occurring while washing with acetone during the filtration procedure. A possible solution to this problem would be to purify the crude, unrinsed product directly after filtration.

It is important to note that in the reaction detailed in **Scheme 15** above, the *β*-naphthylene group can potentially add in two possible ways, leading to two alternate orientations shown in **Figure 7** and **Figure 8** below. However, through rigorous spectroscopic and crystallographic studies performed in the Wits laboratory suite, it was confirmed that the orientation, shown in the structure of compound **43** above, is indeed the preferred orientation. These studies were conducted by another Wits research group prior to the commencement of this project and the findings remain unpublished. As a result no supporting data was included and a detailed discussion of the differences between the orientations will also not be expanded upon.

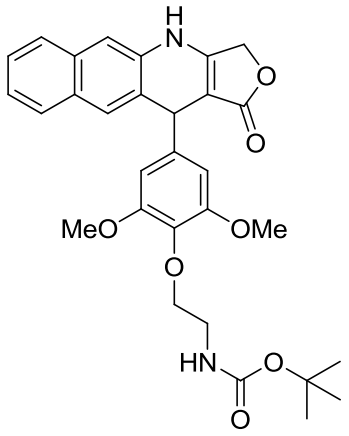

Figure 7

The structure of the purified product was elucidated through the use of mass spectrometry, infrared spectroscopy, ^{1}H NMR and ^{13}C NMR spectroscopy.

The infrared spectrum revealed a medium intensity, amide C=O stretch occurring at 1721 cm^{-1}, another medium intensity carbonyl stretch at 1653 cm^{-1} and a strong C-O band at 1121 cm^{-1}. An additional band that was split into a doublet at 1215 cm^{-1} (as) and 1213 cm^{-1} (sy) was assigned to two C-O-C vibrations. In addition, low-resolution mass spectrometry gave promising results. A

molecular ion ($[M+H]^+$) of mass 533.00 correlated well with the expected isotopic mass of 533.6012 for $C_{30}H_{33}N_2O_7$.

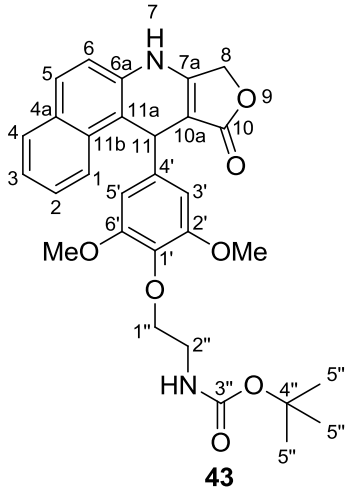

43

Figure 8

For further confirmation of the success of the reaction it was anticipated that the ^{1}H NMR spectrum would clearly reveal the absence of the aldehyde proton (H-7) observed for compound **40**, combined with the emergence of the entire range of proton signals assigned for compound **47**. Upon inspection of the ^{1}H NMR spectrum, the absence of the aldehyde hydrogen atom signal in the chemical shift range of 9.0-9.8 ppm was keenly observed. Furthermore, all of the signals corresponded fairly well with those observed for compound **40** and compound **47**, as though the two ^{1}H NMR spectra had been overlapped.

In the ^{13}C NMR spectrum, the aldehyde carbon signal (C-7, compound **40**) was not detected at a chemical shift of 190.0 ppm and in its place a new carbon signal corresponding to the stereogenic centre, C-11, was found at a chemical shift of 55.9 ppm. The remaining ^{13}C NMR signals were identified in the same chemical shift range as those assigned for compound **40** and compound **47**.

Based on the weight of the spectroscopic data, the synthesis of compound **43** was deemed a success and the pure sample was therefore carried over to the next step in the synthesis.

2.2.3 Step 3: Deprotection of the Boc-group on the Ethylamine Tether

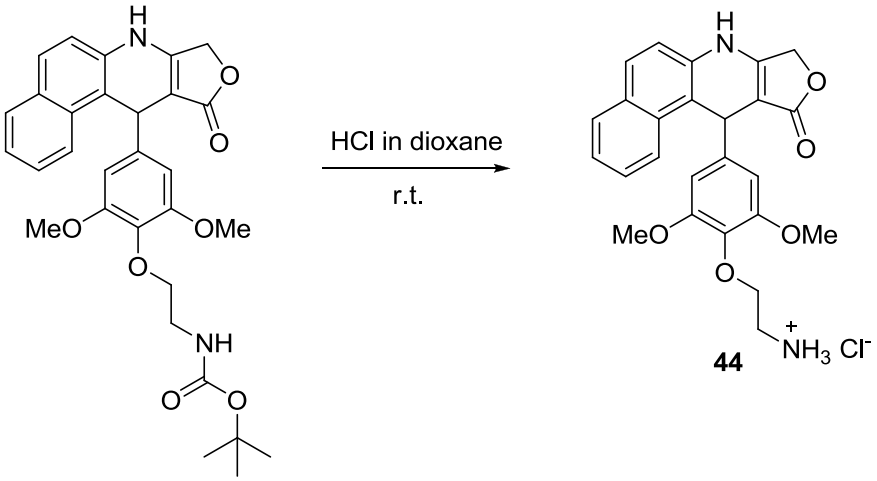

43 **44**

Scheme 16

According to the procedure outlined by Brouwer *et al.*[61], the Boc-protecting group was readily cleaved by stirring a mixture of compound **43** and a solution of hydrogen chloride in dioxane (4 M). This reaction was performed at room temperature for 90 minutes, to reveal, after *in vacuo* removal of the solvent, a beige-coloured flaky powder of the hydrochloride salt, compound **44**, in a quantitative yield of 100% after drying in vacuo for 12 hours.

The structure of compound **44** was substantiated using mass spectrometry, infrared analysis, ^{1}H NMR and ^{13}C NMR spectroscopy.

Favourably, low-resolution mass spectrometry gave a base-peak ($[M+H]^+$) of mass 433.22 which corresponded with the expected isotopic mass of 433.1763 for $C_{25}H_{25}N_2O_5$. The infrared spectrum revealed the absence of the amide C=O stretch, observed for compound **43**, and confirmed the presence of a NH_3^+ group which was assigned to a medium-intensity broad stretch occurring at 2899 cm^{-1} (*lit.*[62] 2000-3000).

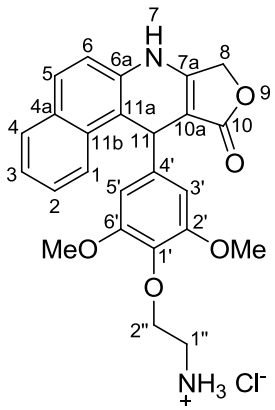

44

Figure 9

In the ^{1}H NMR spectrum of compound **44**, the signal corresponding to the tertiary butyl group (H-5*) for compound **43** was clearly absent from the spectrum (at an expected chemical shift of 1.42 ppm). Furthermore, the ^{1}H NMR spectrum integrated for twenty-one protons, which is nine protons fewer, than the total number of hydrogen atoms integrated for in the ^{1}H NMR spectrum of compound **43**. These findings served to confirm that the tertiary butyl moiety, bearing nine hydrogen atoms, was indeed missing from the structure of compound **44**, as anticipated. However, in the ^{1}H NMR spectrum of compound **44** there appeared to be three additional signals not accounted for in the experimental section: the solvent residual peak for DMSO was observed at 2.50 ppm, an intense water peak at 3.40 ppm was attributed to HDO and some remaining solvent, dioxane was identified at 3.57 ppm. Further drying of the compound should ensure that the dioxane solvent impurity disappears from the ^{1}H NMR spectrum.

The ^{13}C NMR data was less definitive than anticipated; the amide carbon atom, typically observed at a chemical shift of 155.9 ppm for compound **43** was not observed in the spectrum but an additional peak at 152. 5 ppm evaded assignment. On a more promising note, the tertiary butyl signal at 28.4 ppm was entirely absent from the spectrum; in fact, no further peaks occurred upfield from 38.7 ppm.

Overall, the spectroscopic data accounted for the anticipated findings and served to suggest that the synthesis of compound **44** was a success.

2.2.4 Step 4: Coupling Reaction with Photophore to form the Photosensitive Ligand

The final step in our synthetic scheme necessitated the extension of the MCR core with a reactive unit that could be activated by photosensitization with light of a defined wavelength. After meticulous inspection of the literature, it was decided to employ pentafluorobenzoyl chloride to install the "warhead" of the probe. It was envisaged that the amide formation, with this commercially available reagent, would be facile, which was a significant consideration due to the project's time constraints. However, it was important to acknowledge a potential pitfall associated with the proposed scheme; the presence of a competing, undesired reaction of the acyl chloride unit with the secondary amine moiety in the MCR scaffold. Nevertheless, it was anticipated that the precursors would assemble according to our desired outcome; with acylation of the primary amine occurring exclusively.

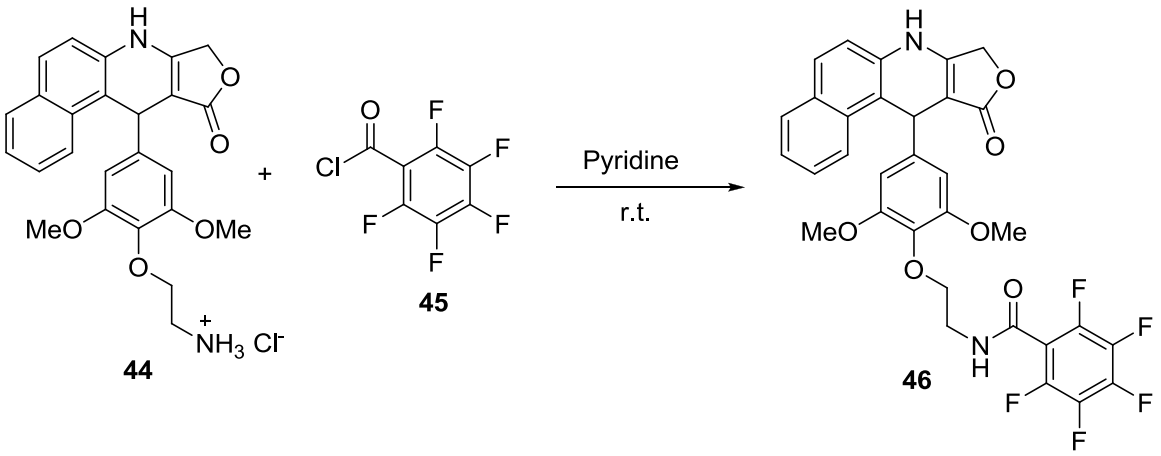

Scheme 17

Compound **47** was thus prepared through a coupling reaction between pentafluorobenzoyl chloride (**45**) and the hydrochloride salt of the ligand. Accordingly, the hydrochloride salt was dissolved in

dry pyridine and stirred at room temperature. To the resulting solution, the commercial reagent, pentafluorobenzoyl chloride, was added at a rate of one drop per minute via an air-tight syringe. The reaction solution was then thoroughly stirred under an inert argon atmosphere overnight. The remaining pyridine was subsequently removed under reduced pressure to reveal a light-brown oil of the crude product that was subsequently partitioned between water and ethyl acetate. Next, the organic layer was washed with three successive quantities of water, dried over anhydrous sodium sulfate and filtered under reduced pressure. Finally, the filtrate was evaporated in vacuo to reveal a bright-yellow oil that was purified by flash column chromatography to afford **46** as a white crystalline powder in a yield of 36 %.

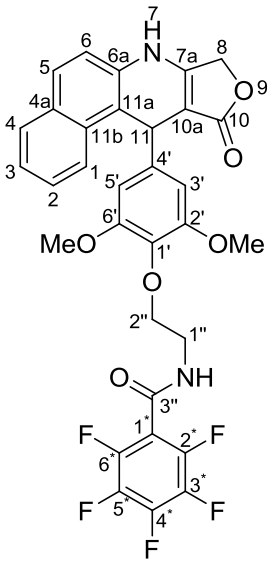

46

Figure 10

High-resolution mass spectrometry gave promising results and served to confirm the identity of the desired target molecule, compound **46**. The molecular ion peak (M^+) which corresponded to the base peak at 626.15265, matched the calculated isotopic mass of 626.1476 ($C_{32}H_{23}F_5N_2O_6$). In the infrared spectrum, a medium intensity amide C=O stretch was observed at 1726 cm^{-1} and another medium-intensity C-F stretch was located at 1233 cm^{-1} (*lit.*[62] 1400-1000 cm^{-1}).

Through the addition of the pentafluoro-photophore, no additional hydrogen atoms are added to the structure. Therefore, it was anticipated that the ^{1}H NMR spectrum of compound **44** would overlap with the ^{1}H NMR spectrum of compound **46**. It was readily observed that all of the ^{1}H NMR signals for **44** were found in the ^{1}H NMR spectrum of compound **46**. However, the solvent impurities encountered in the ^{1}H NMR spectrum of **44** were largely absent from the spectrum of the target molecule.

It is important to note however, that if the acyl group of the photophore had added directly to the secondary amine moiety we would expect to see shifting of the H-8 signal. Conversely, if the photophore had added in the desired position we would expect to observe shifting of the H-1″ signal. In the ^{1}H NMR spectrum the H-8 signal shifted from 6.54 ppm for **44** to 6.51 ppm for **46** and the H-1″ signal shifted from 3.94 ppm for **44** to 3.83 ppm for **46**. Neither signal, showed significant shifting to allow for definitive assignment of the position of the photophore. However, crystallographic studies conducted in the future should reveal more information regarding its true orientation in the molecule **46**.

The successful synthesis of the target molecule was further confirmed in the ^{13}C NMR spectrum by the presence of four additional aromatic peaks and the existence of a quaternary amide signal at a chemical shift of 172.0 ppm. It was not possible to assign the C-F aromatic carbon signals definitively, due to the ambiguous nature of the spectrum and evidence of additional splitting of the carbon signals through coupling to ^{19}F. The use of C-H correlated 2-D NMR, NOSEY, ^{19}F NMR and DEPT spectroscopy in the future should allow for a less equivocal assignment of the aromatic carbon signals.

The weight of the spectroscopic evidence suggests that the synthesis of the photoprobe, compound **46**, was effectively achieved. Although further spectroscopic and crystallographic studies must be conducted in the future to allow for definitive claims regarding the regioselectivity of the reaction product.

CHAPTER 3: CONCLUSIONS AND FUTURE POSSIBILITIES

An analogue of 4-aza-podophyllotoxin was successfully constructed utilizing a variation of the Hantzsch dihydropyridine MCR. Furthermore, as was our aim, a photophore, the commercially available pentafluorobenzoyl chloride, was tethered to the 4-aza-podophyllotoxin scaffold to allow for photoaffinity labelling experiments. However, the site at which the photophore added could not be unambiguously determined by ^{1}H NMR alone. In the future, crystallographic experiments conducted on the target photoprobe **46** should reveal valuable structural information regarding the site at which the acyl group tethers to the hydrochloride salt **44**.

One major assumption that had to be made is that the MCR product, containing the tether and "warhead" **46**, would still dock into the active site originally occupied by the original 4-aza-podophyllotoxin derivatives. The first step undertaken in biochemical testing of this compound would be to run a cytotoxicity screen to determine whether or not the photoprobe **46** is still biologically active. If the screening tests reveal that the probe is not active, then it does not occupy the relevant binding site and further cross-linking experiments would be useless. These findings would necessitate the synthesis of another probe, wherein the cross-linking moiety is moved to another position on the scaffold or another photophore is potentially used as the cross-linking agent.

If the cytotoxicity tests reveal that the photoprobe is biologically active - with the desired functional probe in hand we would be in a position to use this molecule in biochemical experiments designed to afford additional information concerning the mode of action of these proposed podophyllotoxin analogues. This information would be very useful in guiding the further development of these compounds as anti-cancer agents.

It is thus envisaged that our biochemical collaborators in the USA will now incubate the probe with the putative target enzymes, for instance tubulin, hopefully allowing for the molecule to dock into the active site. This will then be followed by treatment with a suitable wavelength light source to promote cross-linking of the reactive pentafluoro- moiety with amino acid resides in close

proximity to the molecule. Next a trypsin digest would result in a polypeptide “soup” which would then be analysed by peptide mass spectroscopic techniques. Identification of polyamino segments containing the additional mass of the probe should provide information on the regions of the protein where the probe was docked before photo cross-linking, thus helping to confirm the identity of the active sites. This important information could then be utilized in future design of inhibitors and would be invaluable for *in silico* molecular docking experiments.

CHAPTER 4: EXPERIMENTAL PROCEDURES

4.1 General Experimental Procedures

4.1.1 Purification of Solvents and Reagents

All solvents utilized for preparative chromatography and for reactions occurring under anhydrous or inert conditions were distilled prior to use. Absolute ethanol was distilled from clean, dry magnesium turnings and triethylamine from calcium hydride. *N*,*N*-dimethylformamide (DMF) was distilled from and stored over potassium hydroxide. Pyridine was distilled from a 1:1 mixture of potassium hydroxide and 4 Å molecular sieves and stored over potassium hydroxide. All reagents were obtained from commercial sources and used without further purification.

4.1.2 Thin-layer Chromatography and Chromatographic Separations

Thin-layer chromatography (TLC) was conducted on Macherey-Nagel Alugram Sil G/UV_{254} platespre-coated with 0.25 mm silica gel 60. Compounds were detected under ultraviolet light (254 nm or 366 nm) in a Bayer UV-cabinet II (BYL00596) to generate the quoted R_f (retention factor) values. Macherey-Nagel Kieselgel 60 silica gel (particle size 0.063-0.020 mm), with a mass 30 times that of the material to be purified, was used as the absorbent for conventional preparative column chromatography. The desired product was then loaded onto the surface of wet-packed silica and coated with a thin layer of acid-washed sand. Elution was accomplished using solvent-mixtures of EtOAc and hexane or EtOAc, Et_3N and MeOH as the mobile phase.

4.1.3 Physical and Spectroscopic Data

^{1}H nuclear magnetic resonance (NMR) spectra were recorded on a Bruker AVANCE 300 (300.13 MHz) or a Bruker 400 (400.13 MHz) spectrometer. Unless otherwise indicated, the NMR spectra were measured in deuterated chloroform ($CDCl_3$) and the chemical shifts were reported in parts per million (ppm) downfield from tetramethylsilane, the internal standard. Coupling constants are given in Hertz. Abbreviations used include: s-singlet, d-doublet, t-triplet, q-quartet and m-multiplet. NMR data are reported as follows: chemical shift (integration of signal, splitting pattern, coupling constant(s), assignment).

^{13}C NMR (^{1}H decoupled) spectra were recorded on a Bruker ADVANCE 300 (75.47 MHz) or Bruker 400 (100.63 MHz) spectrometer. Unless noted to the contrary, spectra were recorded in $CDCl_3$ and chemical shifts were reported in ppm relative to the central signal of $CDCl_3$, taken as δ 77.00.

Infrared Spectra (IR) were recorded on a Bruker TENSOR 2007 IFS-25 Fourier Transform spectrometer. The spectra were then manipulated and analysed using OPUS™ software. Signals were defined as a st-stretch, rock, or δ oop of vw-very weak, w-weak, m-medium or s-strong intensity. IR spectral data are reported as follows: wavenumber (intensity, assignment).

Mass spectra were recorded on a Kratos MS 9/50, VG70EMS or a VG70SEQ mass spectrometer at 70ev and 200μA utilizing **EI** (electron impact), **ESI** (electrospray ionization) or **APCI** (atmospheric pressure chemical ionization) systems.

4.1.4 Other General Procedures

Evaporation of a solvent under reduced pressure refers to the removal of a solvent on a rotary evaporator at approximately 45°C.

Evaporation of a solvent *in vacuo* refers to the removal of a solvent on a rotary evaporator at approximately 45°C followed by further evaporation under high-vacuum.

Evaporation of a solvent under high vacuum refers to the removal of a solvent under high-vacuum exclusively.

4.2 Testing the Waters – Practise MCR

4.2.1 Synthesis of 11-(4-hydroxy-3,5-dimethoxyphenyl)-8,11-dihydrobenzo[f]furo[3,4-b]quinolin-10(7H)-one by MCR (compound 47)

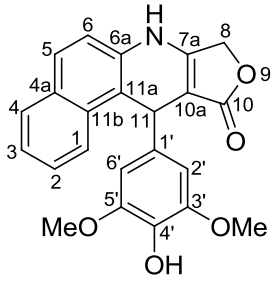

47

A mixture of β-naphthylamine (132.2 mg, 1.000 mmoles, 1.0 equiv.), tetronic acid (100.1 mg, 1.000 mmoles, 1.0 equiv.) and syringaldehyde (182.2 mg, 1.0 mmoles, 1.0 equiv.) in absolute ethanol (2.00 cm^3) was refluxed in a reaction vessel exposed to the atmosphere. The reaction was monitored by thin-layer chromatography (50%EtOAc: Hexane) every hour until the disappearance of reactants was noted under UV-light at 4 hours. Thereafter, the reaction mixture was allowed to cool to room temperature and the precipitated product was collected by filtration and washed with absolute ethanol (2.00 cm^3) chilled by submersion in liquid nitrogen. The solid product was then dried *in vacuo* to reveal a light brown powder (101.4 mg, 54%, $C_{23}H_{19}NO_5$, 389.40 $g.mol^{-1}$); **mp** (these molecular scaffolds do not melt but rather decompose at higher temperatures); **IR** : $\nu_{max}(cm^{-1})$ = 3500 (w, st, N-H), 3260 (w, st, O-H), 1645 (s, st, C=O), 1534 (s, st, C=C), 1196 (m, st, as, C-O-C), 1181 (m, st, sy, C-O-C), 1107 (s, st, C-O) 1107 (C-O), 772 (m, ar, C-H oop); **LRMS *m/z*(EI)** Found M^+, 389.17. (M^+ 75%, $C_{23}H_{19}NO_5$ requires 389.4028), 391 (4), 390 (31), 387 (39), 356 (10), 326 (7), 284 (14), 238 (12), 237 (71), 236.1 (100) 208 (31);**^{1}H NMR** δ_H (300 MHz, DMSO)δ_H (300 MHz, DMSO) 10.23 (1 H, s, NH), 8.16 (1 H, bs, OH), 7.96 – 7.76 (3 H, m, ArH, H-2 and H-3 and H-6), 7.52 – 7.20 (3 H, m, ArH, H-1 and H-4 and H-5), 6.44 (2 H, s, H-2′ and H-6′), 5.58 (1 H, s, H-11), 4.93 (2 H, dd, *J* 15.01 and 15.00 Hz, H-8), 3.59 (6 H, s, OCH_3);**^{13}C NMR** 172.2 (C-10), 156.9 (C-7a), 147.8 (ArC), 136.4 (ArC), 135.0 (ArC), 134.3 (ArCH), 134.2 (ArCH), 132 (ArC), 131.7

(ArC), 131.0 (ArC), 130.7 (ArCH), 114.9 (ArC), 106.6 (ArCH, C-2′ and C-6′), 104.5 (ArCH), 97.4 (C-10a), 58.8 (C-8), 57.0 (OMe), 55.1 (C-11).

4.3 Synthesis of the Photosensitive Ligand

4.3.1 Synthesis of tert-butyl [2-(4-formyl-2,6-dimethoxyphenoxy)ethyl]carbamate (compound 40)

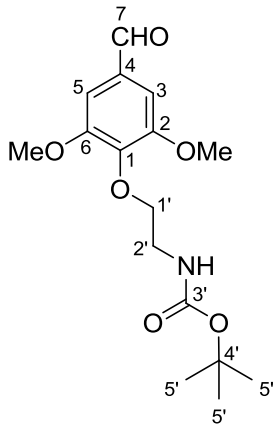

40

A mixture of syringaldehyde (3.00 g, 16.5 mmoles, 1.0 equiv.), 2-(Boc-amino)ethyl bromide (3.69 g, 16.5 mmoles, 1.0 equiv.), potassium carbonate (K_2CO_3) (9.10 g, 65.9 mmoles, 4.0 equiv.) and anhydrous *N*,*N*-dimethylformamide (DMF) (60 cm^3) was stirred at 40°C for three days until the complete disappearance of syringaldehyde, as revealed by thin-layer chromatography (2-(Boc-amino)ethyl bromide is not visible under UV light). Thereafter, the reaction mixture was filtered over diatomaceous earth and concentrated *in vacuo*. The resulting residue was partitioned between ethyl acetate and water. The organic layer was washed with water, an aqueous solution of 5% $NaHCO_3$ and brine, dried over anhydrous sodium sulfate (Na_2SO_4), filtered under water pressure and concentrated *in vacuo*. The crude product was then purified by column chromatography (eluent: 50% EtOAc:Hexane) on silica gel to afford a cream coloured solid **40** in a yield of 34%, after drying *in vacuo* overnight (1.8278g, 34%, $C_{16}H_{23}NO_5$, 325.36 $g.mol^{-1}$); **mp** (these molecular

scaffolds do not melt but rather decompose at higher temperatures); $\mathbf{R}_f$ = 0.5 (50% EtOAc: Hexane); **IR**: $\nu_{max}(cm^{-1})$ = 3383 (m, st, N-H), 1727 (s, st, C=O amide), 1687 (s, st, C=O), 1585 (m, st, ar C-C), 1390 (w, st, CH_3), 1329 (s, st, C-N), 1123 (s, st, C-O), 843 (m, ar, C-H oop); **LRMS *m/z*(EI)** Found M^+, 325.86. (M^+ 10%, $C_{16}H_{23}NO_5$ requires 325.1525), 523 (11),369 (4), 413 (6); **^{1}H NMR** δ_H (300 MHz, $CDCl_3$) 9.88 (1 H, s, H-7), 7.28 (1 H, s, NH), 7.14 (2 H, s, H-3 and H-5), 4.15 (2 H, t, *J* 4.8 Hz, H-1′), 3.95 (6 H, s, OMe), 3.41 (2 H, dd, *J* 6.0 and 9.0 Hz, H-2′), 1.45 (9 H, s, H-5′); **^{13}C NMR** 190.9 (C-7), 156.1 (C-3′), 153.7 (ArC, C-2 and C-6), 142.2 (ArC, C-1), 132.1 (ArC,C-4), 106.5 (ArCH, C-3 and C-5), 79.0 (C-4′), 73.4 (C-1′), 56.18 (OMe), 40.7 (C-2′) 28.4 (C-5′).

4.3.2 Synthesis of tert-butyl {2-[2,6-dimethoxy-4-(10-oxo-7,8,10,11-tetrahydrobenzo[f]furo [3,4-b]quinolin-11-yl)phenoxy]ethyl}carbamate (compound 43)

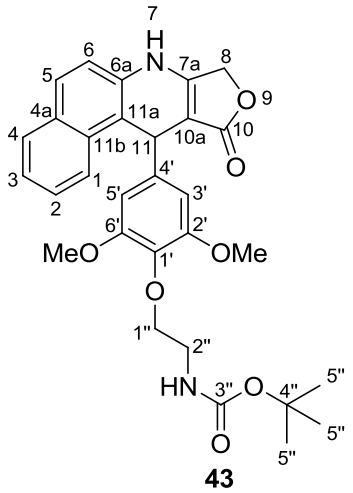

43

A mixture of β-naphthylamine (0.722 g, 5.46 mmoles, 1.0 equiv.), tetronic acid (0.547 g, 5.46 mmoles, 1.0 equiv.) and *tert-butyl 2-(4-formyl-2,6-dimethoxyphenoxy)ethylcarbamate* (1.778 g, 5.5 mmoles, 1.0 equiv.) in absolute ethanol (17.00 cm^3) was refluxed in a reaction vessel exposed to the atmosphere. The reaction was monitored by thin-layer chromatography (50% EtOAc: Hexane) every hour until the disappearance of reactants was noted under UV-light at 5 hours. Thereafter, the reaction mixture was allowed to cool to room temperature and the precipitated product was collected by filtration and washed with absolute ethanol (2.00 cm^3) chilled by submersion in liquid

nitrogen.The solid product was then purified by flash column chromatography (eluent: 50% EtOAc:Hexane) on silica gel to afford **40** as a white, fluffy, crystalline powder in a yield of 19% after drying *in vacuo* for 12 hours (543.5 mg, 19%, $C_{30}H_{32}N_2O_7$, 532.58 g.mol^{-1}); **mp** (these molecular scaffolds do not melt but rather decompose at higher temperatures); $\mathbf{R}_f$= 0.6 (EtOAc); **IR** : ν_{max}(cm^{-1}) = 2937 (w, st, N-H), 1721 (m, st, C=O amide), 1653 (m, st, C=O), 1588 (m, st, ar C-C), 1531 (m, st, C=C), 1364 (w, st, CH_3), 1323 (w, st, C-N), 1215 (w, st, as, C-O-C), 1213 (w, st, sy, C-O-C), 1121 (s, st, C-O), 1010 (m, st, C-N), 744 (m, ar, C-H oop); **LRMS *m/z*(APCI)** Found $[M+H]^+$, 533.00. ($[M+H]^+$ 46%, $C_{30}H_{33}N_2O_7$ requires 533.6012), 534 (24), 434 (26), 433 (100), 431 (10); **^{1}H NMR**δ_H (300 MHz, $CDCl_3$) 7.86 (1 H, broad s, NH), 7.82 – 7.67 (3 H, m, H-2 and H-3 and H-6), 7.44 – 7.31 (3 H, m, H-1 and H-4 and H-5), 7.14 (2 H, d, *J* 8.7 Hz, H-3′ and H-5′), 6.48 (2 H, s, H-8), 5.79 (1 H, s, H-11), 4.12 (2 H, q, *J* 7.1 Hz, H-2″), 3.68 (6 H, s, OCH_3), 3.40 – 3.20 (2 H, m, H-1″), 1.42 (9 H, s, H-5″); **^{13}C NMR** 173.1 (C-10), 156.3(C-3″), 155.9 (C-7a), 153.7 (ArCH), 140.8 (ArC),134.9 (ArC), 134.5 (ArCH),129.4 (ArC), 128.4 (ArCH), 127.3 (ArCH), 124.5 (ArC), 123, 6 (ArC),114.9 (ArC), 104.7 (ArC), 99.5 (C-10a), 99.0 (C-4″), 58.9 (C-1″), 65.3 (OMe), 55.9 (C-11), 37.5 (C-2″), 28.4 (C-5″).

4.3.3 Synthesis of 2-[2,6-dimethoxy-4-(10-oxo-7,8,10,11-tetrahydrobenzo[f]furo[3,4-b]quinolin-11-yl)phenoxy)ethanaminium chloride (compound 44)

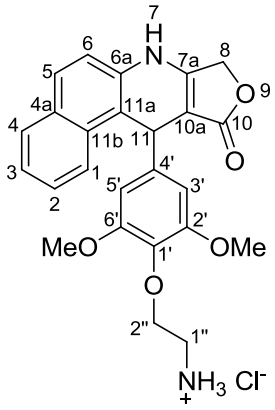

44

Compound **43** (0.535 g, 1.0 mmoles, 1.0 equiv.) was added to a solution of hydrogen chloride in dioxane (0.45 ml, 1.1 mmoles, 4 M, 1.1 equiv.) and the resulting mixture was stirred for 1.5 hours

at room temperature. Thereafter, the excess solvent was removed under reduced pressure and the residue was concentrated *in vacuo* overnight to reveal the hydrochloride salt as a light brown flaky powder in quantitative yield (0.479 g, 100%, $C_{25}H_{25}ClN_2O_5$, 468.93 g.mol^{-1}); **mp** (these molecular scaffolds do not melt but rather decompose at higher temperatures); **IR** : ν_{max}(cm^{-1}) = 2899 (m broad, st, NH_3^+), 1660 (m, st, C=O), 1586 (m, st, ar C-C), 1533 (m, st, C=C), 1346 (w, st, CH_3), 1323 (w, st, C-N), 1216 (s, st,C-O-C),1118 (s, st, C-O), 1000 (w, st, C-N), 754 (m, ar, C-H oop); **LRMS *m/z*(ESI)** Found $[M+H]^+$, 433.22. ($[M+H]^+$ 88%, $C_{25}H_{25}ClN_2O_5$ requires 468.1452), 567 (9), 517 (9),431 (46), Found $[M+M]^+$, 866.44. ($[M+M]^+$ 100%, $C_{50}H_{25}ClN_2O_4$ (dimer) requires 936.2904), 861 (70), 803 (25), 802 (20); **^{1}H NMR**δ_H (300 MHz, DMSO) 10.59 (1 H, s, NH_3^+), 7.96 – 7.72 (3 H, m, H-2 and H-3 and H-6), 7.47 – 7.25 (3 H, m, H-4 and H-1 and H-5), 6.81 (1 H, bs, NH), 6.54 (2 H, s, H-8), 5.67 (1 H, s, H-11), 4.95 (2 H, q, *J* 15.9 Hz, H-1′′), 3.94 (2 H, t, *J* 5.1 Hz, H-2′′), 3.63 (6 H, s, OCH_3); **^{13}C NMR** 172.1 (C-10),152.5 (C-7a), 142.3 (ArC), 135.1 (ArC), 133.9 (ArCH), 129.0 (ArCH), 128.4 (ArC), 126.8 (ArCH), 123, 6 (ArC), 114.9 (ArC), 104.7 (ArC), 96.9 (C-10a), 69.0 (C-8), 65.3 (OMe), 55.8 (C-11).

4.3.4 Synthesis of N-(2-(2,6-dimethoxy-4-(10-oxo-7,8,10,11-tetrahydrobenzo[f]furo[3,4-b]quinolin-11-yl)phenoxy)ethyl)-2,3,4,5,6-pentafluorobenzamide (compound 46)

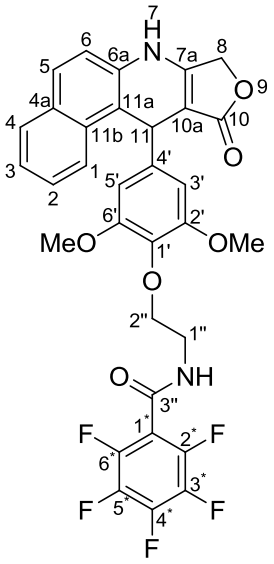

46

The hydrochloride salt, compound **44** (55 mg, 0.12 mmoles, 1.1 equiv.), was dissolved in anhydrous pyridine and stirred at room temperature. To the resulting solution, pentafluorobenzoyl chloride (0.015 cm^3, 24 mg, 0.11 mmoles, 1.0 equiv.) was added at a rate of a drop a minute. The reaction contents were then stirred under an inert argon atmosphere for 12 hours. Excess pyridine was removed under reduced pressure to reveal a light brown oil of the crude product that was partitioned between water and ethyl acetate. The organic layer was washed with 3 volumes of tap water, dried over anhydrous Na_2SO_4 and filtered under reduced pressure. Evaporation of the filtrate *in vacuo* revealed a bright yellow oil that was purified by flash column chromatography (eluent: 50% EtOAc:Hexane) on silica gel to afford **46** as a white powder in a yield of 19% after drying *in vacuo* for 12 hours (23.90 mg, 36%, $C_{32}H_{23}F_5N_2O_6$, 626.53 $g.mol^{-1}$); **mp** (these molecular scaffolds do not melt but rather decompose at higher temperatures); $\mathbf{R}_f$ = 0.2 (50% EtOAc: Hexane); **IR** : $\nu_{max}(cm^{-1})$ = 3259 (broad, st, N-H), 2953 (w, str, N-H), 1726 (m, st, C=O amide), 1652 (s, st, C=O), 1590 (m, st, ar C-C), 1501 (s, st, C=C), 1356 (w, st, CH_3), 1324 (m, st, C-N), 1233 (m, st,C-F), 1214 (s, st, C-O-C),1122 (s, st, C-O), 990 (s, st, C-N), 746 (m, ar, C-H oop); **HRMS *m/z* (EI)** Found M^+, 626.15265. (M^+ 100%, $C_{32}H_{23}F_5N_2O_6$ requires 626.1476); 628 (10), 627 (35), 623 (9), 624 (35), 625 (20); **LRMS *m/z* (EI)** Found $[M+H]^+$, 628. ($[M+H]^+$100%), 626 (38), 628 (40), 608 (14), 629 (10); **^{1}H NMR** δ_H (300 MHz, DMSO) 10.29 (1 H, s, NH), 7.99 – 7.76 (3 H, m, H-2 and H-3 and H-6), 7.52 – 7.17 (3 H, m, H-1 and H-4 and H-5), 6.51 (1 H, bs, NH), 6.54 (2H, s, H-2′ and H-3′), 5.65 (1 H, s, H-11), 4.94 (1 H, dd, *J* 15.01 Hz and 12.01 Hz, H-8), 3.94 (2 H, t, *J* 6.0 Hz, H-2″), 3.83 (2 H, d, *J* 5.3 Hz, H-1″), 3.59 (6 H, s, OCH_3); **^{13}C NMR** 172.0 (C-10), 157.2 (C-3″), 156.7 (C-7a), 152.6 (ArC), 141.8 (ArC), 135.0 (ArC), 134.5 (ArCH), 130.6 (ArC), 130.6 (ArC),128.3 (ArC), 126.8 (ArC), 123.2 (ArC), 123.2 (ArC), 117.5 (ArC), 114.9 (ArC), 105.0 (ArCH), 97.0 (C-10a), 70.6 (C-1″), 73.4 (C-8), 65.3 (C-2″), 60.2 (OMe).

CHAPTER 5: REFERENCE LIST

1. M. L. Bolognesi, N. Calonghi, C. Mangano, L. Masotti and C. Melchiorre, *J. Med. Chem.*, 2008, **51**, 5463-5467.
2. S. Keinan, W. D. Paquette, J. J. Skoko, D. N. Beratan, W. Yang, S. Shinde, P. A. Johnston, J. S. Lazo and P. Wipf, *Org. Biomol. Chem.*, 2008, **6**, 3256-3263.
3. V. K. Tandon, B. C. Rakeshwar, R. V. Singh, S. Rai and D. B. Yadav, *Bioorg. Med. Chem. Lett.*, 2004, **14**, 1079-1083.
4. *Medical Dictionary - Anthracyclines*, http://www.medterms.com/script/main/art.asp?articlekey=20134, Accessed 10/05/2010, 2010.
5. S. Ko, C. Lin, T. Zhijay, Y.-F. Wang, C.-C. Wang and C.-F. Yao, *Tetrahedron Lett.*, 2006, **47**, 487-492.
6. M. Brisson, T. Nguyen, P. Wipf, B. Joo, B. W. Day, J. S. Skoko, E. M. Schreiber, C. Foster, P. Bansal and J. S. Lazo, *Mol. Pharmacol.*, 2005, **68**, 1810-1820.
7. R. P. Verma, *Anti-Cancer Agents Med. Chem.*, 2006, **6**, 489-499.
8. N. Calonghi, E. Pagnotta, C. Parolin, C. Mangano, M. L. Bolognesi, C. Melchiorre and L. Masotti, *Biochem. Biophys. Res. Commun.* , 2007, **342**, 409-413.
9. Z. Chen, Y. Yang, N. Zhang, J. A. Turpin, R. W. Buckheit, C. Osterling, J. J. Oppenheim and O. M. Z. Howard, *Antimicrob. Agents Chemother.*, 2003, **47**, 2810-2816.
10. A. L. Baggish and D. R. Hill, *Antimicrob. Agents Chemother.*, 2002, **46**, 1163-1173.
11. J. Zhou, L. Duan, H. Chen, X. Ren, Z. Zhang, F. Zhou, J. Liu, D. Pei and K. Ding, *Bioorg. Med. Chem. Lett.*, 2009, **19**, 5091-5094.
12. G. J. Kapadia, M. A. Azuine, V. Balasubramanian and P. Sridhar, *Pharmacol. Res.*, 2001, **43**, 363-367.
13. T.-S. Lin, L.-Y. Zhu, S.-P. Xu, A. A. Divo and A. C. Sartorelli, *J. Med. Chem.*, 1991, **34**, 1634-1639.
14. E. A. Couladouros, Z. F. Plyta and V. P. Papageorgiou, *J Org. Chem.*, 1996, **61**, 3031-3033.
15. V. V. Russkikh, *Russ. Chem. Bull.*, 1992, **41**, 555-561.
16. R. A. Illos, D. Shamir, L. J. W. Shimon, I. Zilbermann and S. Bittner, *Tetrahedron Lett.*, 2006, **47**, 5543-5546.

17. C. Joachim and J. K. Gimzewski, in *Molecular Machines and Motors*, ed. J.-P. Sauvage, Springer-Verlag, Heidelberg, Berlin, Editon edn., 2001, vol. 99, p. 307.
18. B. Liu and S.-J. Ji, *Synth. Commun.*, 2008, **38**, 1201-1211.
19. B. K. Banik, M. Fernandez and C. Alvarez, *Tetrahedron Lett.*, 2005, **46**, 2479-2482.
20. Y. Kita, H. Tohma, M. Inagaki, K. Hatanaka and T. Yakura, *J. Am. Chem. Soc.*, 1992, **114**, 2175-2180.
21. J. L. Luche, C. Einhorn and J. Einhorn, *Tetrahedron Lett.*, 1990, **31**, 4125-4128.
22. T. J. Mason, *Chemical Society Reviews*, 1997, **26**, 443-451.
23. X.-F. Zeng, S.-J. Ji and S.-Y. Wang, *Tetrahedron* 2005, **61**, 10235-10241.
24. J.-T. Li, W.-Z. Yang, G.-F. Chen and T.-S. Li, *Synth. Commun.*, 2003, **33**, 2619-2625.
25. R. Cella and H. A. Stefani, *Tetrahedron*, 2009, **65**, 2619-2641.
26. G. Cravotto and P. Cintas, *Chem. Soc. Rev.*, 2006, **35**, 180-196.
27. G. Cravotto and P. Cintas, *Chem.--Eur. J.*, 2007, **13**, 1902-1909.
28. R. Mietchen, *Ultrasonics*, 1992, **30**, 173-179.
29. M. L. D. Palacios and R. Pellón, *Synth. Commun.*, 2003, **33**, 1777-1781.
30. S.-J. Ji and S.-Y. Wang, *Synlett*, 2003, 2074-2076.
31. D. D. Perrin and W. L. F. Armarego, *Purification of Laboratory Chemicals*, 4th edn., Pergamon Press, Oxford, 1998.
32. E. Pretsch, P. Bűhlmann and C. Affolter, *Structure Determination of Organic Compounds: tables of spectral data*, 3rd edn., Springer-Verlag, Berlin, Heidelberg, Germany, 2000.
33. S. N. Singh and R. S. Singh, *Spectrochim. Acta*, 1967, **24A**, 1591-1597.
34. S. Gunasekaran and B. Anita, *Indian J. Pure Appl. Phys.*, 2008, **46**, 833-838.
35. E. Perozo-Rondón, R. M. Martín-Aranda, B. Casal, C. J. Durán-Valle, W. N. Lau, X. F. Zhang and K. L. Yeung, *Catal. Today*, 2006, **114**, 183-187.
36. S.-J. Ji, S.-Y. Wang, Y. Zhang and T.-P. Loh, *Tetrahedron*, 2004, **60**, 2051-2055.
37. B. J. Leslie and P. J. Hergenrother, *Chem. Soc. Rev.*, 2008, **37**, 1347-1360.
38. E. P. Solomon, L. R. Berg and D. W. Martin, *Biology*, 6th edn., Thompson Brooks/Cole, USA, 2002.
39. G. Dormán and G. D. Prestwich, *Trends Biotechnol.*, 2000, **18**, 67-77.
40. A. Singh, R. Thornton and F. H. Westheimer, *J. Biol. Chem.*, 1962, **237**, PC 3006-PC 3008.
41. K. A. Schnapp, R. Poe, E. Leyva, N. Soundararajan and M. S. Platz, *Bioconjugate Chem.*, 1993, **4**, 172-177.
42. N. Soundararajan and M. S. Platz, *J. Org. Chem.*, 1989, **55**, 2034-2044.

43. F. Kotzyba-Hibert, I. Kapfer and M. Goeldner, *Angew. Chem. Int. Ed.*, 1995, **34**, 1296-1312.
44. C. Canel, R. M. Moraes, F. E. Dayan and D. Ferreira, *Phytochem.*, 2000, **54**, 115-120.
45. M. Gordaliza, P. A. García, J. M. Miguel del Corral, M. A. Castro and M. A. Gómez-Zurita, *Toxicon*, 2004, **44**, 441-459.
46. I. V. Magedov, M. Manpadi, S. Van Slambrouck, W. F. A. Steelant, E. Rozhkova, N. M. Przheval'skii, S. Rogelj and A. Kornienko, *J. Med. Chem.*, 2007, **50**, 5183-5192.
47. S. Tu, Y. Zhang, J. Zhang, B. Jiang, R. Jia, J. Zhang and S. Ji, *Synlett*, 2006, **17**, 2785-2790.
48. C. Tratrat, S. Giorgi-Renault and H.-P. Husson, *Org. Lett.*, 2002, **4**, 3187-3189.
49. Y. Hitotsuyanagi, M. Fukuyo, K. Tsuda, M. Kobayashi, A. Ozeki, H. Itokawa and K. Takeya, *Bioorg. Med. Chem. Lett.*, 2000, **10**, 315-317.
50. D. I. Macdonald and T. Durst, *J. Org. Chem.*, 1988, **53**, 3663-3669.
51. F. E. Ziegler and J. A. Schwartz, *J. Org. Chem.*, 1978, **43**, 985-991.
52. A. S. Kende, M. L. King and D. P. Curran, *J. Org. Chem.*, 1981, **46**, 2826-2828.
53. L. H. Klemm, D. R. Olson and D. V. White, *J. Org. Chem.*, 1971, **36**, 3740-3743.
54. Y. Wu, J. Zhao, J. Chen, C. Pan, L. Li and H. Zhang, *Org. Lett.*, 2009, **11**, 597-600.
55. I. V. Magedov, M. Manpadi, E. Rozhkova, N. M. Przheval'skii, S. Rogelj, S. T. Shors, W. F. A. Steelant, S. Van Slambrouck and A. Kornienko, *Bioorg. Med. Chem. Lett.*, 2007, **17**, 1381-1385.
56. R. B. Silverman, *The Organic Chemistry of Drug Design and Drug Action*, 2nd edn., Elsevier Academic Press, MA, USA, 2004.
57. A. Dőmling, *Chem. Rev*, 2006, **106**, 17-89.
58. A. Saini, S. Kumar and J. S. Sandhu, *J. Sci. Ind. Res.*, 2008, **67**, 95-111.
59. *Hantzsch Dihydrioyridine (Pyridine) Synthesis*, www.organic-chemistry.org/namedreactions/hantzsch-dihydropyridine-synthesis.shtm, Accessed 22/02/2011, 2011.
60. L.-M. Wang, J. Sheng, L. Zhang, J.-W. Han, Z.-Y. Fan, H. Tian and C.-T. Qian, *Tetrahedron*, 2005, **61**, 1539-1543.
61. A. J. Brouwer, S. J. E. Mulders and R. M. J. Liskamp, *Eur. J. Org. Chem.*, 2001, 1903-1915.
62. E. Pretsch, P. Bűhlmann and C. Affolter, *Structure Determination of Organic Compounds*, Springer-Verlag, Berlin, Heidelberg, 2000.

APPENDIX

A 1.1: ^{1}H and ^{13}C NMR Spectra for Compounds Successfully Synthesized

A 1.1.1: ^{1}H NMR Spectrum of Compound 1

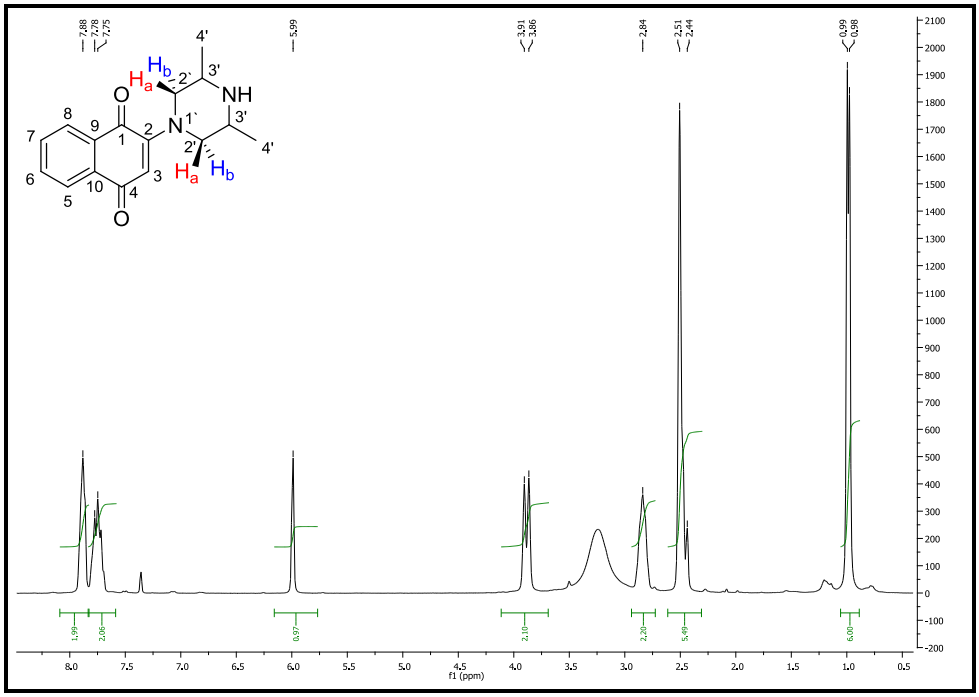

A 1.1.2: ^{13}C NMR Spectrum of Compound 1

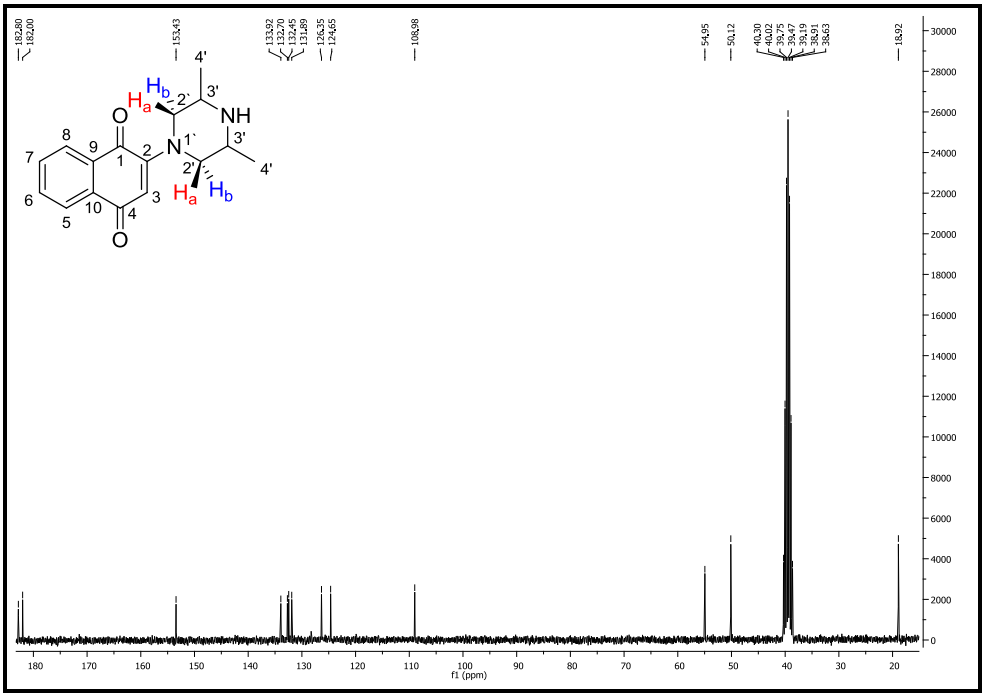

A 1.1.3: HSQC 2-D NMR Spectrum of Compound 1

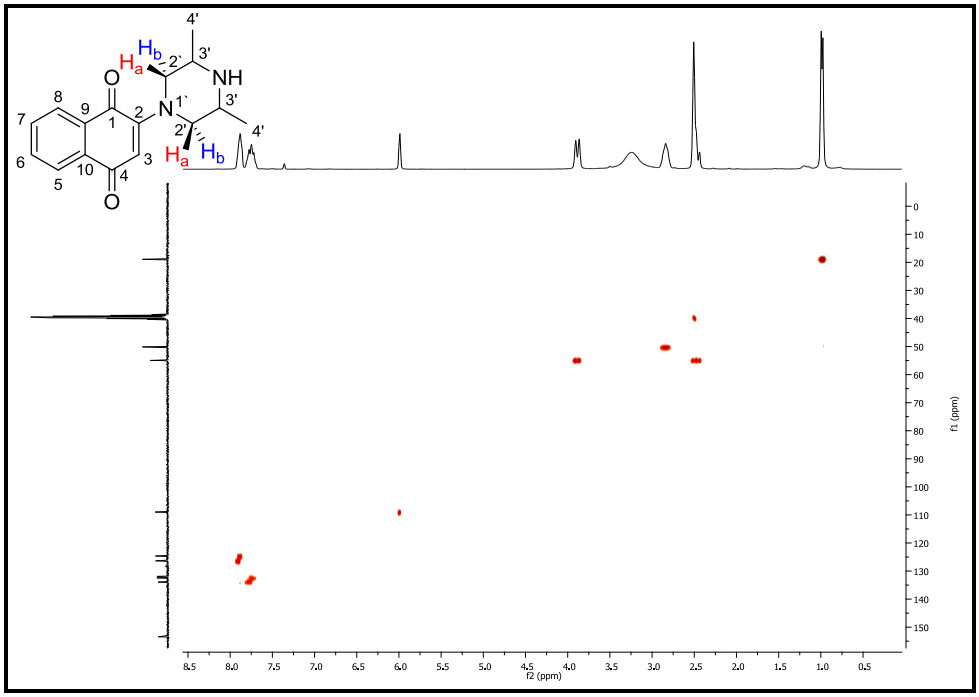

A 1.2.1: ^{1}H NMR Spectrum of Compound 2

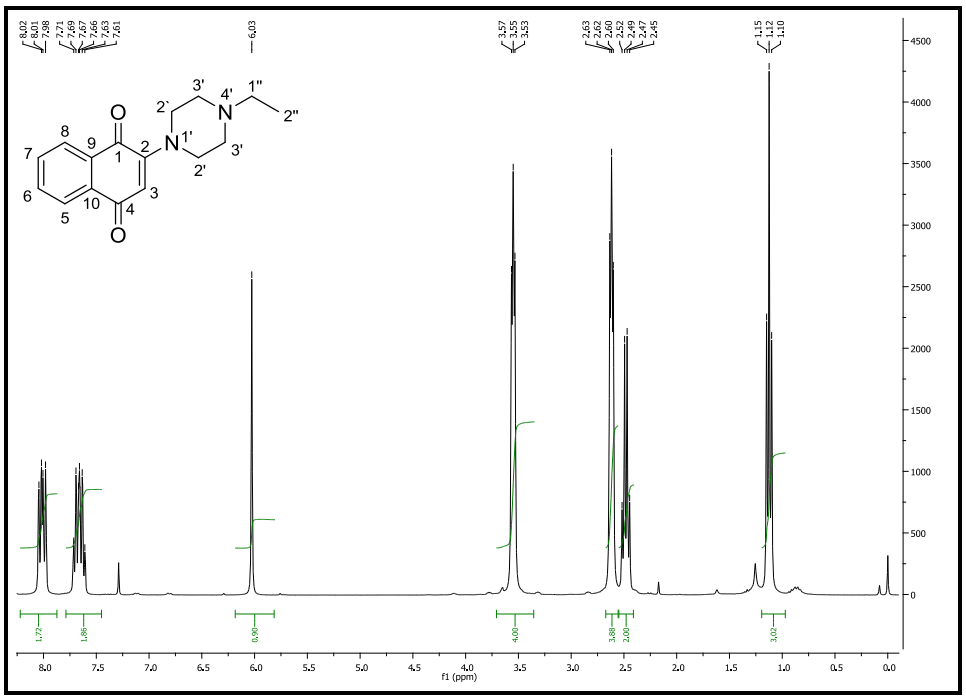

A 1.2.2: ^{13}C NMR Spectrum of Compound 2

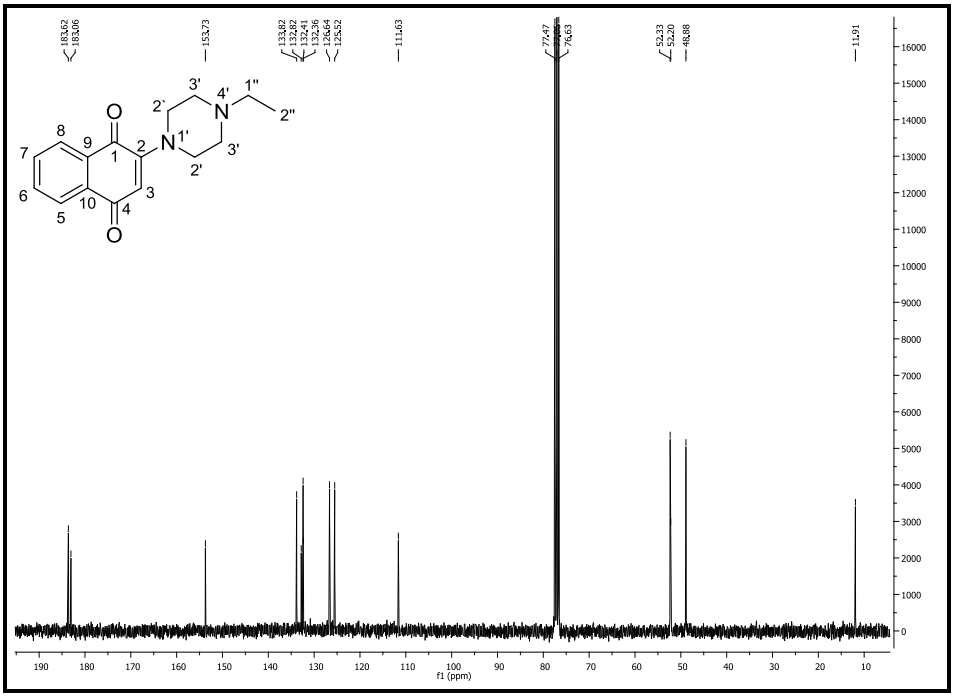

A 1.2.3: HSQC NMR Spectrum of Compound 2

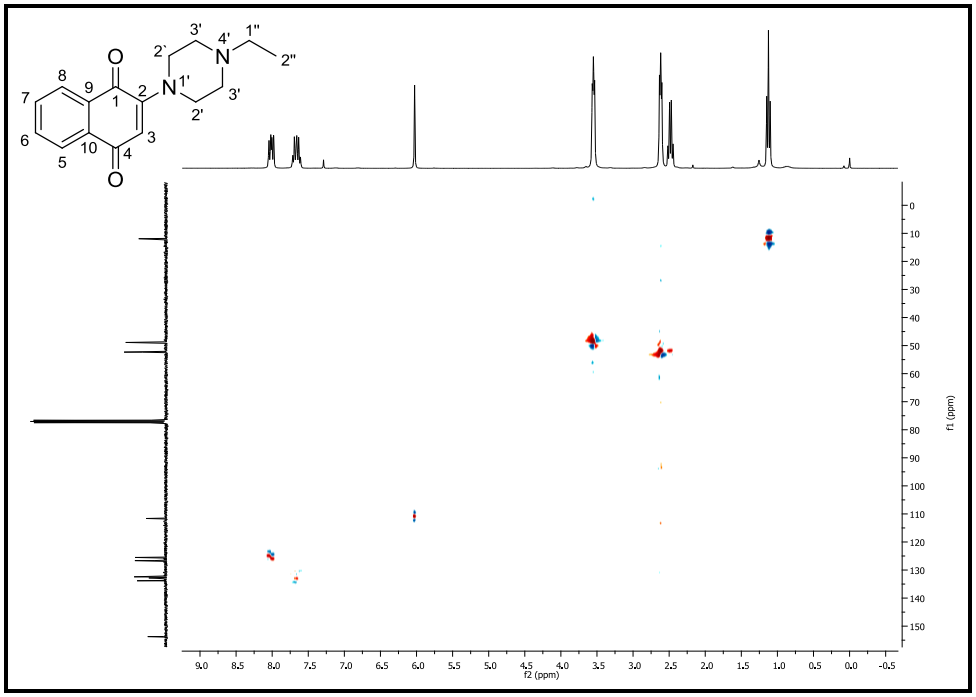

A 1.3.1: ^{1}H NMR Spectrum of Compound 3

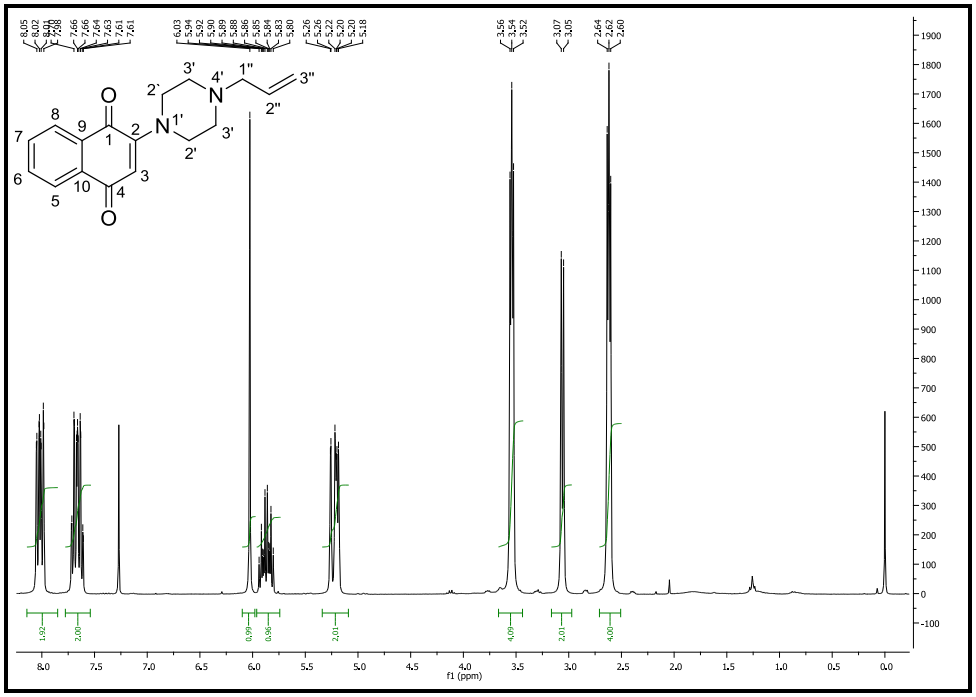

A 1.3.2: ^{13}C NMR Spectrum of Compound 3

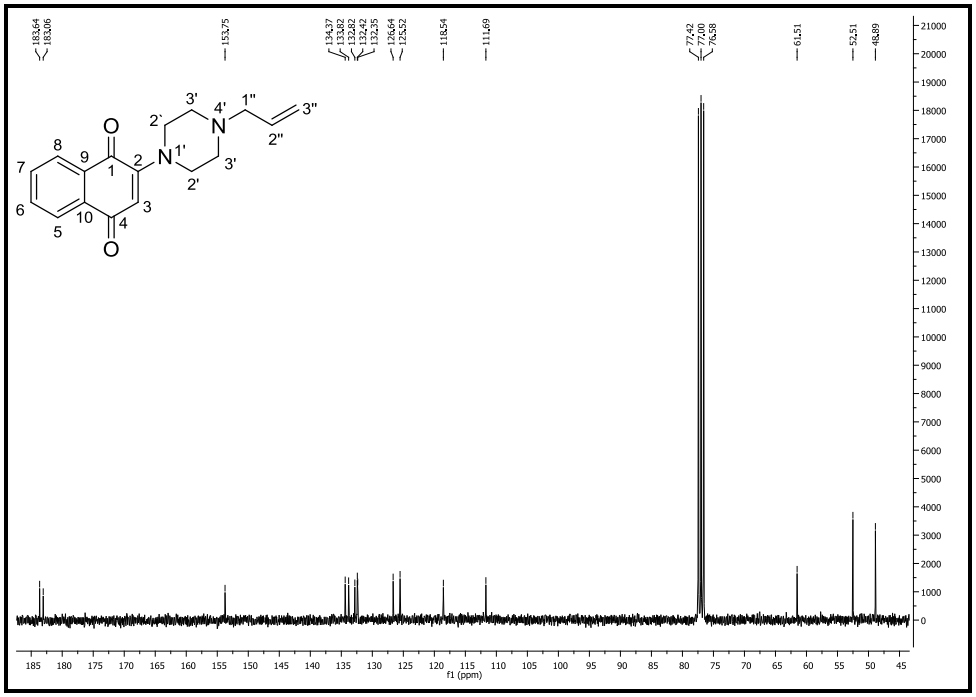

A 1.3.3: HSQC 2-D NMR Spectrum of Compound 3

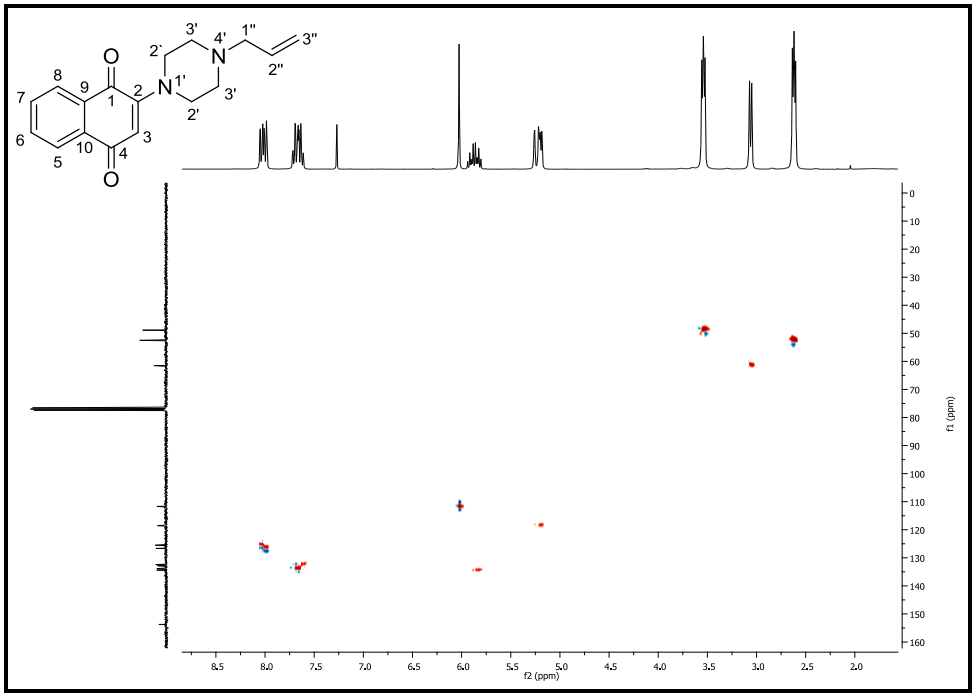

A 1.3′.1: ^{1}H NMR Spectrum of Compound 3

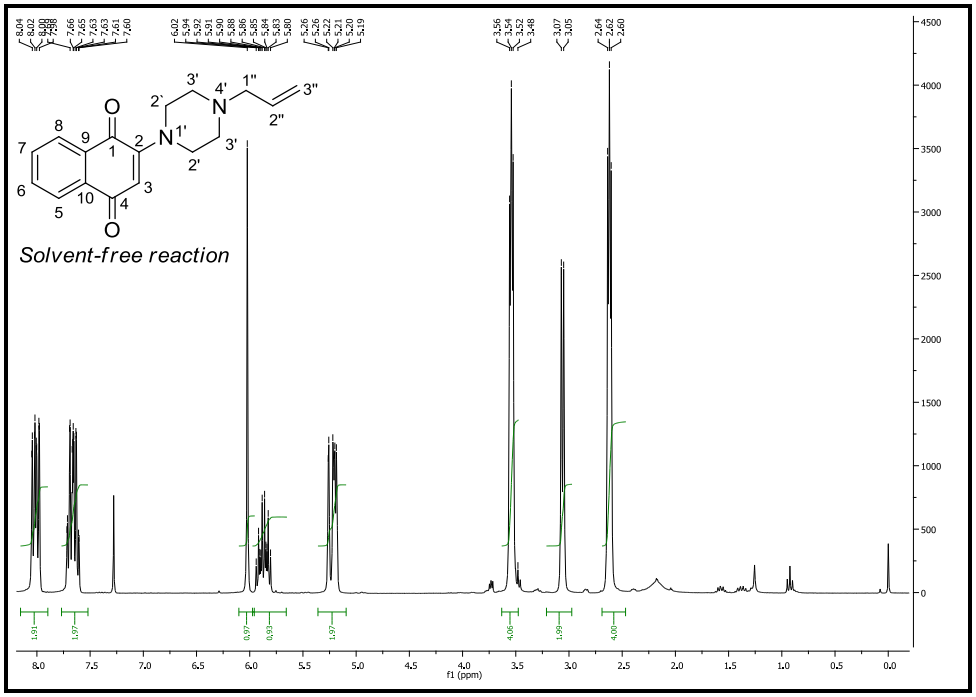

A 1.3′.2: ^{13}C NMR Spectrum of Compound 3

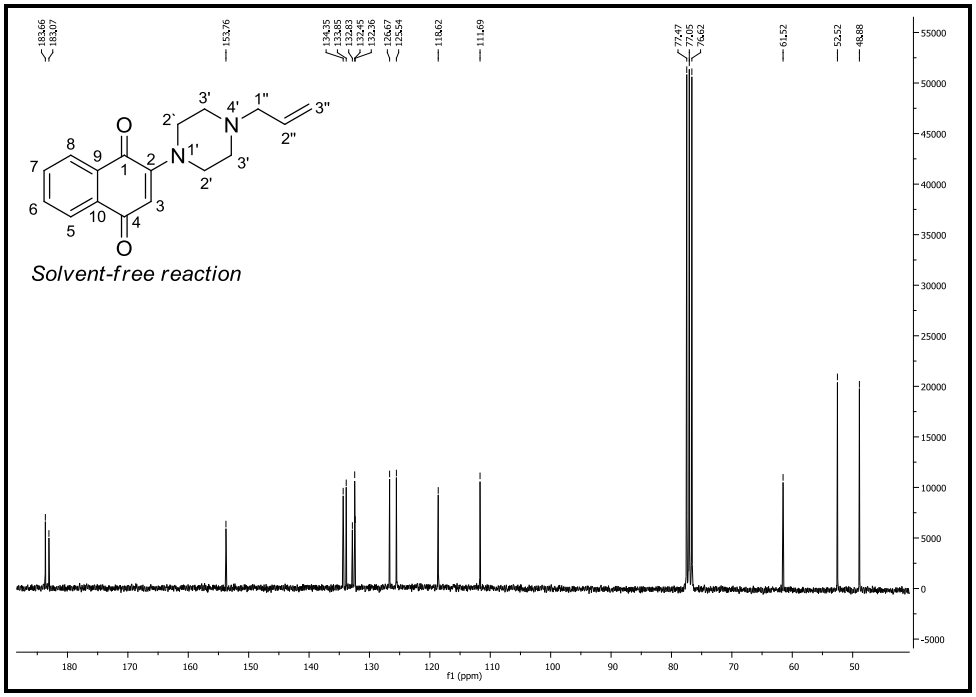

A 1.4.1: ^{1}H NMR Spectrum of Compound 4

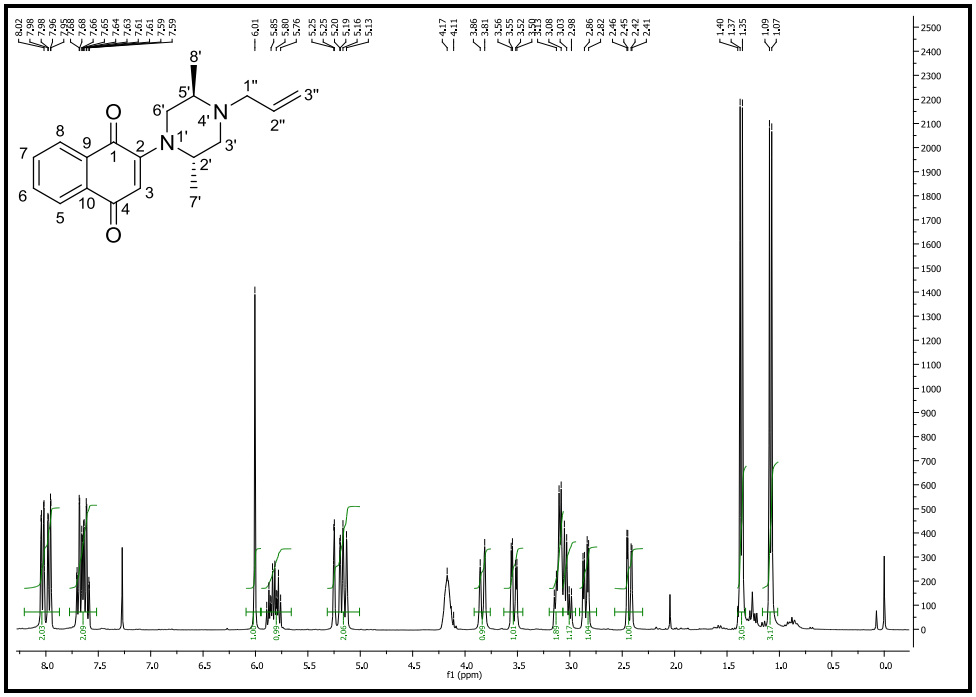

A 1.4.2: ^{13}C NMR Spectrum of Compound 4

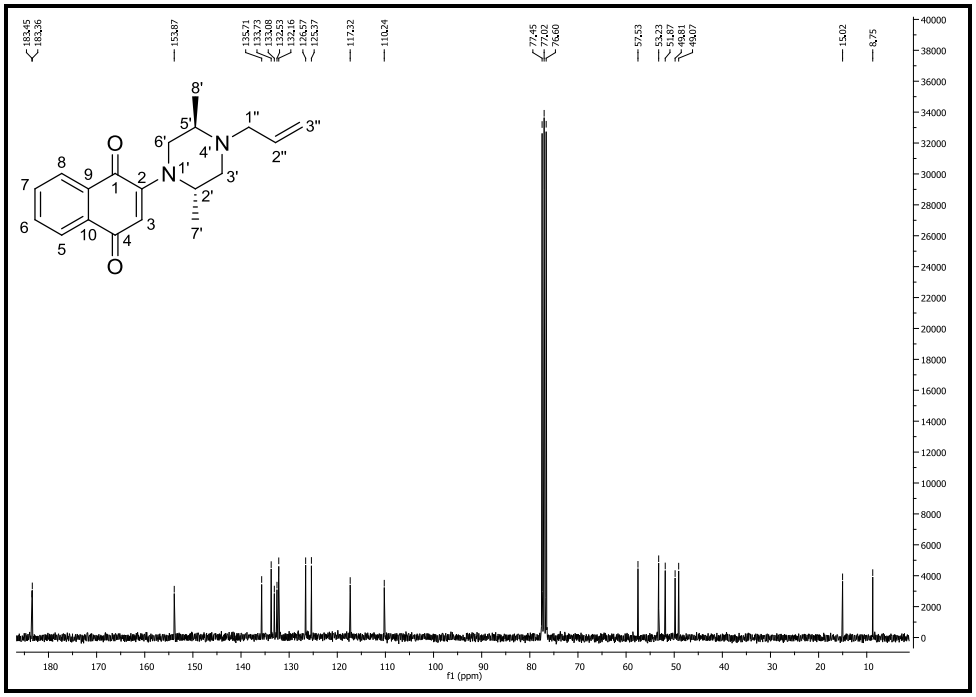

A 1.4.3: HSQC 2-D NMR Spectrum of Compound 4

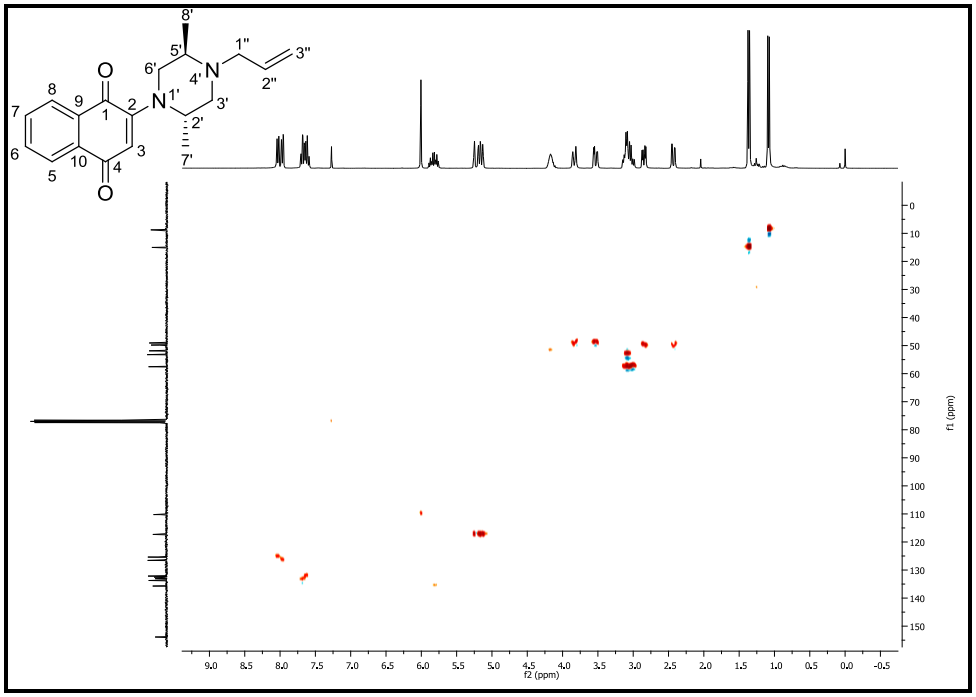

A 1.5.1: ^{1}H NMR Spectrum of Compound 5

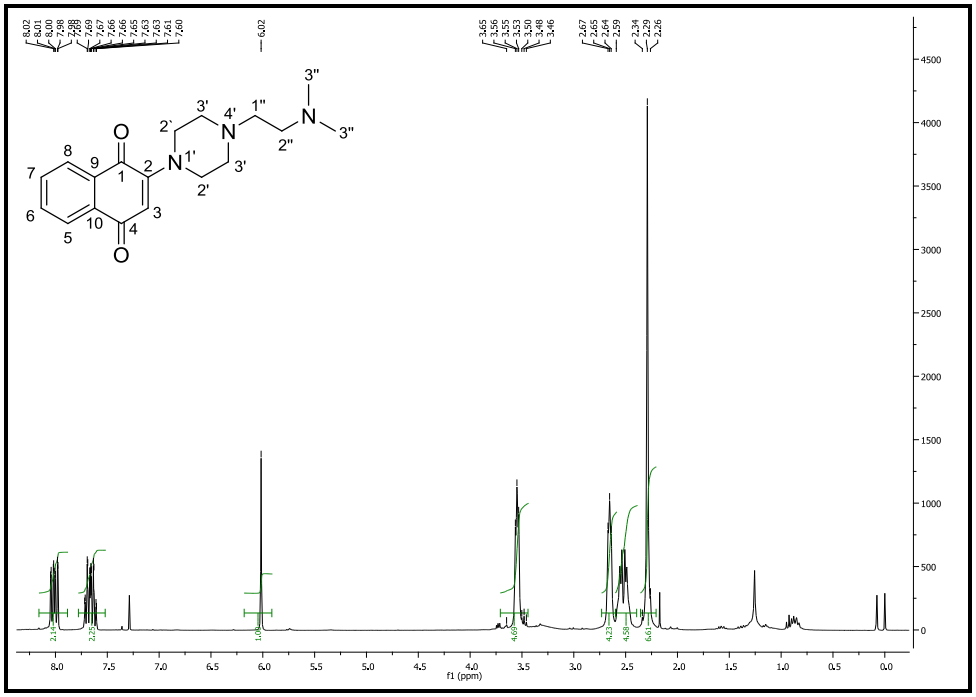

A 1.5.2: ^{13}C NMR Spectrum of Compound 5

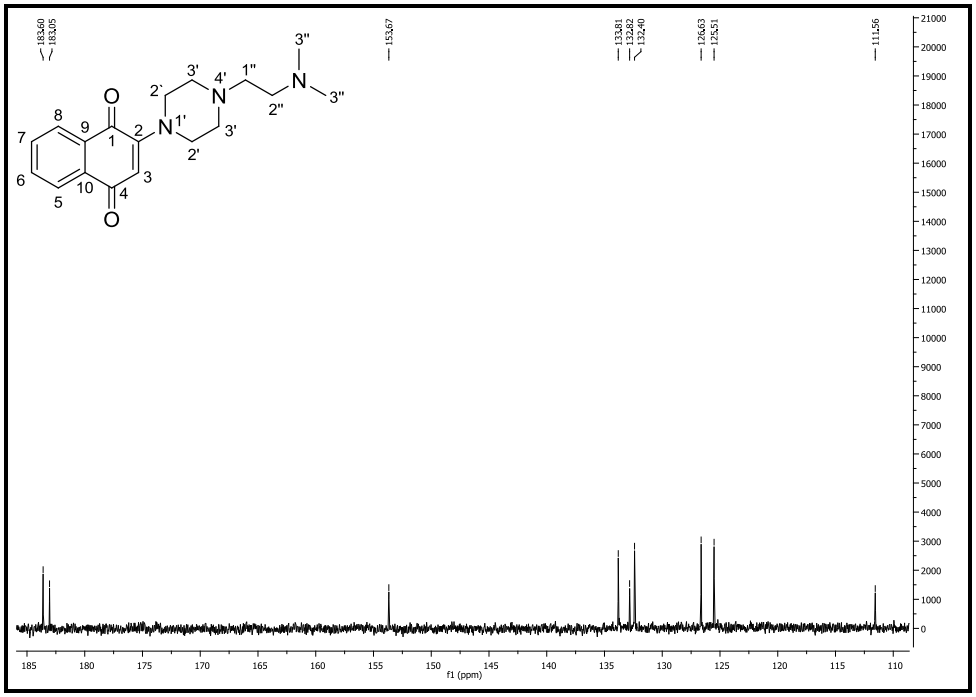

A 1.5.3: HSQC 2-D NMR Spectrum of Compound 5

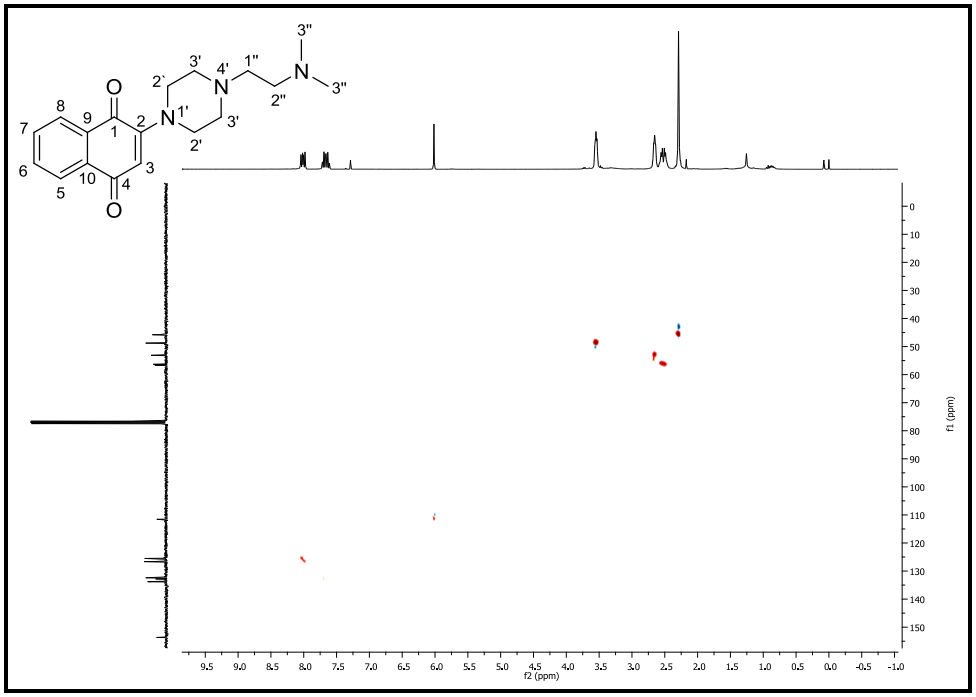

A 1.6.1: ^{1}H NMR Spectrum of Compound 6

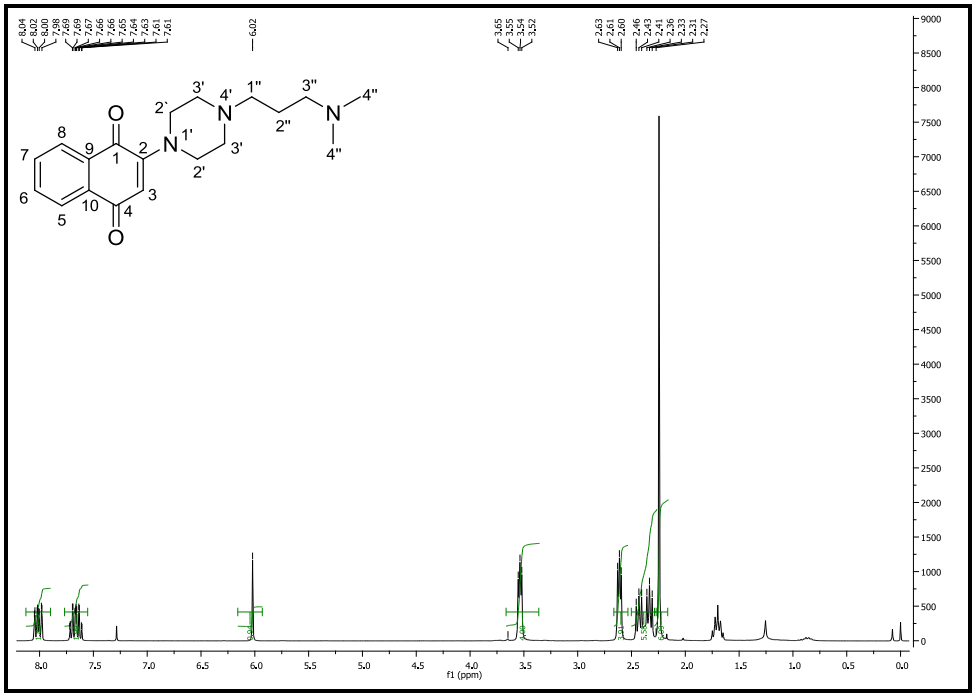

A 1.6.2: ^{13}C NMR Spectrum of Compound 6

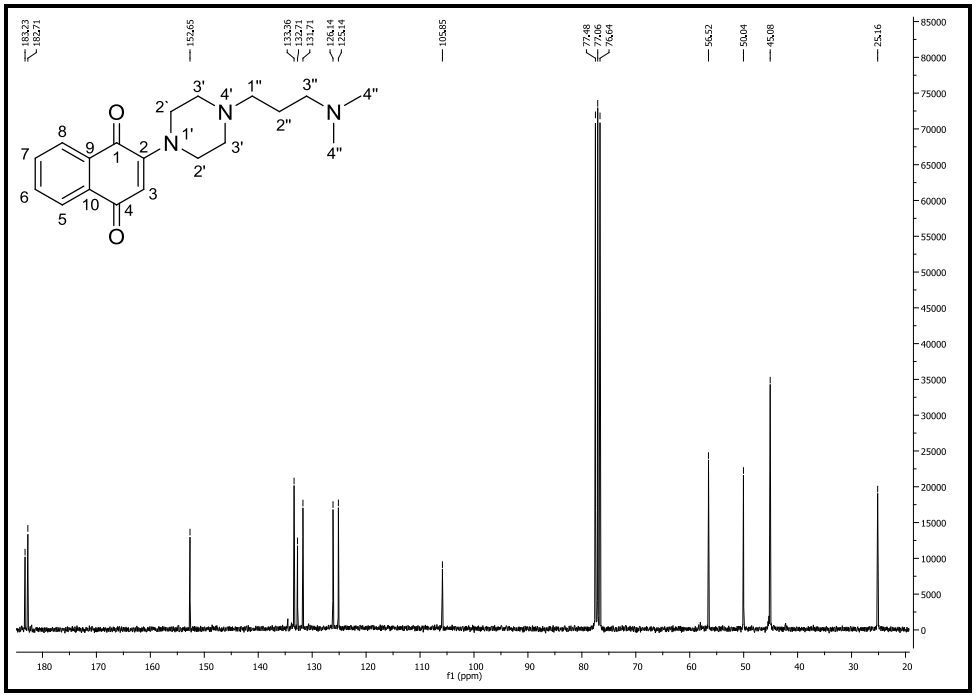

A 1.6.3: HSQC 2-D NMR Spectrum of Compound 6

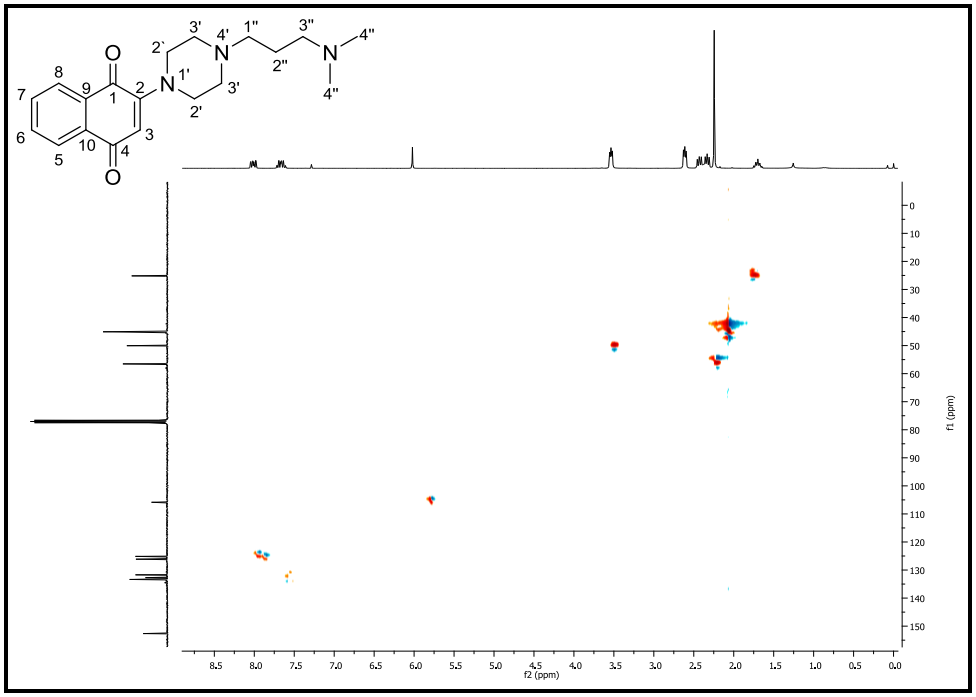

A 1.7.1: ^{1}H NMR Spectrum of Compound 7

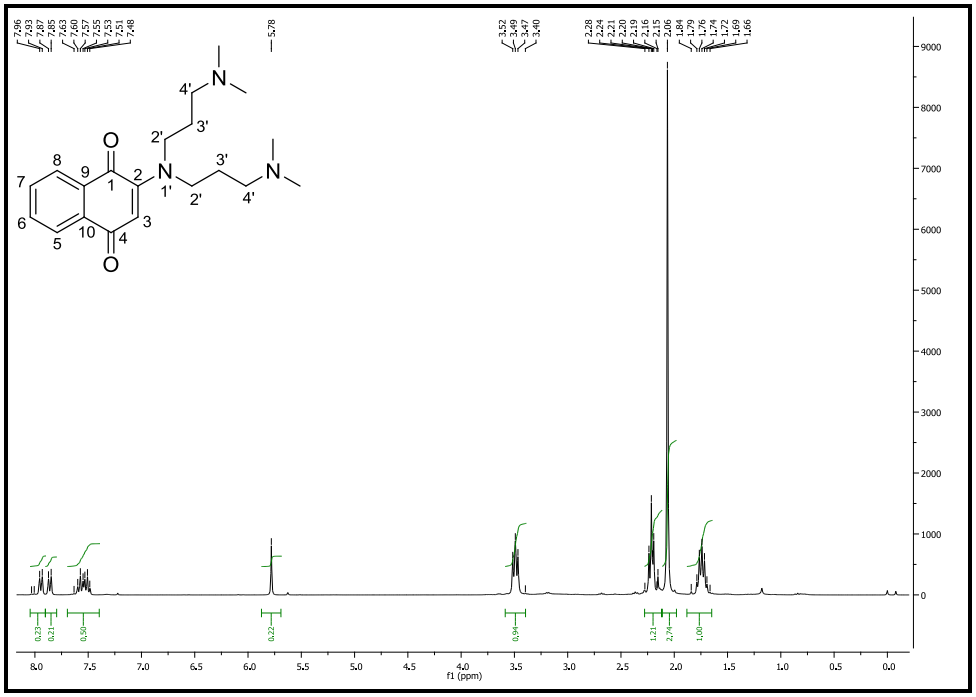

A 1.7.2: ^{13}C NMR Spectrum of Compound 7

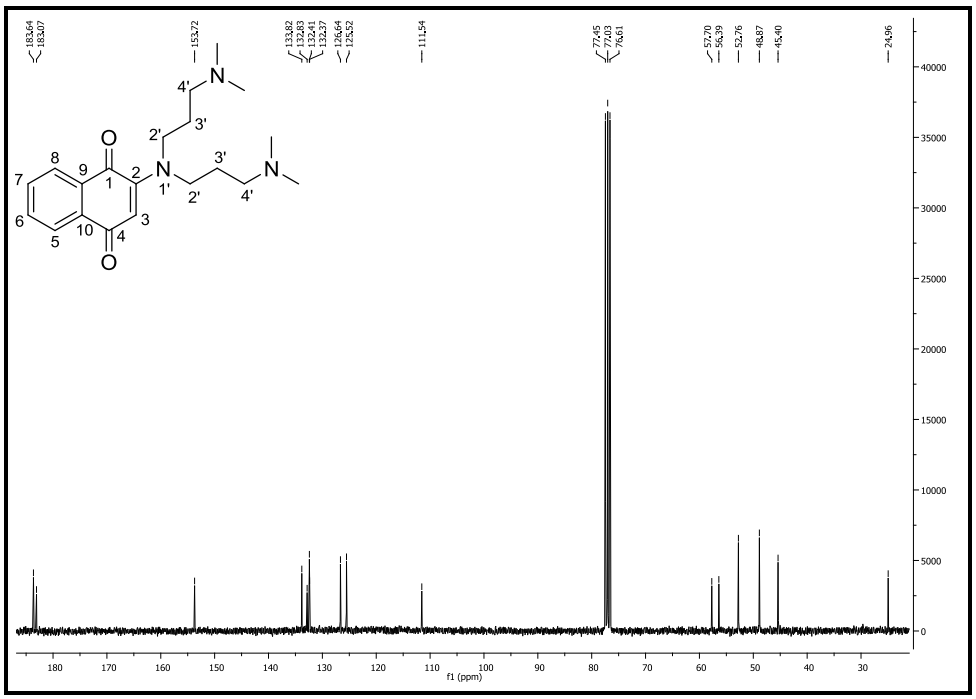

A 1.7.3: HSQC 2-D NMR Spectrum of Compound 7

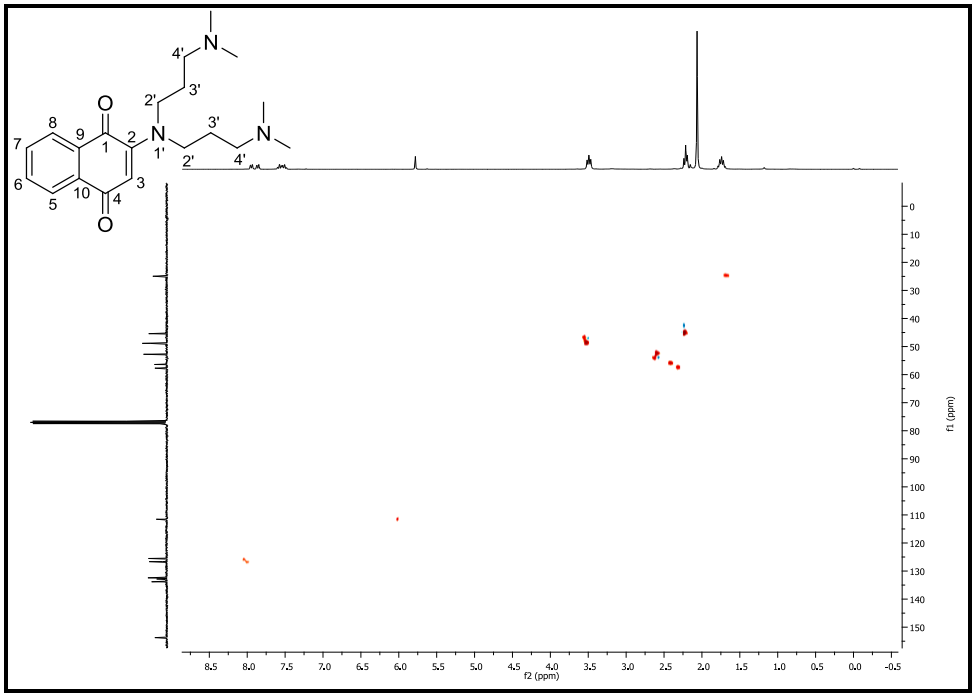

A 1.8.1: ^{1}H NMR Spectrum of Compound 8

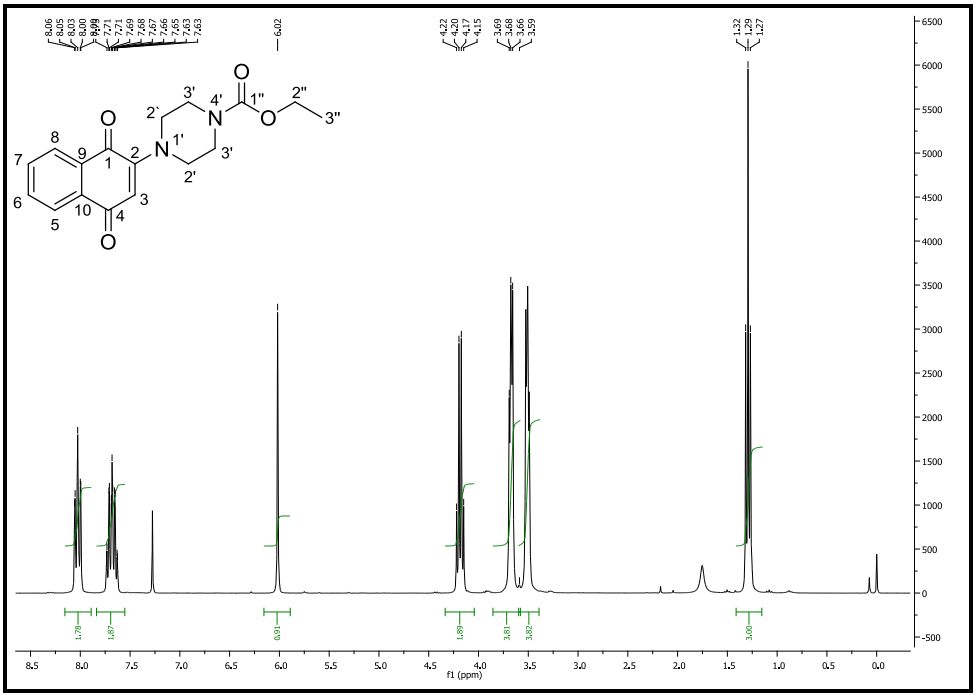

A 1.8.2: ^{13}C NMR Spectrum of Compound 8

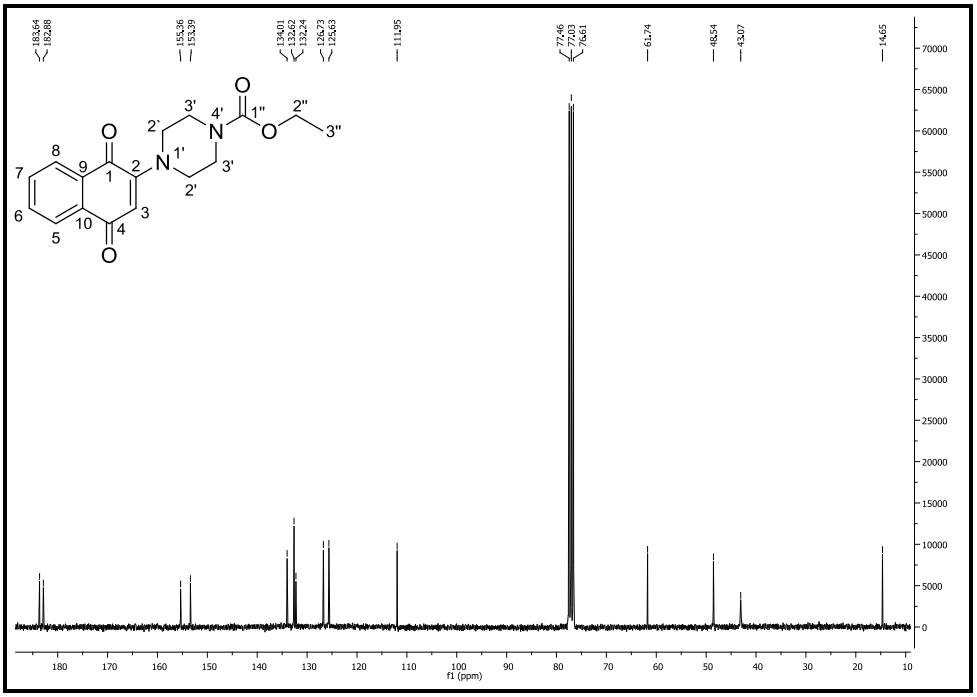

A 1.9.1: ^{1}H NMR Spectrum of Compound 10

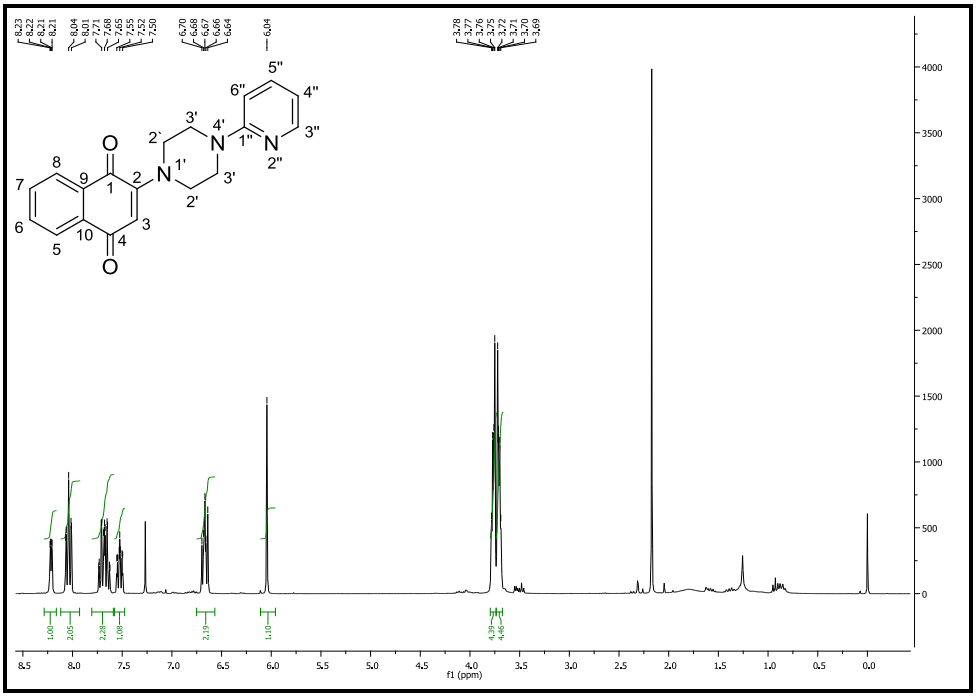

A 1.9.2: ^{13}C NMR Spectrum of Compound 10

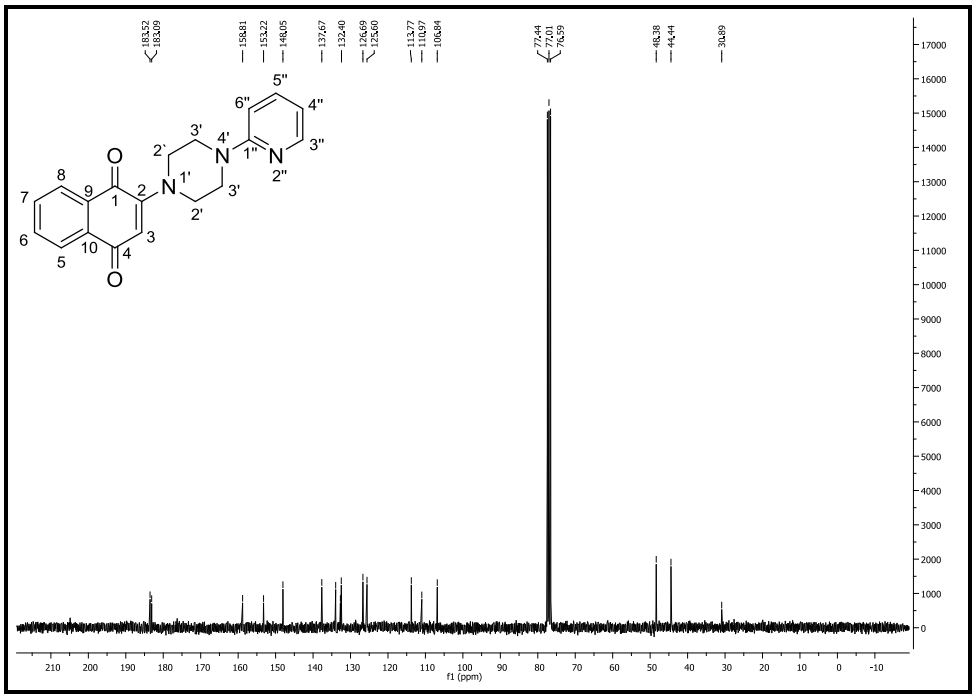

A 1.10.1: ^{1}H NMR Spectrum of Compound 11

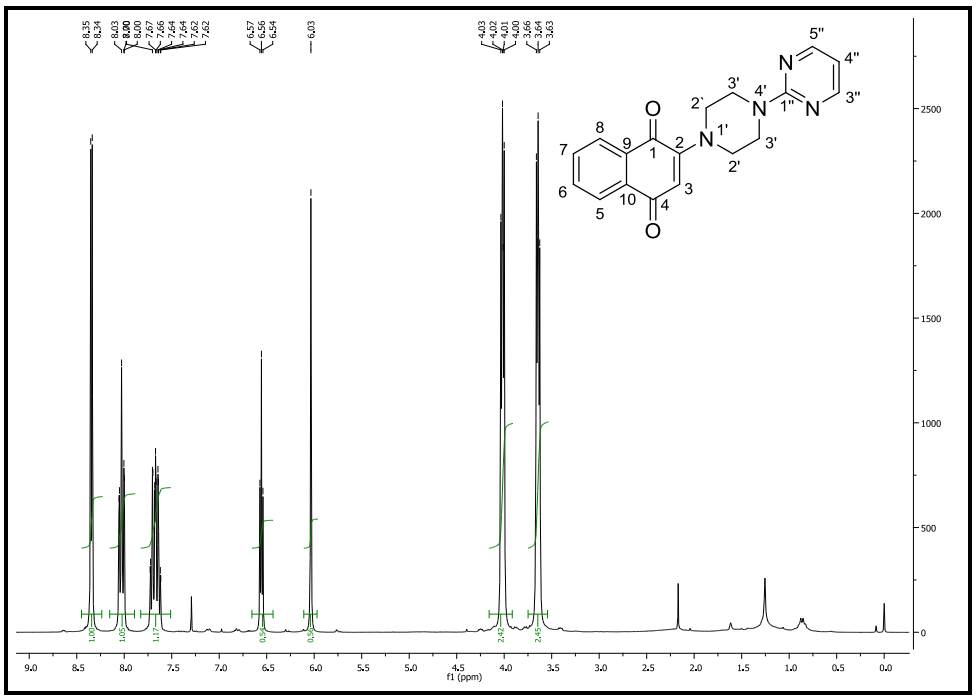

A 1.10.2: ^{13}C NMR Spectrum of Compound 11

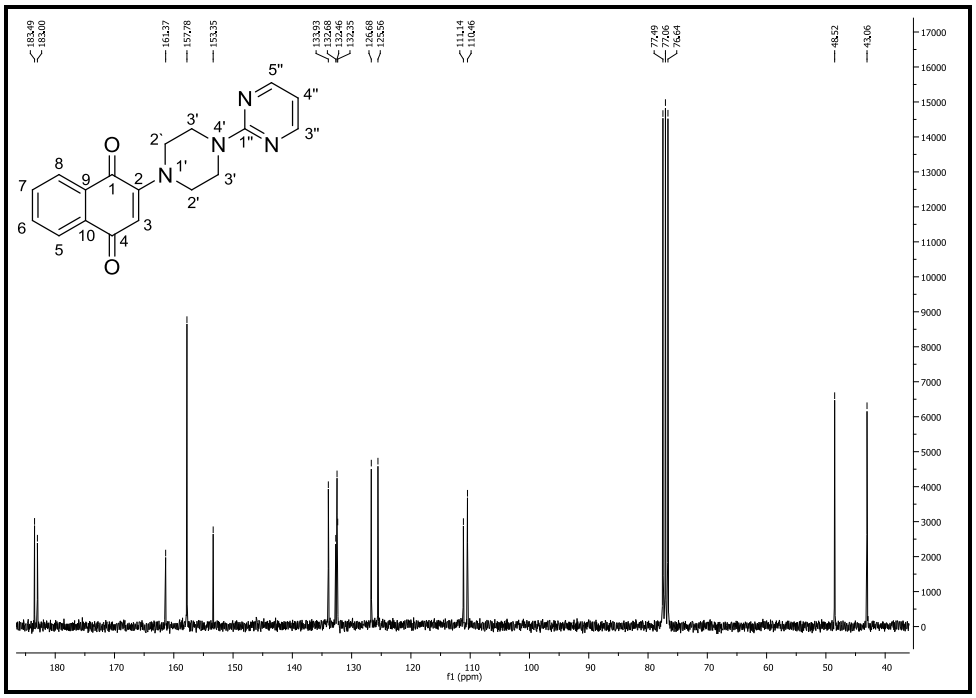

A 1.11.1: ^{1}H NMR Spectrum of Compound 47

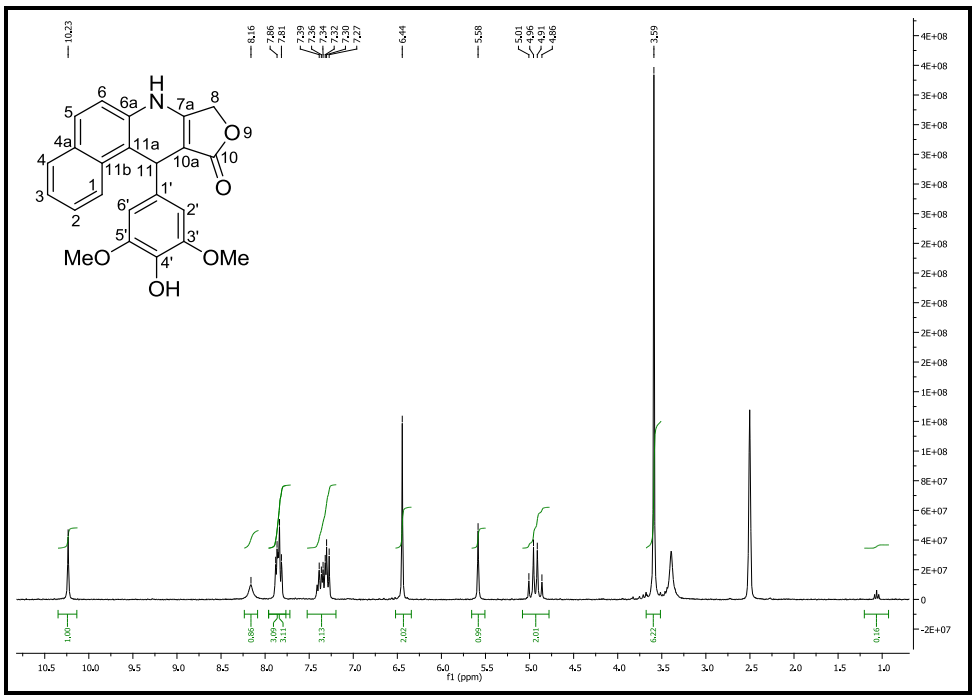

A 1.11.2: ^{13}C NMR Spectrum of Compound 47

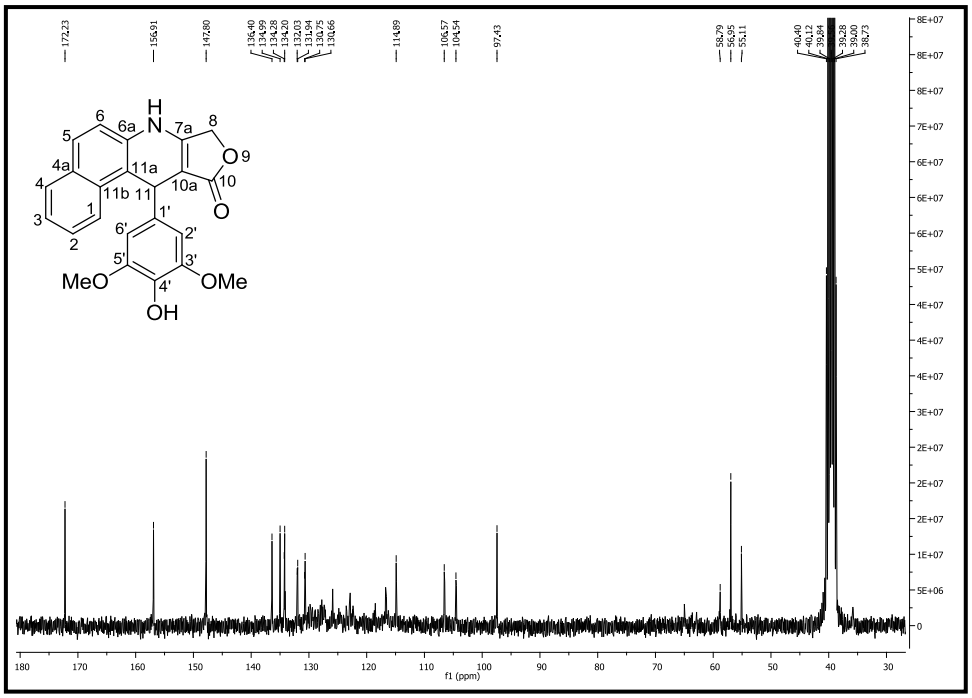

A 1.12.1: ^{1}H NMR Spectrum of Compound 40

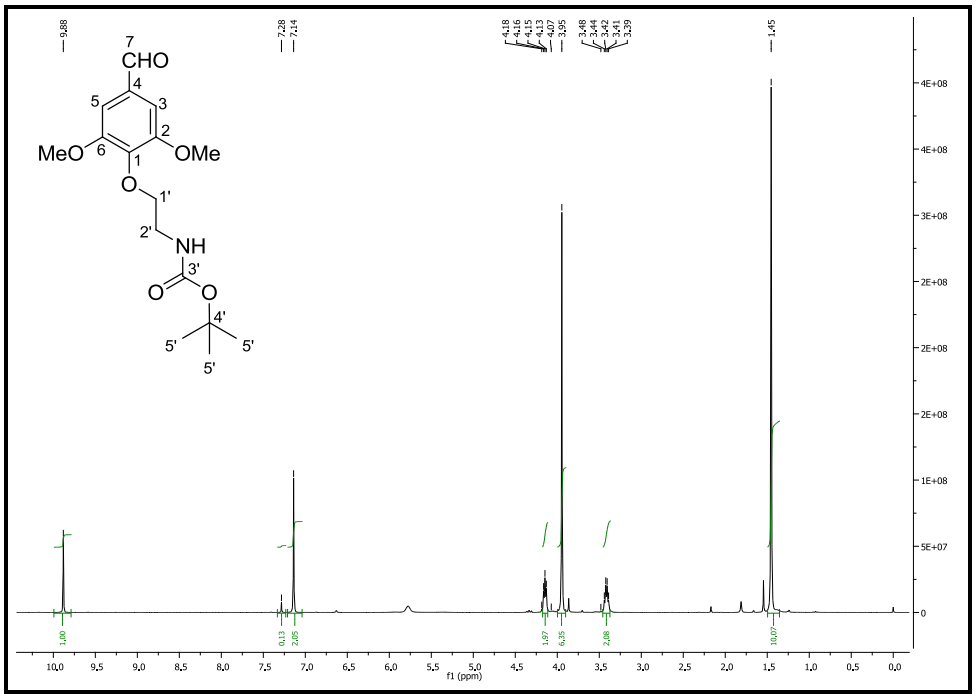

A 1.12.2: ^{13}C NMR Spectrum of Compound 40

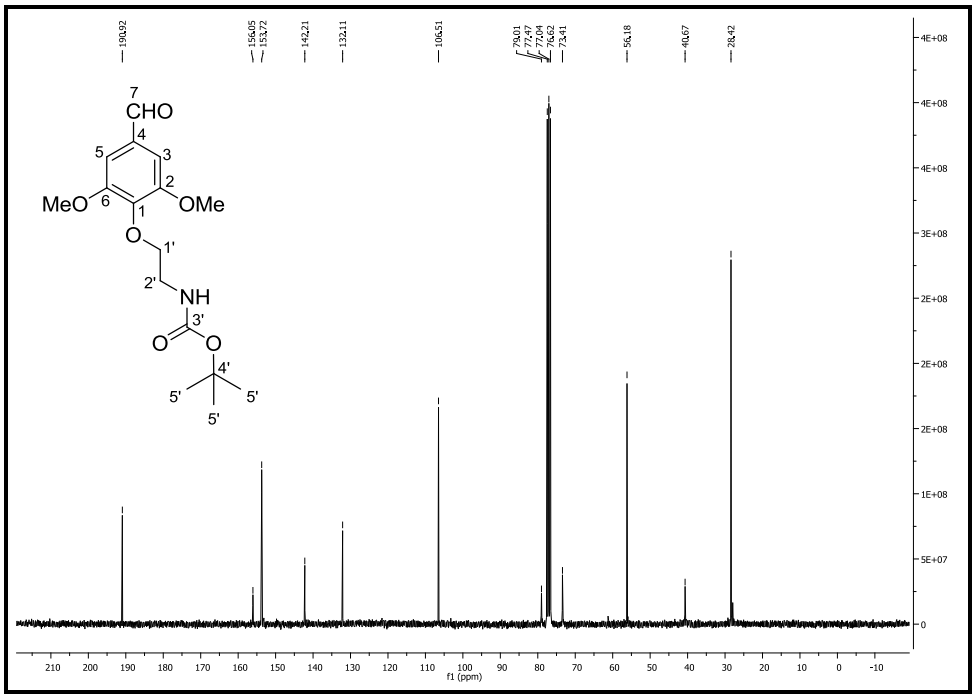

A 1.13.1: ^{1}H NMR Spectrum of Compound 43

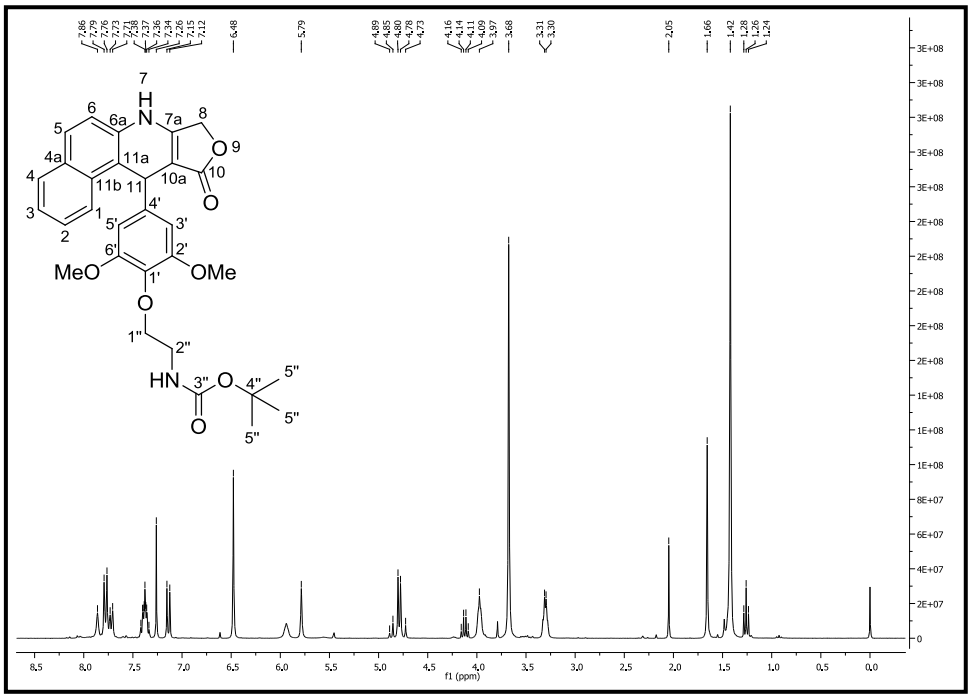

A 1.13.2: ^{13}C NMR Spectrum of Compound 43

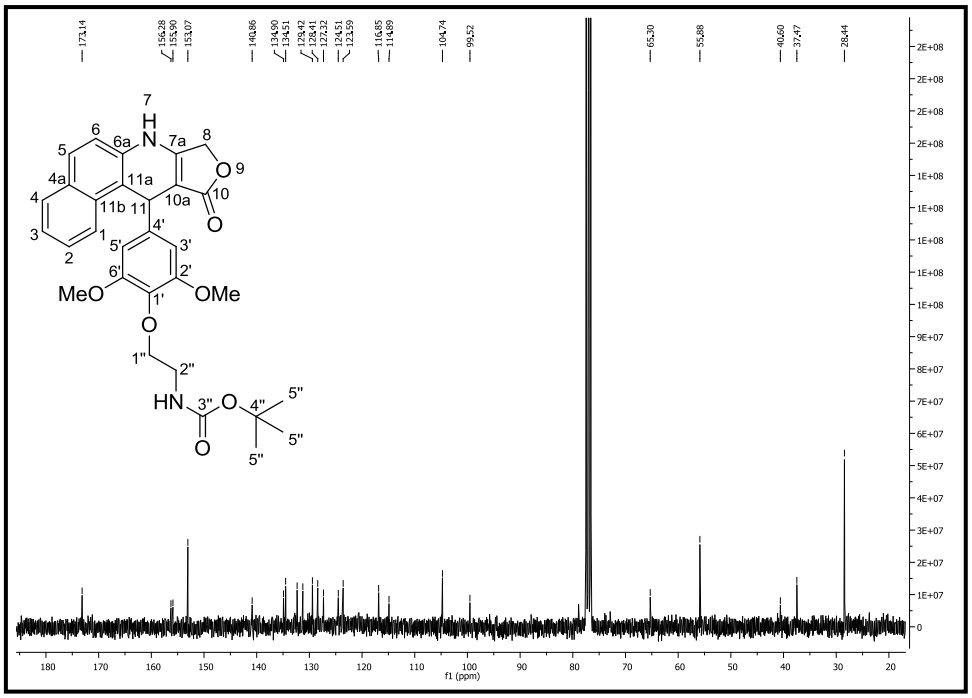

A 1.14.1: ^{1}H NMR Spectrum of Compound 44

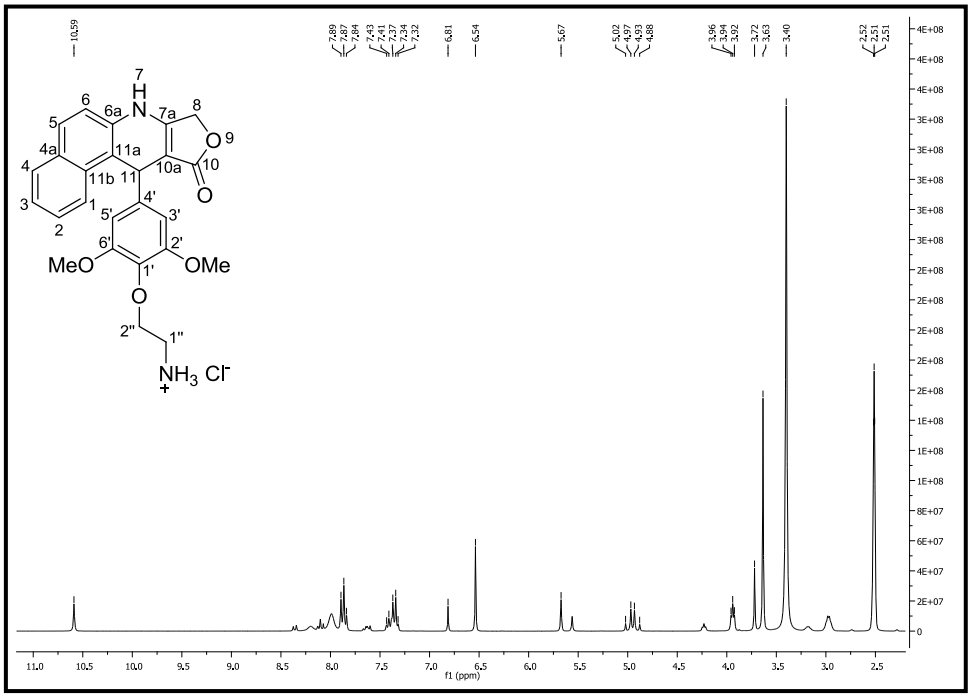

A 1.14.2: ^{13}C NMR Spectrum of Compound 44

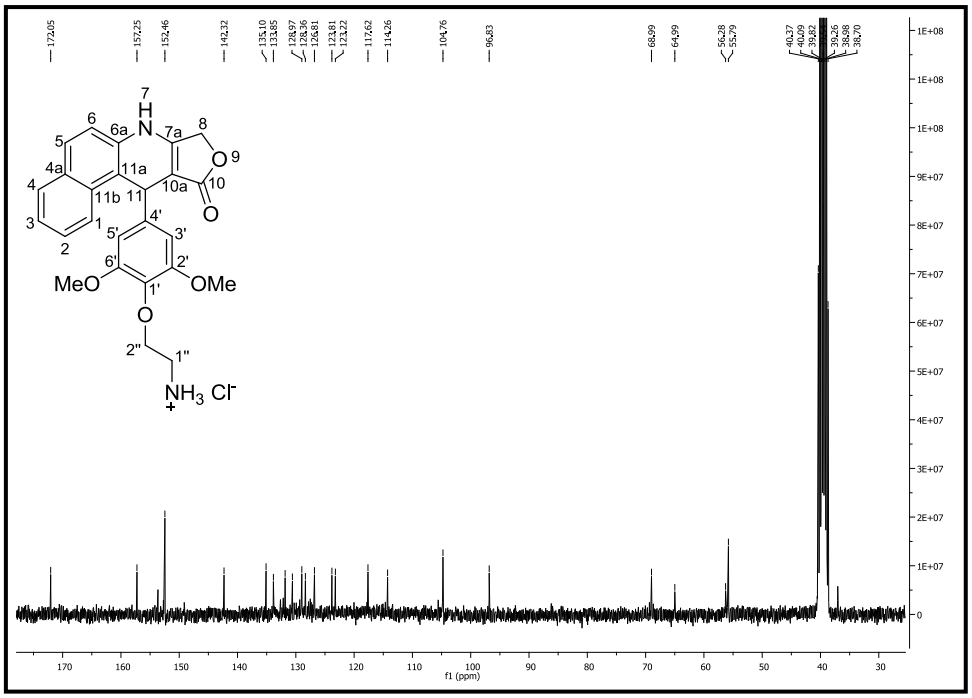

A 1.15.1: ^{1}H NMR Spectrum of Compound 46

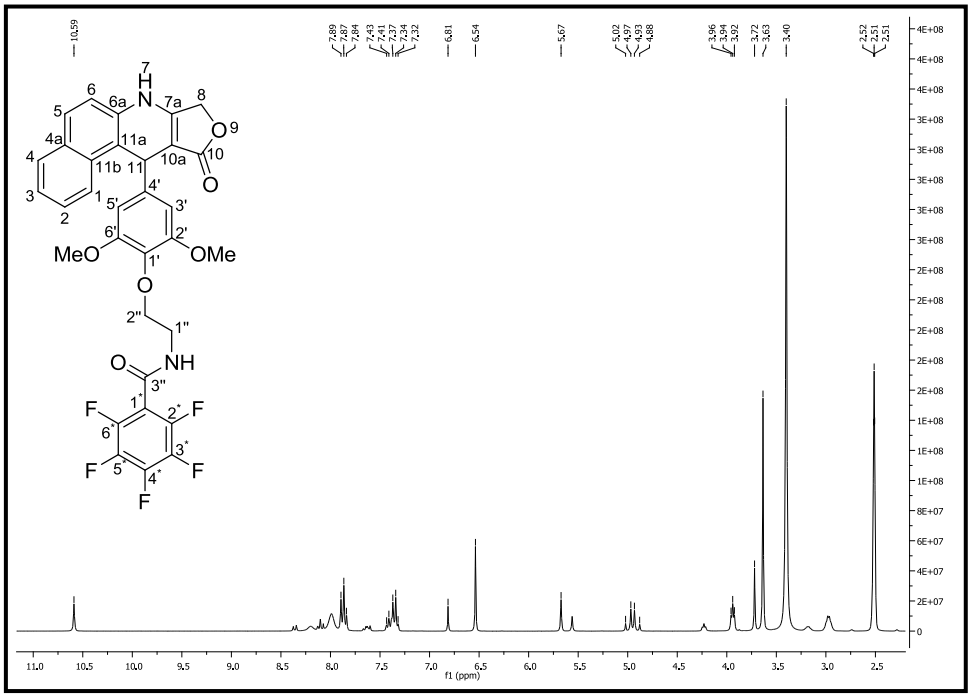

A 1.15.2: ^{13}C NMR Spectrum of Compound 46

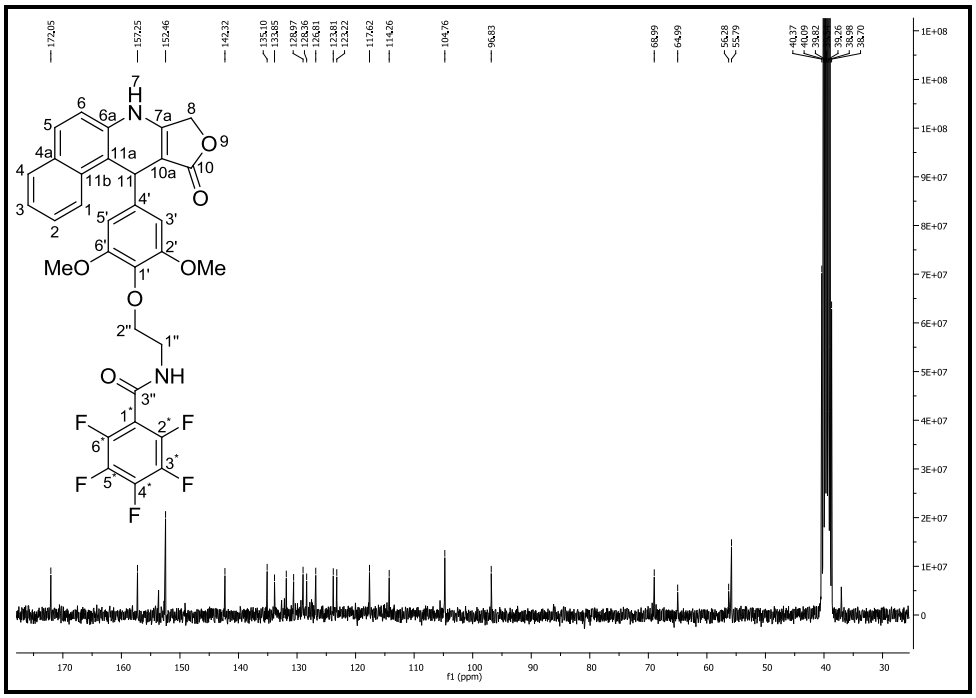

It is again among us, in a glass of milk. It is inserted in a very complex, long chain, yet such that almost all of its links are acceptable to the human body. It is swallowed; and since every living structure harbours a savage distrust toward every contribution of any material of living origin, the chain is meticulously broken apart and the fragments, one by one, are accepted or rejected. One, the one that concerns us, crosses the intestinal threshold and enters the bloodstream: it migrates, knocks at the door of a nerve cell, enters, and supplants the carbon which was part of it. This cell belongs to a brain, and it is my brain, the brain of the me who is writing; and the cell in question, and within it the atom in question, is in charge of my writing, in a gigantic miniscule game which nobody has yet described. It is that which at this instant, issuing out of a labyrinthine tangle of yeses and nos, makes my hand run along a certain path on the paper, mark it with these volutes that are signs: a double snap, up and down, between two levels of energy, guides this hand of mine to impress on the paper this dot, here this one.

Primo Levi, on Carbon